Investigation of the mechanisms underlying the effects of hyperglycaemia on cardiac structural and electrical remodelling

By

Hamida Aboalgasm

ABLHAM002

SUBMITTED TO THE UNIVERSITY OF CAPE TOWN
In fulfilment of the requirements for the degree
Doctor in Medicine (Physiology)
(HUB 6001W)

Supervisor: **A/Prof. Asfree Gwanyanya**
Co-supervisor: **Dr. Robea Ballo**

Department of Human Biology
Faculty of Health Sciences
University of Cape Town
Date of submission: 06 June 2022

Declaration

I, **Hamida Aboalgasm**, hereby declare that the work on which this dissertation/thesis is based is my original work (except where acknowledgements indicate otherwise) and that neither the whole work nor any part of it has been, is being, or is to be submitted for another degree in this or any other university. I empower the university to reproduce for the purpose of research either the whole or any portion of the contents in any manner whatsoever.

Signature: Signed by candidate

Date: 06 June 2022

Acknowledgements

I would like to express my appreciation and thanks to my supervisor, **Associate Professor Asfree Gwanyanya** for your support, guidance, and patience throughout my PhD study. Your enthusiasm for science has encouraged me and I am grateful for all you have taught me. I must also give thanks for your help in writing this thesis and for keeping me motivated throughout the study period. Without your support I could not have completed this dissertation. My co-supervisor, **Dr. Robea Ballo**, thank you for imparting your knowledge of mouse stem cell culture and for your advice, encouragement, and assistance during my study. Thanks for your guidance and valuable feedback toward writing this thesis.

Ms. Thulisa Mkatazo, I am not sure what I would have done without your technical assistance with mouse stem cell culture. Thank you for helping to troubleshoot all the issues. Your advice helped me to move forward all the time. Mrs. Desiree Bowers, thank you for your support and patience in teaching me the basic cell culture techniques, and for all your assistance throughout this study. Prof. Dirk Lang and Mrs. Susan Cooper, thank you for your assistance with confocal microscope imaging.

I would like to thank all the members of the Cardiovascular laboratory and Stem Cell laboratory for their support throughout my study.

I would like also to thank the Libyan Ministry of Higher Education and the Libyan Embassy in South Africa for the financial support of my postgraduate study.

I would like to thank my family, my father, sisters, and brothers who supported me during my study. This thesis is dedicated to the memory of my mother. Everything I do, I do in the hope that it would make you proud. I miss you. Finally, great thanks to my husband for his endless support and encouragement throughout my PhD.

Research outputs

Journal publications:

1. **Aboalgasm, H.**, R. Ballo, and A. Gwanyanya. 2021. "Organisational alteration of cardiac myofilament proteins by hyperglycaemia in mouse embryonic stem cell-derived cardiomyocytes." Journal of Muscle Research and Cell Motility. doi: 10.1007/s10974-021-09607-9.

2. **Aboalgasm, H.**, R. Ballo, T. Mkatazo, and A. Gwanyanya. 2021. "Hyperglycaemia-Induced Contractile Dysfunction and Apoptosis in Cardiomyocyte-Like Pulsatile Cells Derived from Mouse Embryonic Stem Cells." Cardiovascular Toxicology 21 (9):695-709. doi: 10.1007/s12012-021-09660-3.

3. **Aboalgasm, H.**, M. Petersen, and A. Gwanyanya. 2021. "Improvement of cardiac ventricular function by magnesium treatment in chronic streptozotocin-induced diabetic rat heart." Cardiovasc J Afr 32 (3):141-148. doi: 10.5830/cvja-2020-054.

Conference presentations:

1. Physiology Society of Southern Africa (AAPS-PSSA) (12-15 September 2021). Amanda Menzele, **Hamida Aboalgasm**, Robea Ballo, Asfree Gwanyanya. Hyperglycaemia-induced impairment of the autorrhythmicity of mouse embryonic stem cell derived cardiomyocytes.

2.The 11th Annual BRIP Research Symposium (18-19 October 2021).
Amanda Menzele, **Hamida Aboalgasm**, Robea Ballo, Asfree Gwanyanya. Hyperglycaemia-induced impairment of the autorrhythmicity of mouse embryonic stem cell derived cardiomyocytes.

3. The 4th European-South Africa Cardiovascular Research (EU-SASCAR) Conference (April 2019). Stellenbosch, South Africa. **Hamida Aboalgasm**, Asfree Gwanyanya.
Improvement of cardiac ventricular function by magnesium in chronic streptozotocin-induced diabetic rats.

Seminar presentations:

Hamida Aboalgasm, Presenter at a Division of Physiological Sciences Seminar, Department of Human Biology, University of Cape Town (6 October 2021). Investigation of the mechanisms underlying the effects of hyperglycaemia on cardiac structural and electrical remodelling.

Table of Contents

List of figures and tables

List of abbreviations

Symbol	Description
AGE	Advanced glycation end products
AP	Action potential
Bcl-2	B-cell lymphoma 2
BSA	Bovine serum albumin
Ca^{2+}	Calcium
Caspases	Cysteine aspartyl-specific proteases
Cxs	Connexins
EB	Embryoid body
ESC	Embryonic stem cells
ECL	Enhanced chemiluminescence
ESC	Embryonic stem cells
FBS	Foetal bovine serum
GDM	Gestational diabetes mellitus
HRP	Horseradish peroxidase
iMEFs	Inactivated primary mouse embryonic fibroblasts
K	Potassium
LV	Left ventricle
LIF	Leukaemia inhibitory factor
mESCs	Mouse embryonic stem cells
MHC	Myosin heavy chain

NFAT Calcineurin-nuclear factor

Na^+ Sodium

OPA1 Optic Atrophy 1

PI3K Phosphatidylinositol 3-kinase

PBS Phosphate-buffered saline

PFA Paraformaldehyde

PVDF Polyvinylidene fluoride

RAGE Receptor of advanced glycation end product

RIPA Radioimmunoprecipitation

ROS Reactive oxygen species

RyR Ryanodine receptor

rcf Relative centrifugal force

SA South Africa

SERCA Sarcoplasmic/endoplasmic reticulum Ca^{2+}-ATPase

SARS-2 Severe acute respiratory syndrome-type 2

Na^+ Sodium

TGF Transforming growth factor

TNF Tumour-necrosis factor

WHO World Health Organisation

Abstract

Background: Diabetes mellitus with uncontrolled hyperglycaemia is a major cause of cardiovascular complications and mortality. The developing foetal heart *in-utero* is particularly susceptible to hyperglycaemia through pathological remodelling, which results in life-long structural abnormalities such as cardiomyopathy and electrical defects like arrhythmias. However, the underlying mechanisms and potential therapeutic drug targets remain unclear. In this study, a cardiac developmental cellular model was used to study hyperglycaemia-induced remodelling.

Methods: Mouse embryonic stem cells (mESCs) were differentiated into pulsatile, cardiac-like cells via embryoid body (EB) formation and cultured under baseline- or high glucose conditions. A Ca^{2+}-sensitive fluorescent dye Fluo-4 was used to measure calcium transients and a voltage-sensitive dye di-4-ANEPPS was used to record action potentials. Cellular biomarkers were detected using immunocytochemistry, confocal microscopy, and Western blotting as well as terminal deoxynucleotidyl transferase dUTP nick-end labelling (TUNEL) and 5-ethynyl-2-deoxyuridine (EdU) assay.

Results: Undifferentiated mESCs were positive for pluripotent transcription factors Nanog and Oct3/4, whereas the cardiac differentiated mESCs were positive for cardiac proteins troponin T, α-actinin 2, connexin 43, sarco-endoplasmic reticulum calcium ATPase 2 (SERCA 2) and α- and β-myosin heavy chain. Hyperglycaemia decreased the number of beating EBs, their beating rate, and their amplitude of contraction. It also decreased the calcium transient amplitude and the contractile response to ryanodine receptor stimulation by caffeine but did not alter the SERCA 2 expression. The amplitude and duration of action potentials in beating EBs were not altered by hyperglycaemia. However, structural changes included a decrease in EB size and expression of myofilament proteins, α-actinin and α- and β-myosin heavy chain and a disruption of the striated organization of the myofilaments. Hyperglycaemia increased the proportion of TUNEL-positive cells and the expression of the pro-apoptotic marker cytochrome c and decreased the anti-apoptotic protein B-cell lymphoma 2 but did not alter the mitochondrial staining with Mitotracker. It also increased the oxidative stress marker nitrotyrosine but did not alter the extent of EdU

nuclear staining nor the expression of the receptor of advanced glycation end-product. The antioxidant n-acetyl cysteine decreased the fraction of hyperglycaemia-induced TUNEL-positive cells and improved the α-actinin striated pattern. **Conclusion:** Hyperglycaemia suppressed the cardiac differentiation and contractile activity of mESCs as well as disrupted the cardiac myofilament organisation and expression. These effects of hyperglycaemia were likely mediated by mitochondrial-dependent apoptosis triggered by oxidative stress as well as by the abnormalities in calcium signalling. These results have potential clinical implications in foetal diabetic cardiac disease and add novel insights into the mechanistic factors that represent new therapeutic drug targets in the developing foetal heart.

Chapter 1: Introduction

1.1 Diabetes mellitus, a growing metabolic disease

Diabetes mellitus is a leading cause of death, and has overtaken other common conditions such as infectious diseases, which include human immunodeficiency virus and tuberculosis (Roglic et al. 2005). As such, diabetes is one of the major global causes of morbidity and mortality, increased health expenditure, and economic loss. Lately, diabetes has also been associated with an increase in the morbidity of infectious diseases such as severe acute respiratory syndrome (SARS-2) (Gregg, Sophiea, and Weldegiorgis 2021). Diabetes has been reported to have caused 1.5 million deaths world-wide in 2019 (WHO 2021), and its global prevalence in 2019 was estimated to be 136 million people, and is projected to increase to 195 million by the year 2030 and 276 million by the year 2045 (Sinclair et al. 2020). The global increase in the prevalence of diabetes has been attributed to factors such as urbanization, aging populations, and changes in lifestyle factors such as smoking, unhealthy diet, and sedentary life (Mayosi et al. 2009, Ramachandran et al. 1999). Furthermore, the prevalence of diabetes is higher in developing countries, where it is estimated to increase to 69% by the year 2030 compared to 20% in developed countries (Shaw, Sicree, and Zimmet 2010). In Sub-Saharan Africa, the projected prevalence of diabetes is 98% and is expected to increase from 12 million in 2010 to 23 million in 2030 (Hall et al. 2011). Specifically, in South Africa, the burden of diabetes mellitus was 5.5% in 2000 (Bradshaw et al. 2007), but increased to 9% in 2013 (Bertram et al. 2013). Therefore, South Africa has a huge burden of diseases due to high rates of infectious diseases, non-communicable diseases, maternal and child mortality (Mayosi et al. 2009). The economic burden is further worsened by the disease generally affecting working-age people in Africa, thereby causing a decrease in economic productivity (Peer et al. 2014).

Diabetes mellitus is a metabolic disease with various subtypes, all having the common feature of hyperglycaemia, which is a major cause of diabetic complications

and a key parameter monitored during diabetes treatment. Type 1 or insulin-dependent diabetes constitutes about 5-10% of diagnosed diabetic patients (Maahs et al. 2010). Type 1 diabetes is due to autoimmune destruction of pancreatic β-cells through cell-mediated inflammatory responses and occurs mainly in children and adolescents (Devendra, Liu, and Eisenbarth 2004). The presence of autoantibodies against pancreatic islet cells is a characteristic of immune destruction of pancreatic β-cells in type 1 diabetes mellitus and include islet cell autoantibodies to insulin, protein tyrosine phosphatase, and zinc transporter protein (Vermeulen et al. 2011). Autoimmune destruction of pancreatic β-cells has various genetic predispositions such as human leukocyte antigen associations (Noble et al. 1996) and is also linked to environmental factors. Type 2 or non-insulin dependent diabetes mellitus affects about 90% of diagnosed adult diabetic patients. It is characterized by insulin resistance and is associated with a sedentary lifestyle and obesity (Ramachandran et al. 1999). Over time, the disease increases the requirements for insulin in insulin-sensitive tissues and decreases insulin secretion, thereby transforming type 2 diabetes from being insulin independent to insulin dependent (Druet et al. 2006). Another less-recognised subtype of diabetes is gestational diabetes (GDM), which occurs during pregnancy. The uniqueness of GDM is in its effect on both the mother and the foetus, thereby inducing life-long health problems for both. Diabetes in pregnant mothers with poorly monitored hyperglycaemia is linked with foetal birth defects in 5–10% of pregnancies and spontaneous abortion in 15–20% of pregnancies (Reece 2012). GDM occurs in 2% of pregnancies (Pauliks 2015), and according to the International Diabetes Federation (2017), it affects approximately 14% of pregnancies world-wide, corresponding to around 18 million births. The risk factors for GDM include obesity, a previous history of gestational diabetes, maternal age, polycystic ovary syndrome, and exposure to toxic factors (Galtier 2010). However, there is incomplete evidence in the existing literature about the mechanisms through which GDM affects the foetus.

1.2 Diabetes mellitus as a cardiovascular disease

The main causes of diabetic morbidity and mortality are systemic complications, which include acute metabolic conditions such as hyperglycaemia with ketoacidosis and hypoglycaemia. Other causes include chronic complications in various body systems such as cardiovascular, renal, visual, neurological, and gastrointestinal systems. Among the chronic diabetic complications, cardiovascular diseases constitute about half of them, and are the main cause of diabetic morbidity and mortality (Rao Kondapally Seshasai et al. 2011, Soedamah-Muthu et al. 2006). This contribution of cardiovascular complications is more so in African countries where the complications account for over 60% of diabetic deaths (Bos and Agyemang 2013). Apart from affecting the heart through conditions such as myocardial infarction, diabetes also presents as vasculopathy in the retina, kidneys, brain, and peripheral arterial disease (Krentz, Clough, and Byrne 2007). Because of these various cardiovascular manifestations and the effects in either adults or in the foetus of a diabetic mother, diabetes mellitus is primarily considered as a cardiovascular disease (Grundy et al. 1999).

Maternal complications in GDM include hypertension, preeclampsia, and an increased risk of caesarean section delivery (Rosenn 1998). The condition is associated with long-term complications to the offspring including high risk of glucose intolerance, diabetes mellitus, and obesity (Dabelea and Pettitt 2001). Poor maternal glycaemic control, especially in the case of pre-existing diabetes, increases the risk of foetal malformations. The foetuses of diabetic mothers are at a high risk of perinatal morbidity and mortality due to congenital anomalies, also known as congenital malformations, that occur for the duration of intrauterine life (Evers, de Valk, and Visser 2004). Congenital malformations are the second predisposing reason of infant death after prematurity, causing about 20% of infant deaths (Almli et al. 2017). The congenital malformations include cardiac anomalies such as transposition of great arteries, ventricular and atrial septal defects, central nervous system defects such as neural tube defects, and gastrointestinal malformations such as duodenal atresia, and skeletal and genitourinary tract anomalies (McLeod and

Ray 2002). Of these malformations, congenital heart diseases (Alyousif et al. 2021, Wren, Birrell, and Hawthorne 2003) and abnormalities of the nervous system are more common (Li et al. 2012), since both start developing in the early embryonic developmental stage. The prevalence of foetal cardiac malformations reportedly increases to 8.5% in diabetic mothers with poor glycaemic control (Starikov et al. 2013). Moreover, GDM suppresses the expression of transcription factors, which are critical for cardiac lineage specification, suggesting that GDM negatively influences cardiogenesis during early embryonic development (Kumar, Dheen, and Tay 2007).

1.3 Diabetic adult- and foetal cardiac complications

1.3.1 Adult heart complications

The main consequence of diabetic-induced structural changes is diabetic cardiomyopathy, a condition that occurs independently of other cardiac factors such as coronary heart disease and valvular heart diseases (Hayat et al. 2004). Diabetes-induced cardiomyopathy affects cardiac tissue structural components such as cardiomyocytes and the interstitium, thereby imposing a substantial risk factor for left ventricle (LV) hypertrophy (Galderisi et al. 1991). The cardiac structural changes in diabetes mellitus result in changes in cardiac cell size and interstitial deposition of collagen fibres leading to changes in the ventricular mass and ultimately hypertrophy of the LV, which is more frequently affected than the right ventricle (Devereux et al. 2000). Cardiomyocyte alterations involve cellular hypertrophy and death; hypertrophy may be linked to increased fat and protein synthesis within the cardiac cells (Veille et al. 1993). Cardiac fibrosis is an important structural derangement in a diabetic heart since it is associated with cardiac dysfunction and poor prognosis. As such, interstitial fibrosis is one of the important causes of increased ventricular stiffness and diastolic dysfunction in diabetes mellitus (van Heerebeek et al. 2008). In adult diabetic cardiac dysfunction, the diastolic impairment occurs early in diabetes mellitus, and precedes the systolic dysfunction (Karamitsos et al. 2007).

Diabetes mellitus is also linked with changes in the electrical function of the heart that cause cardiac arrhythmias. The abnormalities include defects in cardiac action potential (AP) conduction or repolarization phases, due to a complex interaction of ion channel and electrophysiological alterations. The arrhythmogenesis can be due to irregularities in conduction, which could be mediated by myocardial ischaemia (Desouza et al. 2003), ion channel dysfunction, increased adrenergic drive, and calcium (Ca^{2+}) overload (Tse et al. 2016). In addition, the alteration in the neuronal pathway of the cardiac autonomic innervation of the heart can further promote arrhythmogenesis (Coumel 1993). Diabetes mellitus is also associated with disturbances in the sinoatrial node function (Howarth, Al-Sharhan, et al. 2007) and vascular responses, which increases the incidence of silent cardiac ischemia (Fava et al. 1993). Therefore, alterations in the electrophysiological characteristics of the heart are some of the main underlying causes of cardiac arrhythmias (Soltysinska et al. 2014, Wang and Hill 2010).

1.3.2 Foetal cardiac complications

Several factors predispose to foetal cardiac structural damage including metabolic derangements, disturbances in structural proteins, autonomic dysfunction, impairment in ion homeostasis, and interstitial fibrosis (Tziakas, Chalikias, and Kaski 2005). Common cardiac structural anomalies in infants of mothers with GDM involve ventricular septal defects, transposition of great arteries, tetralogy of Fallot, and aortic stenosis (Moazzen et al. 2014). The defects in great arteries that are more common in infants of diabetic mothers include truncus arteriosus and double outlet right ventricle (Ferencz et al. 1990). Notably, hypertrophic cardiomyopathy has been diagnosed in up to 50% of new-born infants of diabetic mothers (Kulkarni et al. 2017). Foetal hypertrophic cardiomyopathy involves heart enlargement and disproportionate septal hypertrophy. In severe conditions, foetal myocardial hypertrophy causes ventricular stiffness which could influence diastolic filling and systolic function of the heart (Ullmo et al. 2007). Foetal cardiac hypertrophy and myocardial remodelling are triggered primarily by cardiomyocyte hyperplasia, and

disorganization of the normal pattern of cardiac myofibrils, changes that are similar to those seen in cardiomyopathy in adults (Dowling et al. 2014, Lehtoranta et al. 2013). Moreover, the infants who survive the intrauterine diabetic condition have a possibility of developing congenital malformation and cardiomyopathies that predispose to cardiac dysfunction later in life (Depla et al. 2021, Hoodbhoy et al. 2019).

GDM causes cardiac foetal functional impairments even in the absence of detectable structural changes. These functional alterations include changes in heart rate and impaired ventricular filling, which predispose the foetal cardiac dysfunction. Cardiac foetal diastolic dysfunction has been detected in the earliest days of foetal doppler ultrasound in mothers with GDM (Hatém et al. 2008). As such, alterations in foetal cardiac function are correlated with neonatal morbidity (Bhorat, Pillay, and Reddy 2018). The alterations in foetal cardiac function have been observed previously in the first trimester of pregnancy in foetuses of diabetic mothers in comparison with non-diabetic controls (Russell et al. 2008).

An initial marker of foetal cardiac dysfunction in mothers with GDM could be the foetal heart rate, which observed to be higher in foetuses from diabetic mothers with poor glycaemic control (Costa et al. 2009). In addition, foetal cardiac arrhythmias have been diagnosed in 1–3% of pregnancies (Aggarwal, Czaplicki, and Chintala 2009). The disturbances in the electrical conduction system of the heart also include alterations in the gap junction proteins, which play a key part in intercellular impulse transmission within the myocardium. Gap junctions in the heart consist of proteins called connexins (Cxs), which are expressed in the adult myocardium (van Kempen et al. 1991) and have been linked to electrophysiological defects in adult diabetic hearts (Howarth, Nowotny, et al. 2007). The remodelling of the gap junction proteins is likely to occur in Cx 43 (Lin et al. 2006) since it has been demonstrated in previous studies in an adult diabetic model that there is an association between structural remodelling of such Cxs and development of cardiac arrhythmias in the adult diabetic heart (Howarth et al. 2008, Howarth, Nowotny, et al. 2007). However, whether the

developing heart exposed to diabetic conditions could show changes in the gap junction protein is still unknown.

The basis for cardiac complications in diabetes mellitus either in adult or in foetal hearts occur through a maladaptation process called cardiac remodelling. Pathological cardiac remodelling is a group of cardiac cellular, and interstitial changes that leads to modifications in cardiac structure and function. The pathological cardiac remodelling occurs in response to a pathological stimulus such as diabetes (Sekaran et al. 2017). Cardiac remodelling changes can occur in various cardiac tissue such as cardiomyocytes, ventricular myocardium, intestinal matrix, vascular and smooth muscle cells. Cardiomyocytes are the functional component of the heart, and are the key elements of cardiac health and disease (Fountoulaki, Dagres, and Iliodromitis 2015).

1.3.3 Foetal cardiac remodelling

Although cardiac remodelling is often diagnosed in adults, the foetal heart is more susceptible to damage when exposed to a pathological factor such as diabetes mellitus (Rizzo et al. 2020). In addition, babies of mothers with GDM are at a higher risk for cardiovascular disease and death in later life because of cardiac remodelling that disturbs the myocardium affecting cardiac structure and ventricular function (Garg et al. 2014).

During the development of the heart, several cardiac progenitor cells contribute to the different cardiac cell types (Schleich et al. 2013). GDM is correlated with alterations in the expression of the genes controlling normal cardiac development, which cause disturbances in the differentiation of tissue such as the cardiac ganglia (Kumar, Dheen, and Tay 2007). Cardiac development occurs from mesoderm layer, which is identified as the first heart fields, second heart fields lineages, the migrating neural crest cells and epicardial cells for heart morphogenesis (Brade et al. 2013). Cardiogenesis begins from specification of cardiac progenitor cells, which promote the major portions of heart development. Subsequently, after cardiomyocyte lineage

specification, the developed cardiomyocytes undertake proliferation and terminal differentiation to generate fully differentiated functional cardiomyocytes (Kelly, Buckingham, and Moorman 2014). The neural crest originating from the neural plate border, is a group of pluripotent cells that go through induction, maintenance, differentiation, migration, and can contribute to almost every organ system in vertebrates including the heart (Hall 2008).

Cardiomyocytes proliferate rapidly during foetal life, but the proliferation ends after birth (Lopaschuk, Spafford, and Marsh 1991) when the cardiomyocytes exit the cell cycle and become terminally differentiated cells, thereby being unable to divide. These cells therefore respond to pathological stimuli by increasing in size rather than increasing in number (Anversa, Ricci, and Olivetti 1986). The developing cardiomyocytes also respond to pathological stimuli by altering their gene expression through the reactivation of foetal genes programme. Such foetal genes include the production of defective cellular elements that result in ineffective tissue proliferation and differentiation (Gidh-Jain et al. 1998). The reactivation of the foetal genes programme is indicated by the induction of mRNA for genes such as the glucose transporter isoform and α-myosin heavy chain (Depre et al. 2000). The re-activation of foetal genes induces abnormal cell growth through alteration in protein synthesis resulting in cardiomyocyte hypertrophy (Lauriol et al. 2014). These maladaptive changes eventually lead to adverse ventricular remodelling via increased mechanical stress, initiation of aberrant signalling and impaired contractility function, which all finally cause heart failure (Yung et al. 2004). Therefore, understanding the cellular remodelling changes in diabetes, especially in developing cardiac cells may facilitate preventative treatment of heart failure.

1.3.4 Mechanisms underlying foetal cardiac remodelling in GDM

GDM is associated with several disturbances that lead to cellular remodelling especially in the developing cardiac cell. Such factors include general metabolic disturbances like lipid disorders, insulin insufficiency and hyperglycaemia. Among

these factors, hyperglycaemia causes significant alteration especially at the cellular level. Although high maternal glucose concentration is linked with foetal heart problems, the cellular and subcellular consequences of GDM on embryonic heart development is still unknown. Therefore, investigation of the mechanisms leading to diabetic developmental cardiac pathology might be a starting point for establishing preventative and treatment protocols. The mechanisms connecting compromised molecular signalling to congenital heart diseases in babies of diabetic mothers are becoming of increasing interest.

1.3.4.1 Role of insulin resistance

Insulin resistance in diabetes is one of the pathological factors that precipitates pathological cardiac cellular remodelling either in the adult or in the foetal heart. Foetal hyperinsulinemia has been observed in infants of a diabetic mothers intrauterine (Weiss et al. 2000), and after birth by sampling of umbilical cord blood (Dornhorst et al. 1994). Foetal insulin production seems to be linked to the level of metabolic irregularity in the foetus and is prognostic of compromised glucose tolerance and obesity in later life (Lindsay et al. 2003). Insulin resistance is expected to allow the foetus to get a sufficient supply of glucose by shifting the maternal energy metabolism from carbohydrates to lipids (Di Cianni et al. 2003). Hyperglycaemia in the blood returning from mother to foetus through the placenta activates insulin secretion in the foetus, which enhances cardiac foetal septal hypertrophy (El-Ganzoury et al. 2012). Foetal hyperinsulinaemia increases glucose transport from diabetic mother across the placenta (Paauw et al. 2020) and triggers the increased expression of insulin receptors and foetal organomegaly in the heart and other insulin-sensitive tissues (Boucher, Kleinridders, and Kahn 2014). Foetal hypertrophic cardiomyopathy is also triggered by foetal hyperinsulinemia and insulin-like growth factors that enhance hypertrophy in cardiomyocytes (Hagemann and Zielinsky 1996), thereby predisposing to proliferation and hypertrophy of cardiac cells (Buchanan and Kitzmiller 1994).

1.3.4.2 Role of lipid disorders

The alterations in the lipid metabolism of new-born babies of diabetic mothers could predispose to development of coronary heart diseases later in life (Eslamian et al. 2013). Hyperglycaemia is linked to reduced free fatty acid oxidation and increased glucose oxidation, which enhances accumulation of triglycerides, thus inducing lipid toxicity. Aberrant metabolic pathways have been recognized as the main mediators of teratogenesis in mouse embryos, involving modified metabolism of inositol, arachidonic acid, and prostaglandins (Baker et al. 1990). In addition, hyperglycaemia enhances low density lipoprotein oxidation in the adult heart through the superoxide-dependent pathway, which leads to free radical production (Kawamura, Heinecke, and Chait 1994). Compared to the adult heart, the foetal heart utilizes mostly glucose and lactate as source of energy, instead of fatty acids. GDM with poor glycaemic control triggers transport of lipids from mother to foetus, leading to hyperlipidaemia (Merzouk et al. 2000). Postnatally, the infant heart shows increased expression of some genes implicated in triglyceride and fatty acid metabolism (Lehman and Kelly 2002). Furthermore, it has been proposed that maternal obesity could be a risk factor for foetal congenital heart disease, independent of diabetes mellitus (Madsen et al. 2013). Incidentally, it has been shown in a previous study that the increased lipid and glucose indicators in diabetic mother are closely connected to impaired cardiac ventricular function in neonates of diabetic mothers (Cade et al. 2017).

1.3.4.3 Role of hyperglycaemia

Hyperglycaemia has been shown to induce pathological cardiac remodelling during early embryological heart developmental stages through factors such as oxidative stress, modulation of gene expression, cellular apoptosis, and protein modifications (Floris et al. 2015, Han et al. 2015). The foetal response to maternal hyperglycaemia is dependent on several factors such as the period of cardiac development, severity of hyperglycaemia, metabolic disorders, and genetic susceptibility. In GDM, glucose is transported through the placenta by a facilitated glucose transporter protein, which induces an increase in foetal blood glucose levels (Ericsson et al. 2007). The

interpretation of the molecular mechanisms of hyperglycaemia-induced cardiac embryopathy is still being explored. Several previous studies have reported that hyperglycaemia is the main risk factor for GDM-induced foetal cardiac damage (Devereux et al. 2000, Rubler et al. 1972). Exposure of cardiac neural crest cells to high glucose caused congenital heart defects in 82% of chick embryos. The malformations identified in chick embryo were in the outflow tracts and pharyngeal arch arteries that develop from neural crest cells (Roest et al. 2007). It has been reported that even mild increases in maternal serum glucose are linked with congenital heart defect in infants from diabetic mothers (Priest et al. 2015). Maternal hyperglycaemia causes an enhanced glucose metabolism in the developing foetus that could modify several molecular chain reactions including changed cell lipid metabolism and increased production of reactive oxygen species (ROS), which induces oxidative stress and subsequently increases the risk of foetal malformations (Chang et al. 2003). In addition, high glucose causes activation of various proteins engaged in cell death and alternative metabolic signalling pathways (Zhao et al. 2009).

Induction of oxidative stress

Oxidative stress is a condition of enhanced production of ROS or the impairment of the antioxidant system. The increased ROS causes significant cardiovascular tissue damage, as it causes cellular alterations via multiple mechanisms such as oxidation and modulation of intracellular signalling pathways (Kwon et al. 2003). The rise in ROS levels in hyperglycaemia could be a consequence of a decrease in destruction or/and rise in the production of catalase (enzymatic/non-enzymatic). The difference in the levels of these enzymes leads to increased vulnerability of the tissue to oxidative stress damage leading to development of cardiac impairment (Lipinski 2001). In particular, maternal hyperglycaemia also causes suppression of the endogenous antioxidant activity in the developing foetus (Li et al. 2011). In hyperglycaemia, ROS formation occurs by non-enzymatic glycation of proteins, glucose oxidation and enhanced lipid peroxidation causing the impairment of enzymes, cellular activities, and increased insulin resistance due to oxidative stress (Maritim, Sanders, and Watkins 2003). In a hyperglycaemic environment, the foetus

increases its oxidative metabolism, causing foetal hypoxaemia (Teramo 2010). In blood vessels, enhanced oxidative stress can lead to harmful vessel hyper-reactivity, vascular smooth muscle cell proliferation, platelet activation, and lipid peroxidation, which all eventually cause vascular complications (Maytin, Leopold, and Loscalzo 1999). Maternal hyperglycaemia associated with reduced levels of an essential intracellular antioxidant, glutathione (El-Bassiouni et al. 2005), which could predispose the developing foetus to oxidative stress damage. The efficiency of using antioxidant treatment to prevent GDM-induced neural tube and heart defects has been demonstrated previously (Al Ghafli et al. 2004, Yang and Li 2010). However, information concerning the role of antioxidants in diabetes-induced changes in early cardiac cellular development is limited.

The principal factor leading to enhanced mitochondrial ROS production is the redox state of the respiratory chain. The mitochondrial dysfunction in diabetes mellitus occurs due to disturbances in the mitochondrial proteins involved in fission and fusion, which are essential active processes that regulate normal morphology of mitochondria in the cell (Sesaki and Jensen 1999). Irregularities in fission and fusion predispose to cardiac cellular apoptosis (Cassidy-Stone et al. 2008). These processes involve several proteins, involving mechanical enzymes which alter mitochondrial membranes, and regulatory proteins that regulate the communication of these mechanical proteins together with organelles. Among these proteins, the mitochondrial GTPase, optic atrophy1 (OPA1) plays an important part in normal mitochondrial fusion, structure, and function. The dynamin related OPA1, situated on the inner mitochondrial membrane, protects the cell from apoptosis by inhibiting the release of cytochrome c from the mitochondria (Frezza et al. 2006). It has been shown that the condition of heart failure is linked to decreased OPA1 in the adult heart and with increased cardiac cell apoptosis, contributing to the progression of heart failure (Chen et al. 2009). A previous study done by Ding et al (Ding et al. 2020) suggested that OPA1 plays a part in modifying the progression of adult diabetic cardiomyopathy. However, the role of OPA1 in developing cardiac cells exposed to hyperglycaemia is still unknown.

The enhanced production of mitochondrial ROS also disturbs endogenous antioxidant activities, activate caspase3/8-dependent apoptosis and decreases cell proliferation in embryonic hearts exposed to maternal diabetes (Sivan et al. 1997, Wang, Reece, and Yang 2015). Previous studies have reported that, GDM triggers oxidative stress and stimulates pro-apoptotic kinase signalling pathways, leading to disturbances in cell proliferation and apoptosis and resulting in defective cardiogenesis (Wang, Reece, and Yang 2015, Yang et al. 2015). The Wnt signalling pathway is one of the most important developmental signalling pathways and has been shown to play an essential role for embryogenesis. Alterations in the Wnt signalling pathway could lead to congenital heart diseases similar to those detected in human diabetic pregnancies (Lin et al. 2007, Schleiffarth et al. 2007). Eriksson and colleagues observed that the supplementation of the free oxygen radical scavenging enzyme, superoxide dismutase in cultured rat embryos protected against the teratogenic effects of hyperglycaemia (Eriksson and Borg 1993).

Oxidative stress also leads to several changes in cardiac tissue such as modifications in gene expression (Cheng et al. 1999), modulation of extracellular matrix (Siwik, Pagano, and Colucci 2001), activation of different cellular hypertrophy kinases and transcription factors such as protein kinase C (Cheng et al. 2005), and cellular apoptosis (von Harsdorf, Li, and Dietz 1999). In addition, oxidative stress causes endothelial dysfunction and impaired production of nitric oxide (Hink et al. 2001). The excess ROS also triggers matrix metalloproteinases, which are proteolytic enzymes that enhance the production and deposition of collagen by cardiac fibroblasts, thereby promoting the development of myocardial fibrosis (Siwik, Pagano, and Colucci 2001). ROS also impairs the contractile function of the heart through alteration of proteins included in excitation–contraction coupling processes. ROS can also modulate Ca^{2+} handling via the stimulation of L-type Ca^{2+} channels and the inhibition of Ca^{2+} uptake by the Ca^{2+} ATPase in the sarcoplasmic reticulum (Zima and Blatter 2006). However, whether oxidative stress could be implicated in early developing cardiac cells disturbances as a result of hyperglycaemia still needs to be clarified.

Disturbances in cellular metabolism

Hyperglycaemia-induced disturbances in cardiac metabolism and mitochondrial dysfunction are mechanisms proposed to underlie diabetic cardiomyopathy (Lee et al. 2015). Mitochondrial dysfunction and reduced adenosine triphosphate are associated with increased oxidative damage through elevated hydrogen peroxide production and decreased glutathione levels (Ghosh et al. 2005). In addition, mitochondrial dysfunction causes the release of pro-death factors such as cytochrome c and, apoptosis-inducing factor (Cai et al. 2002). Defects in the energy metabolism of the heart leads to a decrease in the energy consuming processes and consequently disturbs cardiac contractile activity. In normal conditions, fatty acids and carbohydrates are the main sources used by mitochondria for energy production (Stanley, Recchia, and Lopaschuk 2005), but hyperglycaemia is linked to alterations in the metabolism of glucose due to decreased glucose transporters such as GLUT1 and 4, both of which are regulated by insulin (Russell et al. 1998). The modifications in cardiac mitochondrial oxidative metabolism can also be mediated through changes in the level of gene transcription by peroxisome proliferator activated receptor (PPAR). PPARs are a family of ligand activated transcription nuclear factors, which play a role in controlling glucose and lipid homeostasis (Barger and Kelly 2000). PPAR expression is enhanced in hyperglycaemic conditions, which suggest that it may have a role in diabetic cardiomyopathy (Lee, Kao, et al. 2011).

Hyperglycaemia causes the activation of various metabolic signalling pathways involved in the pathogenesis of diabetic cardiovascular diseases. Such pathways involve the polyol pathway, which contributes to 3% of glucose flux in cells under normal conditions. However, in hyperglycaemia about 30% of glucose enters through the polyol pathway causing tissue destruction via enhancement of ROS production and reduced levels of nitric oxide production (Obrosova et al. 2005, Tang, Martin, and Hwa 2012). The pentose phosphate pathway inhibits cardiomyocyte maturation both in *in-vitro* models of embryonic stem cell-derived cardiomyocytes and in *in-vivo* models of murine diabetic hearts (Nakano et al. 2017). Hyperglycaemia also increases the activation of the protein kinase pathways that control intracellular signalling transduction such as growth factor signalling and endothelial activation.

The increased activation of the protein kinases leads to an alteration in the expression of specific cytokines such as TGF-β and connective tissue growth factor, both of which are involved in the progression of cardiac fibrosis (Way et al. 2002). Moreover, the impairment of the protein kinase pathway incudes the Akt signalling pathway, a signal transduction pathway promoting survival of the cardiac cells through regulation of cellular metabolism, protein synthesis, and glucose uptake (Yao, Han, and Han 2014). The impaired activation of Akt pathway leads to increased signalling activity and the modulation of several factors such as GSK-β, which enhances hypertrophic growth of the heart (Aoyagi and Matsui 2011).

Hyperglycaemia causes shifting of glucose into the hexosamine biosynthetic pathway (HBP), which is responsible for many of the manifestations of hyperglycaemia-induced cardiomyopathy (Kolm-Litty et al. 1998). The HBP pathway is a glycolytic pathway, incorporating 3% of total glucose utilized (Marshall, Bacote, and Traxinger 1991). The major by-product of the HBP pathway is UDP-N-acetylglucosamine, a substrate for *O*-GlcNAc transferase that catalyses the reversible O-GlcNAcylation of serine and threonine residues of various cytosolic and nuclear proteins. The activation of the HBP pathway by hyperglycaemia causes changes in both gene expression and protein function, which together predispose to the pathogenesis of diabetic complications such as diabetic nephropathy (Schleicher and Weigert 2000). The HBP pathway also has a significant role in hyperglycaemia- induced insulin resistance (Buse 2006) and is linked to diabetic complications as it causes inhibition of eNOS activity by hyperglycaemia-produced *O*-acetyl glucosaminylation at the Akt site of the eNOS protein (Du et al. 2001). However, there is limited evidence in previous literature regarding the role of these pathways in the pathogenesis of hyperglycaemia-induced developing cardiac cell alterations.

Degenerative and proliferative changes

Hyperglycaemia is associated with several degenerative or proliferative changes that lead to cardiac cellular alterations. Such changes include post-translational modifications of several intracellular and extracellular proteins/molecules such as

formation of advanced glycation end products (AGEs), matrix deposition and interstitial fibrosis, which all predispose to cardiac cellular hypertrophy and cell death. In addition, hyperglycaemia causes mitochondrial dysfunction and energy deficit, which all leads to cardiac dysfunction.

Post-translational modifications

Hyperglycaemia is associated with post-translational modifications such as the formation of AGEs, which are important contributors to hyperglycaemia-induced cardiac cellular injury. The AGEs are a heterogeneous group of molecules formed through a process known as glycation and occurs due to a non-enzymatic series of irreversible reactions between glucose and plasma proteins (Basta, Schmidt, and De Caterina 2004). The accumulation of AGEs inside the cell causes an alteration in the function of intracellular proteins as well as activation of intracellular signalling pathways such as enhanced production of free radicals leading to cellular damage (Yan et al. 1994). Furthermore, the AGE-induced cardiomyocyte dysfunction in a diabetic heart is coupled with disturbances in the mitochondrial membrane depolarization and decreased inactivation of GSK-β factor, which together enhance the hypertrophic growth of the heart and impaired cardiac contractility (Ma et al. 2009). The deposition of AGEs causes the upregulation of transforming growth factor (TGF), which leads to induction of fibrosis (Striker and Striker 1996), as well as to derangements in enzymatic function of sarcoplasmic reticulum (Bidasee et al. 2004).

Furthermore, the AGE products cause cellular damage through reaction with their specific receptors called receptors of AGE (RAGE), which are expressed in several cell types such as cardiomyocytes and vascular cells (Brett et al. 1993). RAGE stimulate intracellular oxidative stress through activation of NADPH oxidase and inhibition of nitric oxide is well defined in a diabetic condition where both receptor expression and AGE ligand availability are highly expressed (Jandeleit-Dahm and Cooper 2008). The AGE-RAGE interactions have an important role in cardiac dysfunction and pathogenesis of several cardiac structural and electrical alterations. These interactions have been shown to depress sarcoplasmic/endoplasmic reticulum Ca^{2+}-ATPase (SERCA) activity and participate in pathogenesis of diabetic

cardiomyopathy (Arai 2002). In addition, the accumulation of AGEs in the extracellular matrix causes myocardial stiffness and impaired cardiac performance (Deluyker, Evens, and Bito 2017). The AGE-RAGE interactions also cause the release of pro-inflammatory cytokines and free radicals and activation of pleiotropic transcription nuclear factors, which all induce an isoform shift of the normal contractile protein myosin heavy chain (α-MHC) to the impaired β-MHC isoform (Aragno et al. 2006).

Interstitial fibrosis is one of the underlying causes of cardiac cellular derangements. It occurs due to activation of cardiac fibroblasts, which increases production and accumulation of types I and III collagen fibres in the myocardium (Weber 1997). The extracellular collagen composition is controlled through the equilibrium between collagen synthesis and degradation, which are mediated by matrix metalloproteinases and their inhibitors. In addition, the accumulation of AGEs in the extracellular matrix leads to the modification of extracellular proteins leading to cardiac fibrosis, which causes myocardial stiffness and impaired cardiac performance (Deluyker, Evens, and Bito 2017). There is an increase in the activity of matrix metalloproteinases in diabetic cardiac tissue and in the cardiac tissue culture model exposed to high glucose that was reported to be due to ROS formation (Uemura et al. 2001). In addition, transforming growth factor beta1 (TGF-β1) performs an essential role in the modulation of fibroblasts and alterations of gene expression that induces interstitial fibrosis (Rosenkranz et al. 2002). The TGF-β over-expression has been observed in cardiac hypertrophy associated with interstitial fibrosis and in hyperglycaemia (Way et al. 2002, Westermann et al. 2007). Interstitial fibrosis leads to abnormal electrical conduction in the heart causing reduced conduction velocity (Miragoli, Gaudesius, and Rohr 2006).

Cardiac cellular hypertrophy

Cardiac cellular hypertrophy is one of the consequences of proliferative changes due to hyperglycaemia. The increased activation of the calcineurin and nuclear factor of activated T-cell (NFAT) signalling pathway has been implicated in the pathological

hypertrophic growth of the myocardium. The activation of this pathway within the cardiomyocyte depends on the intracellular Ca^{2+} concentration (Wilkins et al. 2004), the Ca2+-dependent calcineurin dephosphorylates NFAT and cause it translocate into the nucleus to stimulate gene expression (Heineke and Molkentin 2006). This pathway is associated with stimulation of the foetal gene program and the induction of cardiac hypertrophy and cardiac arrhythmias (Zhao et al. 2016). Furthermore, the Ca^{2+}/calcineurin-NFAT signalling regulates the cardiac hypertrophic response in coordination with another pathway, such as protein kinase C or mitogen-activated protein kinases (Molkentin 2004).

TGF-β is known to play a crucial role in the early stages of embryonic cardiac development (Bartram et al. 2001). Maternal hyperglycaemia has been reported to suppress TGF-β signalling in the exposed embryonic hearts by downregulating the expression of its receptors such as TGF-β receptor. In addition, maternal hyperglycaemia is also associated with phosphorylation of downstream effectors such as mothers against decapentaplegic (Smad2/3), which may contribute to hyperglycaemia-induced cardiac defects (Wang, Reece, and Yang 2015). The induction of TGF-β expression in diabetic hearts could be mediated via activation of angiotensin II (Toblli et al. 2005), or through the direct actions of hyperglycaemia on the activation and secretion of TGF-β transcription factor (Ziyadeh et al. 1994). The AGE-RAGE interactions are also known to induce fibrosis through upregulation of TGF-β (Striker and Striker 1996). However, the role of post-translational modification in the pathogenesis of hyperglycaemia-induced cardiac cell development changes are still unclear.

Cardiac cell death

Cardiomyocyte death triggers a reduction in myocardium performance and ventricular dilation (Frustaci et al. 2000) and plays a significant role in the development of diabetic cardiomyopathy (Cai et al. 2006). The cardiac tissue of diabetic patients has been shown to have greater numbers of apoptotic cardiomyocytes, endothelial cells, and fibroblasts, in comparison to that in non-diabetic subjects (Frustaci et al. 2000). However, whether cell death could occur in

early development of cardiac cells is still unknown. Myocardial cell death is a significant determinant of cardiac pathogenesis during hyperglycaemia as it leads to damage of contractile units, conduction disturbances, hypertrophy of cardiac cells, and fibrosis (Kang 2001).

Types of cell death

Based on cellular morphological changes three main forms of cell death have been distinguished including apoptosis, autophagy, and necrosis (Dyntar et al. 2006, Frustaci et al. 2000). Autophagy is a self-degradative process characterized by accumulation of vacuoles in the cytoplasm and encapsulated cytoplasmic material and consequent lysosomal degradation (Axe et al. 2008). Necrosis is unprogrammed cell death (caused by factors external to the cells), and characterized by cytoplasmic swelling, dilation of organelles, rupture of cell membranes and leakage of cytoplasmic content (Proskuryakov, Konoplyannikov, and Gabai 2003). Apoptosis is a process of programmed cell death (cell death mediated by intracellular program) characterized by alterations in cellular morphology. Because of its link with diabetes, for the purposes of this project, apoptosis will be further discussed in depth.

The cellular apoptosis features include shrinkage of the cell, cell membrane blebbing, formation of apoptotic bodies and nuclear changes such as chromatin condensation and DNA fragmentation (Trump et al. 1997). Furthermore, hyperglycaemia-induced cardiac cell apoptosis has been also reported in several *in-vitro* studies using cultured endothelial cells (Baumgartner-Parzer et al. 1995) and smooth muscle cells (Peiró et al. 2001), as well as cardiomyocytes (Shizukuda, Reyland, and Buttrick 2002). Generally, apoptosis is initiated by the activation of family of proteases known as cysteine aspartyl-specific proteases (caspases), included in the proteolysis of proteins, which cause biochemical and morphological alterations, which are characteristic of cellular apoptosis. There are two main pathways of cellular apoptosis: the extrinsic and intrinsic apoptotic pathways. The intrinsic pathway also identified as mitochondrial-dependent pathway of apoptosis is triggered by intracellular stimuli that act on several targets within the cell result in release of proteins from mitochondria. The mitochondria-dependent pathways include

generation of ROS and oxidative stress damage (von Harsdorf, Li, and Dietz 1999). Mitochondrial proteins such as cytochrome c, which is associated in the inner membrane of the mitochondria, is a component of the electron transport chain in the mitochondria. In addition, cytochrome c is implicated in the initiation of apoptosis when released into the cytoplasm. It binds apoptotic protease triggering factor-1 to create a complex, which works as a platform for the cleavage and activation of downstream caspases caspase-9 and -3 pathways (Henderson et al. 2005).

Previous studies have been shown that the hyperglycaemia-increased release of mitochondrial protein cytochrome c into the cytoplasm and enhanced activity of cleaved caspase-3 in cell culture condition under high glucose level (Feng et al. 2018) and in an adult diabetic animal model (Cai et al. 2002). The caspases are a family of protease enzymes that plays an essential function in programmed cell death and inflammation. These enzymes are produced as zymogens that are activated after cleavage of their prodomains (Nicholson and Thornberry 1997). The activation of caspases occurs through different pathways and includes the involvement of mitochondria, which release caspase activating proteins into the cytoplasm, thereby triggering apoptosis (Green and Reed 1998). There are two sets of caspases, the initiator and the executioner caspases (Elmore 2007). After cell injury occurs, the initiator caspases (caspases 8 and 9) are activated from inactive procaspases and activate the executioner caspases (caspases 3, 6 and 7). The stimulation of executioner caspases initiates a cascade of events that cause DNA fragmentation, damage of the nuclear proteins and cytoskeleton and development of apoptotic bodies (Martinvalet, Zhu, and Lieberman 2005, Poon et al. 2014).

B-cell lymphoma 2 (Bcl-2) is a family of regulatory proteins that regulate the intrinsic pathway of cellular apoptosis through preventing (anti-apoptotic) proteins such as Bcl-2 and Bcl-XL or inducing (pro-apoptotic) proteins such as Bax, Bak and Bad. The relationship between the apoptotic and anti-apoptotic proteins regulates the cell cycle through mitochondrial regulation. In addition, the stability between pre-apoptotic and anti-apoptotic factors controls the survival of the cells and the process of apoptosis (Hengartner 2000). Bcl-2 is in the outer membrane of mitochondria, where it has a

significant role in helping cellular survival and preventing the actions of pro-apoptotic proteins. The pro-apoptotic proteins induce apoptosis through their action on the mitochondrial membrane to promote permeabilization and release of cytochrome c and ROS (Oltvai, Milliman, and Korsmeyer 1993). The Bcl-2 -associated X protein (BAX) was recognized by its homologous binding to Bcl-2 that enhances apoptosis in response to stress stimuli (Oltvai, Milliman, and Korsmeyer 1993). The balance between the apoptotic and anti-apoptotic proteins regulates the cellular life cycle through mitochondrial function. The ratio of Bcl-2 to Bax known as “death switch” is frequently recognized as an indicator of apoptosis. A rise in this ratio is used to indicate reduction of the apoptotic process, while a decrease in the ratio implies exacerbation of the apoptotic process. However, whether there is increased cardiac cellular apoptosis in developing cardiac cells exposed to hyperglycaemia requires further exploration.

The extrinsic pathway of cellular apoptosis, also recognized as the death receptor pathway, is stimulated by extracellular receptors binding to the cell-surface called death receptors. Death receptors such as Fas are members of the tumour-necrosis factor receptor family which activate apoptosis upon ligand binding (Tartaglia et al. 1993). Once ligands bind to their particular death receptors, the death domains attract the intracellular adaptor protein, which subsequently activates the signalling cascade of the caspase protease family (Salvesen and Dixit 1997). The caspases that are involved in the formation of this death-inducing signalling complex include caspase-8 and caspase-10, which are both cleaved and produce active initiator caspases (Kischkel et al. 2001, Sprick et al. 2000).

The association between cellular proliferation and cell death might correspondingly reveal the fact that cells require survival signals. Deficiency of these indicators causes apoptosis, a phenomenon named ‘death by neglect’. Survival signals consist of hormones, growth factors, cytokines, and additional stimuli, such as the signal induced by adhesion molecules. The survival signals are facilitated via phosphatidylinositol 3-kinase (PI3K)/AKT pathway (Yao and Cooper 1996). The PI3K plays critical roles in many biological cellular activities such as cytoskeletal

organization, cell survival, and apoptosis (Toker and Cantley 1997), with Akt being its most well-known downstream target (Chan, Rittenhouse, and Tsichlis 1999). In addition, AKT has an anti-apoptotic role by inhibiting the release of cytochrome c and apoptosis enhancing factors from mitochondria (Kim et al. 2004). Meng and collaborators (Meng et al. 2017) have proposed that diabetes mellitus could induce neuronal apoptosis in the cerebral cortex through downregulating AKT phosphorylation. In the diabetic heart, the blockage of the PI3K/Akt pathway reduced the expression of eNOS and mTOR, which are both proteins that may regulate the level of apoptosis (Chen et al. 2014). These findings were corroborated by Wang et al (Wang et al. 2019) who showed that the PI3K/Akt signalling affects the anti-apoptotic pathway in a cardiac cell line exposed to high glucose in cell culture conditions.

Excitation- contraction coupling alterations

The coupling between excitation and contraction in cardiomyocytes is mediated through a Ca^{2+} induced Ca^{2+} release mechanism. In cardiac cells, the arrival of electric signals at the sarcolemma causes Ca^{2+} from the extracellular space to enter cardiac cell through voltage-gated L-type Ca^{2+} channels. The entry of Ca^{2+} induces Ca^{2+} release from the sarcoplasmic reticulum through ryanodine receptor type (RyR), and this action is overall referred to as Ca^{2+} induced Ca^{2+} release. The resulting transient increase in intracellular Ca^{2+} concentration can be recorded as Ca^{2+} transient, a vital event in the regulation of the contraction and relaxation of cardiomyocytes. The intracellular Ca^{2+} binds to the myofilament protein troponin C, a molecule of the thin filament of the sarcomere, triggering myocardial contraction. To activate myocardial relaxation, Ca^{2+} is then withdrawn from the sarcoplasm via Ca^{2+} reuptake into the sarcoplasmic reticulum, which is intermediated by SERCA and Na^{+}/ Ca^{2+} exchanger, both being the main Ca^{2+} re-uptake pathways (Bassani, Bassani, and Bers 1994).

It has been shown that the cardiac contractile dysfunction is underlined by Ca^{2+} transient prolongation and changed intracellular Ca^{2+} handling. In addition, the expression of the RyR is decreased, which is closely linked with the development of

hypertrophic remodelling in adult heart (Engelhardt et al. 2001). Changes in the concentration of extracellular Ca^{2+} causes weakening of cell junctions that reserve myocardium tissue integrity leading to arrhythmogenic cardiomyopathy (Moccia et al. 2019). In adult diabetic cardiomyocytes reduced SERCA action and Ca^{2+} sequestration, as well as impaired Na^{+}/Ca^{2+} exchange function was observed (Hattori et al. 2000). In early stages of heart development, it has been shown in the model stem cell derived-cardiomyocytes, the early use of RyR-sensitive stores, and they show rhythmic internal Ca^{2+} transients (Viatchenko-Karpinski et al. 1999). Later developmental stages of the heart require RyR for spontaneous beating (Yang et al. 2002). In addition, a developmental study in stem cell derived cardiomyocytes confirmed the presence of a functional sarcoplasmic reticulum by showing spontaneous local Ca^{2+} events and raised Ca^{2+} release in response to caffeine stimulation as a function of RyR response to *in-vitro* differentiation (Sauer et al. 2001). However, these changes are unknown in developing cardiac cells exposed to hyperglycaemia.

Ca^{2+} overload has been implicated as one of the main causes of cardiomyocyte alterations and cardiac contractile dysfunction (Luo and Anderson 2013). The condition of abnormal depolarization in an adult diabetic heart has been presumed to occur under conditions of Ca^{2+} overload and leads to cardiac arrhythmias (Nordin, Gilat, and Aronson 1985). In addition, Ca^{2+} overload activates Ca^{2+} dependent pathways that mediate maladaptive cardiac remodelling, such pathways include calcineurin-NFAT translocation and activation of other hypertrophic cascade pathways within the cardiomyocytes (Wilkins et al. 2004). Furthermore, Ca^{2+} overload activates the process of cellular cytotoxicity and apoptosis (Kumar, Kain, and Sitasawad 2012). However, the role of Ca^{2+} in hyperglycaemia-induced changes in the developing cardiac cell is still unknown.

It has been shown in previous studies that diabetes mellitus is accompanied by a reduction in the activities of Ca^{2+} ATPase of cardiac myofibrils and myosin isozymes in adult heart (Rupp, Elimban, and Dhalla 1989). The reduced activity of the ATPase of cardiac myofibrils plays a significant role in the development of cardiac contractile

dysfunction and occurs secondary to down-regulation of myosin isoforms and phosphorylation of the contractile proteins leading to cardiac hypertrophy and atrophy in a diabetic heart (Dillmann 1980, Liu, Takeda, and Dhalla 1997). Furthermore, diabetes mellitus is linked with increased phosphorylation of cardiac myofilaments troponin I, without alterations in its gene expression in the adult diabetic heart (Liu, Takeda, and Dhalla 1996). Diabetes mellitus is also connected with decreased activity of SERCA, which results in decreased relaxation in the adult diabetic heart (Ganguly et al. 1983). It has been shown that the Ca^{2+} could control the process of cardiac cell differentiation and heart development (Porter, Makuck, and Rivkees 2003). However, the role of Ca^{2+} in cardiogenesis, especially in pathological conditions such as hyperglycaemia is a complicated process to study especially at the molecular level. It would therefore be invaluable to use the appropriate study model to evaluate early developmental cardiac cellular changes.

1.4 Mouse embryonic stem cells as a tool for cardiac developmental remodelling studies

A main limitation in understanding the cellular mechanisms underlying foetal cardiac remodelling in GDM is the lack of an experimental model that recapitulates the developmental- and pathological changes occurring during the primary stages of cardiac cellular development. Fully differentiated adult cardiomyocytes have a low regenerative capacity (Steinhauser and Lee 2011), and therefore they do not allow the investigation of intermediate cellular developmental processes. In addition, adult cardiomyocytes do not survive for long period *in-vitro* such as cell culture conditions where they undergo spontaneous remodelling (Nag, Lee, and Sarkar 1996). On the contrary, stem cells such as mouse embryonic stem cells (mESC) proliferate physiologically and can differentiate into specific cell types such as cardiomyocytes. In addition, stem cells that undergo cardiac differentiation remain stable under cell culture conditions (Wobus et al. 2002). Furthermore, *in-vitro* mESC-derived cardiomyocytes have been confirmed as one of the cardiac cellular models that help

to evaluate the mechanisms of the cardiotoxicity (Shi et al. 2020) and therefore could be a useful model for studying cardiac glucotoxicity.

The emergence of stem cell differentiation models provides a good tool to study changes during early tissue development (Robbins et al. 1990). Embryonic stem cells (ESC) originate from the inner cell mass of blastocysts and can differentiate into all three primary embryonic germ layers including the mesoderm from which the heart development occurs (Thomson et al. 1998). ESCs are pluripotent, which indicate that they can proliferate indefinitely and have the capacity to differentiate into different cell lineages including cardiomyocytes (Guasch and Fuchs 2005). ESC-derived cardiomyocytes not only provide an *ex-vivo* basis of cardiomyocytes for cell-based heart therapies, but also are a useful model for studying cardiac development. In addition, stem cells form a good model for studying early normal and pathological cardiac developmental processes. The stem cells differentiation culture system into cardiomyocytes has been commonly used as a model to study the early stages of cardiogenesis (Robbins et al. 1990). Moreover, the *in-vitro* stem cell differentiation into cardiac cells could provide a valuable model to analyse the differentiation process in order to understand the mechanisms of cellular remodelling via the creation “Disease-in-a-dish” models (Ballo, Greenberg, and Kidson 2012). During the early developmental stage, cardiomyocytes are difficult to isolate from the embryo because the heart is very tiny, too small to be subjected to single cell preparations (Davies et al. 1996). As such, the stem cell differentiation through embryoid body (EB) formation has been broadly used as a model for the analysis of early cardiac cellular development. Several previous studies have described the utility of EB-derived models for cardiomyogenesis (Hescheler et al. 1997, Wobus, Wallukat, and Hescheler 1991) at ultrastructural (Hescheler et al. 1997), molecular biological (Miller-Hance et al. 1993), and electrophysiological (Ji et al. 1999, Maltsev et al. 1994) levels, which all show a similarity to that observed in murine heart development. Therefore, stem cells derived cardiac-like cells represent a potentially suitable experimental model in understanding the developmental cellular mechanisms underlying foetal cardiac remodelling in a pathological condition such as diabetes.

1.5 Hypothesis and aims

1.5.1 Hypothesis

The hypothesis of this study is that hyperglycaemia causes structural and electrical remodelling in early development of cardiac cells. These alterations are mediated by degenerative changes, oxidative stress, and abnormalities in components of excitation-contraction coupling.

1.5.2 Aims and specific objectives

Aim 1- To establish and validate the model of spontaneous differentiation of stem cells into cardiac-like cells.

Specific objective (a) To validate the pluripotency nature of the mouse embryonic stem cells (mESC).

Specific objective (b) To differentiate mESC into cardiac-like cells and confirm the functional and structural cardiac-like nature.

Specific objective (c) To determine the optimal glucose concentration for differentiation of stem cells into cardiac-like cells.

Aim 2- To evaluate the effect of hyperglycaemia on the differentiation and maturation of mESC into cardiac-like cells.

Specific objective (a) To establish the hyperglycaemia model of stem cell differentiation into cardiac-like cells.

Specific objective (b) To evaluate the effect of hyperglycaemia on the morphological, functional, and electrophysiological characteristics of stem cell differentiation into cardiac-like cells.

Aim 3- To explore the possible underlying mechanisms of hyperglycaemia-induced cardiac cellular remodelling.

Specific objective (a) To investigate the role of degenerative and proliferative changes in hyperglycaemia -induced structural and electrical alterations in stem cell derived cardiac-like cells.

Specific objective (b) To explore the role of changes in excitation-contraction coupling in hyperglycaemia -induced structural and electrical alterations in stem cell derived cardiac-like cells.

Chapter 2: Materials and methods

2.1 Mouse embryonic stem cell (mESC) propagation and *in-vitro* differentiation

Pluripotent mESCs of the OLA 129 (ES-E14) mouse cell line (provided by Prof. F. Brombacher, Department of Immunology, University of Cape Town, SA) were used in the study for differentiation into cardiac-like cells. All cell culture work was performed under aseptic conditions wearing laboratory coats and sterile gloves. Cells were grown at 37 ºC in a water-jacketed incubator (Thermo Scientific, USA) with 95% humidity and 5% CO_2. Cells in culture were regularly checked and imaged on the EVOS XL Core microscope (Life Technologies, USA). The microscope was housed inside the Bio-Flow hood and used to monitor cell growth and to detect any signs of infection. All cell culture chemicals were purchased from Thermofisher Scientific, unless stated otherwise.

The other cell lines used in this study included feeder layers of inactivated primary mouse embryonic fibroblast (iMEFs; ATCC, USA), which were prepared following a standardised technique (for process of MEFs culture and inactivation see Appendix 2.3). The iMEFs were tested for quality and stability before use by checking seeding capacity and how well mESCs could be propagated on them. Inactivated PA6 cells (provided by Professor S. Kidson, A-Star, Singapore) originally derived from new-born mouse calvaria were used to validate the differentiation potential of this mESCs source. All cells were regularly tested to exclude mycoplasma infection using nuclear staining (Appendix 2.4).

2.1.1 mESCs culture and passage

Before plating the iMEF feeder layers, the tissue culture dishes were coated with a 0.1% gelatine and incubated at 37 °C for one hour. Frozen iMEF stocks were thawed

into DMEM/ foetal bovine serum (FBS) medium and plated on the gelatine-coated dishes at a density of 0.15 x10^6 cells/ 35 mm dish.

After 24-48 hours, the mESC were plated on the feeder layers using stem cell culture medium. The culture medium on the iMEFs was replaced at least 2 hours before plating the mESC with ES culture medium containing DMEM 4.5 g/L glucose supplemented by FBS (15%), glutamax (1%), penicillin/ streptomycin (1%), beta-mercaptoethanol (0.1%), and 5 ng/ml leukaemia inhibitory factor (LIF) (Catalog Number A35933, Thermofisher Scientific, SA). The addition of LIF helps to maintain the pluripotency state of the stem cells through activation of intercellular signalling pathways that target key pluripotency transcription factors (Smith et al. 1988). The mESC were retrieved from liquid nitrogen, thawed rapidly at 37 °C and added dropwise to 4 ml ES medium and centrifuged at 1500 rcf for 5 minutes. The supernatant was aspirated, and the cell pellet triturated with 1 ml ES culture medium then plated onto the feeder layer in 2 ml of medium. Dishes were placed at the back of the incubator for 48 hours. Medium was changed every second day. The growth of stem cells was monitored under the microscope daily for the emergence of stem cell colonies which were identified by their morphology, amorphous structure with well-defined borders comprising hundreds of small, rounded cells with high nucleus cytoplasmic ratio. The mESC colonies were allowed to reach 70-80% confluency (confluency is an estimation of the percentage area covered by the cells in the culture dish) for 4-5 days before passaging them into one or more new dishes coated with feeder layers. Care was taken to avoid the colonies being either too sparse or too close to each other which could result in spontaneous differentiation.

Passaging mESC colonies

Colonies were enzymatically dissociated from feeder layers using dispase II solution (Sigma-Aldrich, USA). The dispase solution allows for a gentle dissociation in comparison to other enzymatic solutions. At first, the ES culture medium was aspirated and the dispase solution (5 mg/ml) was added, and the colonies incubated at 37^{o}C for 15-20 minutes. Once the mESC colonies were dissociated from the

feeder layer, the dispase solution was neutralized with an equal amount of ES culture media and the suspension transferred to a 15 ml tube and centrifuged at 1500 rcf for 5 minutes. The supernatant was aspirated, and the cell pellet triturated into a single cell suspension with ES medium and plated in a split of 1:2 onto new feeder layers. The mESC were passaged 1- 2 times, over 10-15 days, to expand the cell line and freeze down cells before induction of differentiation.

2.1.2 mESCs differentiation

2.1.2.1 Differentiation into the 3 germ layers

To validate the pluripotency of undifferentiated mESCs, the cells were differentiated into the three germ layers ectoderm, mesoderm, and endoderm. Undifferentiated mESC colonies were dissociated from feeder layers with dispase solution. After neutralization, the mESC colonies were transferred to a 15 ml conical tube using a wide bore pipette and allowed to settle by sedimentation for 10-15 minutes. The supernatant was aspirated, and the settled colonies were gently triturated about 4 -5 times into small clumps with iMEF medium. The cell suspension was transferred to 10 cm non-adherent bacteriological dishes and incubated at 37°C for 24 hours to allow aggregation and formation of embryoid bodies (EB) in a suspension culture in bacterial-grade non-adherent dishes. The EB is a three-dimensional multicellular aggregate that facilitates intercellular interaction, in which cell-cell contact exists. The EB consists of ectodermal, mesodermal, and endodermal precursors, which resemble the characteristics of cell differentiation during early mammalian embryogenesis and differentiate into derivatives of the three germ layers (Itskovitz-Eldor et al. 2000). After 24 hours, about 50 EBs were transferred using a wide-bore pipette to each of three non-adherent dishes containing differentiation media specific for each of the germ layers as follows. For each of the differentiation processes coverslips were coated with 0.1% gelatine and inserted into 12-well culture dishes. 3-4 EBs plated per coverslip.

Differentiation into endoderm: after 24 hours of EB formation, the iMEF culture medium was changed to EB medium containing KO-DMEM (Catalog number 10829-018, Thermofisher Scientific, SA) supplemented with FBS (10%), glutamax (1%), penicillin/ streptomycin (1%), B-mercaptoethanol (0.1%), and non-essential amino acid (1%), and incubated a further 2-3 days in suspension culture. The EBs were then transferred onto the coverslips in EB medium. The culture medium was changed every second day for a period of 15-20 days.

Differentiation to mesoderm: after 24 hours of EB formation, the iMEF culture medium was changed to EB medium supplemented with 0.5 mM ascorbic acid and cultured in suspension for 2-3 days more in bacteriological dishes. EBs were then transferred onto the coverslips in EB medium containing 0.5 mM ascorbic acid. Medium was changed every 2 days for 15-20 days.

Differentiation to ectoderm: after 24 hours of EB formation, the culture medium was changed to N2/B27 culture medium containing 50% neuronal basal medium with 50% DMEM F12 supplemented with N2 (0.5%), B27 (1%), glutamax (1%), and penicillin/ streptomycin (1%) and cultured in suspension for 2-3 days in bacteriological dishes. A feeder layer of inactivated PA6 cell were plated on gelatine-coated coverslips in multi-well tissue culture plates using DMEM culture medium supplemented with FBS (10%), glutamax (1%) and penicillin/ streptomycin (1%). The EBs were then transferred onto the PA6 feeder layer using N2/B27 culture medium. The culture medium was changed every second day for 15-20 days.

2.1.2.2 Differentiation into cardiomyocytes and interventions

mESC were differentiated into cardiac-like cells through the formation of EBs which have been widely used as a trigger of an *in-vitro* differentiation of stem cells (Kurosawa 2007). There are different methods of EB formation in cell culture such as liquid suspension culture in bacterial-grade dishes and culture in hanging drops (Kurosawa 2007). In our laboratory, we optimized the method of EB formation for mESC differentiation into cardiac-like cells using the hanging drop method to standardise the size of the EBs and minimise the heterogeneity of the formed EB

beating characteristics by using a specific number of cells (1000) suspended in a hanging drop as further described below.

Hanging drop method

The mESC colonies were lifted from the feeder layer with dispase solution as described in section 2.1.1. The cells were counted using a counting chamber haemocytometer (Lasec, SA) (Appendix 2).). In preliminary studies we found that 1000 cells/drop forms a more robust and well-formed EB than 500, and 2000 cells/ drop. For all subsequent experiments the seeding cell suspension was therefore adjusted to 1000 cells /20 µl drop using differentiation culture media.

About 40-50 drops of 20 µl each were placed onto the under surface of the lids of 10-cm culture dishes (Appendix 2.6). The lids were then inverted and placed onto culture dishes filled with 10 ml of phosphate-buffered saline (PBS) to keep the drops from evaporating. The first day in which the hanging drops were formed was called day 1 of differentiation. The drops were incubated at 37^{o}C and left undisturbed for 72 hours to allow the EBs to form. On day 3 of differentiation, the EBs were visible as small white dots in the drops. The EBs were transferred into a bacteriological dish by washing the hanging drops off the lid using differentiation medium, then cultured for a further 4-5 days. Medium was changed a day later by swirling the plates to allow the EBs to collect in the centre. The medium was removed by aspirating from the periphery of the dish using a 1 ml pipette tip, and fresh medium added slowly down the wall of the dish.

On day 7 of differentiation the EBs were transferred individually, with a wide-bore pipette tip to avoid damaging the EBs, onto 0.1% gelatine-coated coverslip at a density of 2-3 EBs/well of a 12-well culture plate or 1-2 EBs/ well of a 24-well culture plate. The EBs were cultured for a further 13 days using the differentiation culture media. The medium was changed on day 3 after the EBs were adhered, and thereafter every second or third day. The EBs were monitored every second day from day 8 of differentiation onward under the EVOS light microscope for

spontaneous beating characteristics (onset of spontaneous beating, number of beating EBs and beating rate) and for morphological changes. Images were taken daily for measuring EB diameter on day 3 of differentiation (day of EB transfer from hanging drop to suspension) and on day 7 of differentiation (day of EB transfer from suspension onto coverslips for attachment).

2.1.2.2.1 Experimental design

Pluripotent mESCs were differentiated under either 25-, or 50-mM glucose concentration for 20 days starting on day 1 (first day of hanging drop formation) which is the point of stem cell differentiation induction (Figure 1). Although 25 mM glucose is high, it was used in this study as the standard condition because it is the default standard glucose concentration used in mESC *in-vitro* cardiac differentiation (Ali et al. 2004, Guan, Fürst, and Wobus 1999). In addition, 25 mM glucose has been shown to enhance mESC cardiac differentiation (Crespo et al. 2010). During the differentiation period, different analyses and treatment interventions were performed at specific time points.

To evaluate the effect of the glucose concentration compared to the corresponding *in-vivo* physiological glucose level, a subgroup of mESCs was differentiated under culture medium with 5.5 mM glucose. In this study we started with 5.5-and 25 mM glucose to evaluate the optimal glucose level for stem cell differentiation into cardiac-like cells, before proceeding to a hyperglycaemia model using 50 mM glucose which has been used previously in a hyperglycaemia model of cardiac-like H9C2 cells (Han et al. 2015, Xu et al. 2020). We note here that the addition of glucose in the preparation of high glucose culture medium would introduce osmolarity changes. However, hyperglycaemia in diabetic patients is characteristically associated with changes in osmolarity, and for this reason in our study we did not correct for the osmolarity changes due to glucose addition.

Antioxidant treatments:

To test the role of antioxidant treatments, a subgroup of differentiated EBs were treated with N-acetyl cysteine (NAC, 100 µM, dissolved in DMSO; Sigma, SA) for 72 hours. According to our preliminary experiments to optimize the NAC dose, we found the dose greater than 1 mM was harmful to mESCs since the EBs stopped beating and detached from the culture dishes.

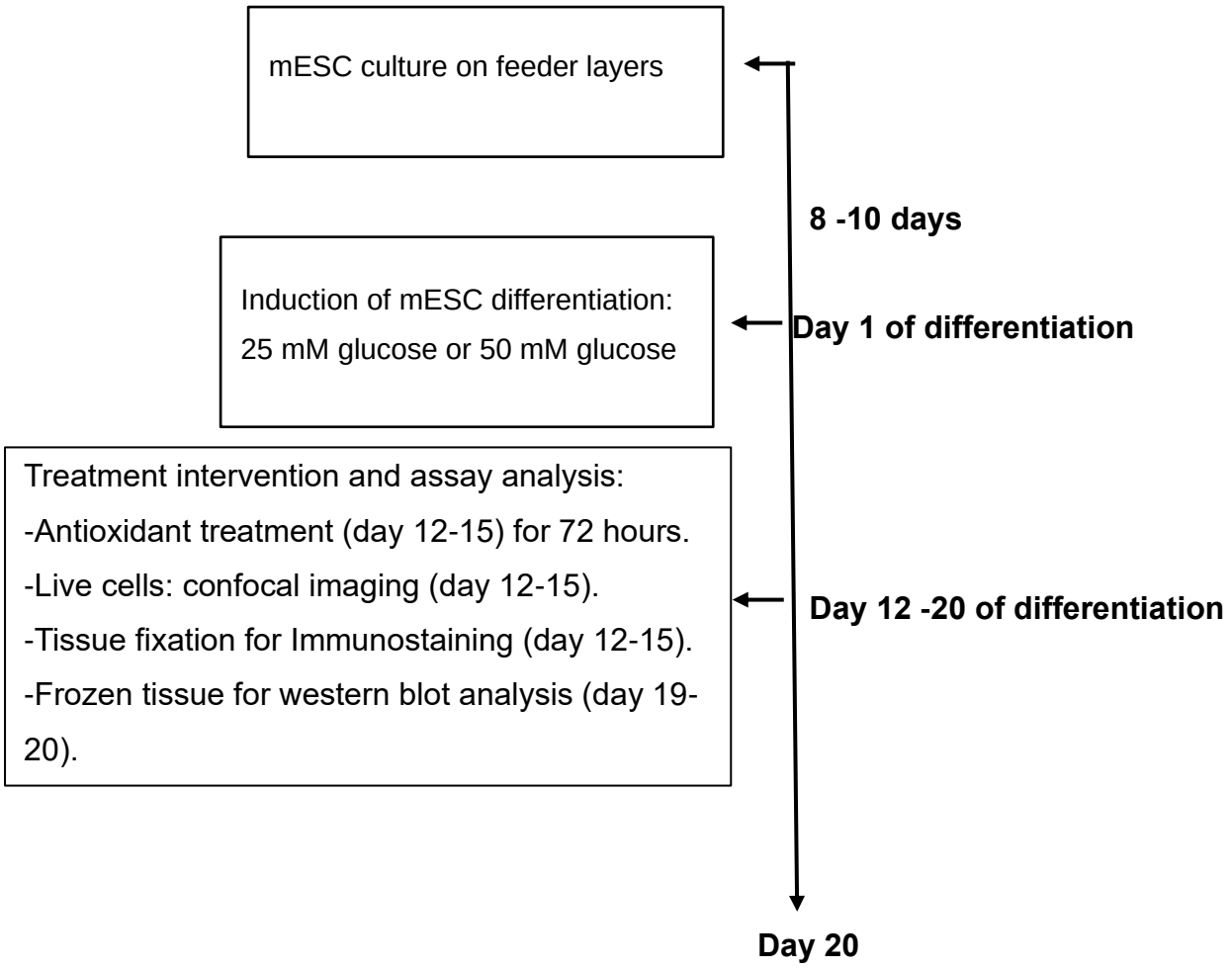

Figure 1: Summary diagram of the experimental protocol. mESC were differentiated under either 25- or 50-mM glucose. Drug treatment and different assays and analysis were done during the time of mESC differentiation.

2.2 Immunocytochemistry

Undifferentiated mESC were immunostained for the expression of stem cell pluripotency nuclear markers: Octamer-binding transcription factor 4 (Oct4) (Nichols et al. 1998) and Nanog (Chambers et al. 2003). Differentiated mESC were immunostained for the markers of three germ layers: alpha smooth muscle actin, B-III tubulin, and alpha-1 fetoprotein. The stem cell derived cardiomyocyte-like cells were immunostained for characteristic cardiomyocyte proteins: cardiac myosin heavy chain (alpha and beta heavy chain specific), alpha actinin 2, cardiac troponin T, and connexin 43. The stem cell derived cardiac-like cells were also immunostained for nitrotyrosine, a marker of oxidative stress.

The undifferentiated mESCs or differentiated EBs (day 12–15) were adhered on glass coverslips, washed with 1x PBS 3 times 3 minutes each then fixed with 4% paraformaldehyde (PFA) (Appendix 1.6), for 15 minutes at room temperature followed by permeabilization with ice-cold methanol for 15 minutes. Samples were blocked with 3% bovine serum albumin (BSA), 0.01% triton -X 100 in 1x PBS for one hour at room temperature. The EBs were then incubated with primary antibodies (Table1) diluted in 1% BSA in 1x PBS at 4^{o}C overnight in a humidifying chamber. The next day, the EBs were washed three times, 10 minutes each with 1x PBS and incubated with the secondary antibodies: Alexa Fluor 488 (1:500 dilution in 1x PBS) or Cy3 (1:1000 dilution in 1x PBS) at room temperature in dark for 2 hours. For nuclei counterstaining, the cells were washed 3 times, 10 minutes each with 1x PBS, then stained with 0.5 µg/ml Hoechst 33258 for 10 minutes at room temperature in the dark. The cells were washed 3 times with 1x PBS 5 minutes each and mounted onto glass slides using mowial mounting medium containing n-Propyl gallate (anti-fade) (Sigma Aldrich, SA). In negative control samples, the primary antibodies were omitted.

The EBs were visualized with the confocal microscope (Carl Zeiss LSM880 and Zeiss LSM 510 Germany) using ZEN software. The confocal setting includes (scan mode: frame, frame size: xy 512, speed:9, bit depth:8bit, number of averging:1,

pinhole is set to one airy unit). To standardize the confocal microscopy image-acquisition, the settings throughout the different slides were kept by use the “Reuse” configuration feature in the ZEN image-acquisition software. This feature applies the setting of the previous imaging onto new experiment. Therefore, it keeps the acquisition parameters constant on different slides and at different magnifications. For confocal microscopy image acquisition, each EB was arbitrarily divided into four quadrants and five images were taken (four from each quadrant and one from the centre). The average data from the five images was taken as a single EB parameter measurement. The confocal images were analysed with image J software (NIH, USA).

Table 1: Antibodies used in immunocytochemistry and western blot.

Type	Antibody class/host species	Catalogue number / Source	Dilution	Short name
Primary antibodies	Rabbit polyclonal anti-Oct4	Ab19857 / Abcam	1:200 for ICC	Oct3/4
	Rabbit polyclonal anti-Nanog	Ab80892 / Abcam	1:200 for ICC	Nanog
	Mouse monoclonal anti- alpha smooth muscle actin	Ab7817 / Abcam	1:100 for ICC	α-SMA
	Mouse monoclonal anti-B-III tubulin	Ab78078 / Abcam	1:300 for ICC	βIII-tubulin
	Mouse monoclonal anti- Alpha-1 fetoprotein	AB45745 / Abcam	1:100 for ICC	α1-fetoprotein
	Rabbit monoclonal anti- alpha actinin 2	701914 / Thermofisher Scientific	1:250 for ICC	α-actinin 2
	Mouse monoclonal anti-cardiac myosin heavy chain (alpha and beta heavy chain specific.)	MA1-26180 / Thermofisher Scientific	1:200 for ICC	MHC
	Mouse monoclonal anti-cardiac troponin T	MA5-12960 /Thermofisher Scientific	1:400 for ICC 1:200	cTnT

			for WB	
	Mouse monoclonal ant- connexin 43	35-5000 /Thermofisher Scientific	1:200 for ICC	Cx43
	Mouse monoclonal anti- Cytochrome c	MA5-11674Thermofisher Scientific	1:500 for WB	Cytochrome c
	Mouse monoclonal anti- B cell lymphoma 2	MA5-11757/ Thermofisher Scientific, SA	1:100 for WB	BCL2
	Mouse monoclonal anti- Nitrotyrosine	32-1900/ Thermofisher Scientific	1:200 for ICC	Nitrotyrosine
	Mouse monoclonal anti-OPA1	MA5-16149 Thermofisher Scientific	1:1000 for WB	OPA1
	Mouse ploYclonal anti RAGE	PA1-075/ Thermofisher Scientific	1:500 for WB	RAGE
	Mouse monoclonal anti- sarco-endoplasmic reticulum calcium transport ATPase 2	MA3-919/ Thermofisher Scientific	1:250 for ICC 1:500 for WB	SERCA2 ATPase
	Mouse monoclonal anti-TGF beta 1	MA5-16949/ Thermofisher Scientific	1:300 for WB	TGF-β
	Mouse monoclonal anti-Bax	MA5-14003/ Thermofisher Scientific	1:500 for WB	Bax
	Mouse monoclonal anti-β-actin	MA515739/ Thermofisher Scientific	1:5000 for WB	β-actin
Secondary antibodies	1-HRP-conjugated goat anti-mouse	G21040/ Thermofisher Scientific	1:8000 for WB	
	2- HRP-conjugated goat anti-rabbit	ab6721/ABCAM	1:8000 for WB	
	3-Alexa Fluor 488	715-546-150	1:500	Alexa Fluor

	donkey anti-mouse	/Amersham	for ICC	488
	4-Alexa Fluor 488 donkey anti-rabbit	711-546-152 /Amersham	1:500 for ICC	Alexa Fluor 488
	5-Cyanine3 donkey anti-rabbit	711-166-152 /Amersham	1:1000 for ICC	Cy3
	6- Cyanine3 donkey anti-mouse		1:1000 for ICC	Cy3
ICC: immunocytochemistry, WB: western blot, HRP: horseradish peroxidase.				

2.3 Calcium transient measurements

Calcium imaging is a microscopy technique to measure Ca^{2+} condition of the cells or tissue. This technique has allowed studies of Ca^{2+} signalling in varied cell types such as neurons and cardiac cells (Bootman and Berridge 1995). Calcium indicators are fluorescent molecules that respond to the binding of Ca^{2+} ions by changing their fluorescence properties.

The EBs were cultured on 0.1% gelatine coated coverslips or in the imaging dishes (glass bottom culture dishes) for Ca^{2+} imaging experiments. The Fluo-4 Ca^{2+} indicator (Fluo-4, AM, cell permeant, Catalogue number: F14201, Thermofisher, SA) were used for Ca^{2+} transient imaging in this study. The stock solution of Fluo-4 was prepared in DMSO by adding 50 µl DMSO to 50 µg Fluo- 4 vial, vortexed to dissolve then were aliquoted and kept at -20ºC protected from light. On day 12-15 of EB differentiation, the Fluo-4 working solution (10 µm) was prepared on the day of the experiments by adding 10 µl from the stock solution of fluo4-AM with 0.02% Pluronic F-127 (to promotes loading of Fluo-4 AM into cells) to the culture media. For Fluo-4 loading, the culture medium was removed, and the medium mixed with fluo 4-AM and Pluronic. The culture dishes were wrapped with foil to protect from light and incubated in the incubator at 37ºC and 5% CO_2 for 20-30 minutes undisturbed. After loading, the culture dishes were transferred to the incubation chamber at 37ºC and 5% CO_2 at the stage of the confocal microscope LSM880 for Ca^{2+} transient imaging using the ZEN software, x20 objective (EC Plan-neofluar 20x /0.50 M27). The EBs were visualized to find the beating area under low illumination to avoid fluorophore

bleaching. Fluo-4 was excited at 488 nm and emitted fluorescence was captured at 490–540 nm. The setting for Ca^{2+} transient imaging includes (dimension: x: 344, y: 256, time: 200, 16-bit, scan mode: plane, time series, camera exposure time: 5.0 ms, scaling x: 2.048 µm, y: 2.048 µm, average: 1, and beam splitters: FW1: FSet38 wf). The recording was done for 200 cycles at 30 frames/second.

Ca^{2+} transient imaging data was analysed with image J (NIH) software using LC_Pro, plugin (Francis et al. 2012). At first the image sequences were exported from ZEN software as a series of images, which was then opened with image j software and saved as tiff files to be analysed with LC_Pro plugin and the output data was analysed with Origin software.

2.4 Recording of action potential

The cardiac action potential was recorded in using a voltage-sensitive dye aminonaphthylethenylpyridinium (ANEP) dye (Di-4-ANEPPS, catalogue number D1199, Thermofisher, SA), which fluoresce in response to the change in the electrical potential in their environment. The Di-4-ANEPPS stock solution was prepared by dissolving the dye powder in DMSO, aliquoted and kept at 4 ^{o}C protected from light. The EBs were cultured on 0.1% gelatine coated coverslips or in the imaging dishes for voltage sensitive dye imaging. On day 12-15 of EB differentiation, the working solution of Di-4-ANEPPS dye (10 µm) was prepared on the day of the experiments in the culture media. For dye loading, the culture medium was removed, and the prepared dye solution was added to the EBs. The culture dishes were wrapped with foil and incubated in the incubator at 37ºC and 5% CO_2 for 15-20 minutes undisturbed. After loading, the EBs were imaged with confocal microscope LSM880. Di-4-ANEPPS dye was excited at 488 nm and emitted fluorescence was captured at 490–540 nm. The setting of the confocal imaging includes (objective: EC Plan-Neofluar 20x/0.50 M27, dimension: x: 344, y: 256, time: 200, 16-bit, scan mode: plane, time series, camera exposure time: 5.0 ms, scaling x: 2.048 µm, y: 2.048 µm, average: 1, and beam splitters: FW1: FSet38 wf). The recording was done for 200 cycles for 6-8 seconds at a frame rate of 30

frames/second. The imaging process and the settings were as for the Ca^{2+} transient imaging in section 2.3. The di-4-ANEPPS imaging data were analysed with image J (NIH) software using LC_Pro, plugin. The output data was analysed with Origin software.

2.5 Measurement of cellular contractility

To evaluate the contractile function of the stem cell derived cardiac-like cells under different glucose concentration, the beating EBs were imaged with the confocal microscope. The EBs (day 12–15 of differentiation) plated on gelatine-coated, glass-bottom imaging dishes were mounted in an incubation chamber (5% CO_2 at 37°C) on the stage of the confocal microscope LSM880 using the ZEN software. At first, the EBs were visualized to find the beating areas and, then transmitted- light microscopy images were captured using the settings 30 frames/s for 200 cycles; exposure time 5 ms; magnification 20x (EC Plan-neofluar 20x /0.50 M27).

To test the effect of caffeine stimulation, caffeine (1 mM; dissolved in water; Sigma, SA) was applied during time-lapse imaging. The time-lapse images were analysed with ImageJ (NIH, USA) using the Myocyter macro, an analytical software tool for the image processing software ImageJ (v. 1.52b) (Grune et al. 2019) (Appendix 4). Amplitude of contraction was derived. The rate of change of amplitude over time [d(Amplitude)/dt], which corresponds to the contractility parameter dP/dt (where P is pressure and t is the time), was calculated as the first derivative of the amplitude-time data.

The chronotropic response of spontaneously beating EBs to β-adrenergic stimulation was evaluated using β-adrenergic receptor agonist isoprenaline (1 µM dissolved in distilled water; Sigma, SA,) for 5 minutes at 37°C. The beating rate was counted before and after application of the drug.

2.6 Mitochondrial staining

The mitochondria were stained using Mitotracker Green (M7514, Thermo-Fisher Scientific). The EBs were cultured on 0.1% gelatine coated coverslips for mitochondrial staining. On days 12-15 of EB differentiation, EBs were incubated with Mitotracker Green (1 µM) in cell culture medium (5% CO_2 at 37°C) for 45 minutes. The samples were then washed and counterstained with Hoechst 33,258 (0.5 µg/mL) and covered with foil to protect from light. The imaging dishes were then mounted in an incubation chamber (5% CO_2 at 37°C) on the stage of the Zeiss LSM880 confocal microscope (magnification 20x) for imaging the beating areas of EBs. The EBs were excited at 488 nm and fluorescence signals were captured using ZEN software. Images were analysed using ImageJ, and the uptake of Mitotracker Green was expressed as the fluorescent intensity in the beating EBs.

2.7 TUNEL assay

DNA damage was identified using the terminal deoxynucleotidyl transferase-mediated biotinylated dUTP ([14- biotin] dUTP) nicked end labelling (TUNEL) assay. The Click-iT Plus TUNEL assays (Thermofisher, SA, Catalog No:C10617) were used in this study. For TUNEL assay, the culture medium was removed, and the samples washed once with 1x PBS. The cells were fixed with 4% PFA for 15 minutes at room temperature followed by permeabilization with 0.25% triton -X 100 in 1x PBS for 20 minutes at room temperature then washed twice with 1x PBS. To perform the TdT reaction the cells were incubated with TdT reaction buffer for 10 minutes at 37°C, thereafter the TdT reaction buffer removed, and the cells incubated with TdT reaction mixture for 60 minutes at 37°C. The reaction mixture was removed, and the cells washed twice for 5 minutes each with 3% BSA in PBS at room temperature. The cells were then incubated with Click-iT Plus TUNEL reaction cocktail for 30 minutes at 37°C protected from light, the samples washed with 3% BSA in1x PBS for 5 minutes at room temperature (details of solution preparation in Appendix 5). The samples were then blocked with 3% BSA in 1x PBS for one hour protected from light at room temperature. The blocking solution was removed and the EBs incubated with

α-actinin 2 antibody (dilution 1: 250 in 1% BSA in 1x PBS) at 4^{o}C overnight in a humidifying chamber.

The following day, samples were washed three times, 10 minutes each, with 1x PBS and incubated with the secondary antibodies: Alexa Fluor 488 (1:500 dilution in PBS) at room temperature in dark for 2 hours. For nuclei counterstaining, the samples were washed 3 times, 10 minutes each, with 1x PBS, then stained with 0.5 µg/ml Hoechst 33258 for 10 minutes at room temperature in the dark. The cells were washed 3 times with 1x PBS, 5 minutes each, and mounted onto glass slides using mowial mounting medium containing anti-fade powder. The cells were visualized with confocal microscope Carl Zeiss LSM880 using ZEN software. The samples were imaged at x40 and x63 objectives where the TUNEL positive cells are co-stained with α-actinin 2. For confocal microscopy image acquisition, the EBs were randomly divided into quadrants and 5 images were taken per EB. The TUNEL positive cells were quantified with Image J software and the results were presented as the percentage of TUNEL positive cells to the total cells (were the nuclear stain also counted in each slide).

2.8 EdU assay

Cell proliferation was assessed using Click-iT EdU (5-ethynyl-2-deoxyuridine) Cell Proliferation Kit (Click-iT EdU Cell Proliferation Kit, Catalog number: C10337, Thermofisher, SA), according to the manufacturer's instructions. The EBs at day 12-15 of differentiation were incubated with 10 µM EdU solution (prepared in DMSO) mixed in cell culture medium for 5 hours in culture conditions. After 5 hours incubation, the culture media was removed and the EBs were fixed with 4% PFA in 1x PBS for 15 minutes at room temperature then the cells were washed twice for 5 minutes each with 3% BSA in 1x PBS. The EBs were then permeabilized with 0.5% triton X-100 in 1x PBS for 20 minutes at room temperature. After permeabilization, the EBs incubated with Click-iT reaction cocktail (used within 15 minutes of the preparation) for 30 minutes at room temperature, protected from light (Appendix 6). The EBs were then washed once with 3% BSA in 1x PBS for 5 minutes. For co-

staining with cardiac specific protein MHC (α and β isoforms), the EBs were then blocked with 3% BSA, 0.01% triton-X 100 in 1x PBS for one hour at room temperature. The EBs were then incubated with MHC antibody (dilution 1:200 in 1% BSA in 1x PBS) at 4^{o}C overnight in a humidifying chamber.

On the next day, the EBs were washed three times, 10 minutes each, with 1x PBS and incubated with the secondary antibodies: Cy3 (1:1000 dilution in PBS) at room temperature in dark for 2 hours. For nuclei counterstaining, the cells were washed 3 times, 10 minutes each, with 1x PBS, then stained with 0.5 µg/ml Hoechst 33258 for 10 minutes at room temperature protected from light. The EBs were washed 3 times with 1x PBS for 5 minutes each and mounted onto glass slides using mowial mounting medium containing n-Propyl gallate (anti-fade).

The EBs were visualized with confocal microscope (Carl Zeiss LSM880) with x40 and x63 objectives and ZEN imaging software. The EdU staining were excited at Alexa Fluor 488 and emitted fluorescence was captured at 490–540 nm, whereas the MHC staining were excited at 530 nm and emitted fluorescence was captured at 560 nm. The images were taken 4-5 areas /EB in the areas were co-stained with MHC and the EdU. The cells were quantified manually with Image J software. The number of EdU-stained nuclei was expressed relative to the total number of the nuclei in MHC-stained cellular areas.

2.9 Western blot analysis

The western blot was performed for mESC derived cardiac-like cells for SERCA2, TGF-β, RAGE, Bcl-2, Bax, OPA1, and cytochrome c. The mESC derived cardiomyocyte was washed twice with ice cold 1x PBS, scraped down with cold rubber tip of a sterile plastic 1 ml syringe using cold radioimmunoprecipitation (RIPA) lysis buffer containing 50 mM Tris-HCl (pH 8), 1% triton x-100, 150 mM NaCl, 0.1% sodium dodecyl sulphate, 0.5% sodium deoxycholate with a protease and phosphatase cocktail inhibitor (Halt protease and phosphatase inhibitor, Thermo Scientific, USA). The cellular lysates were vortexed then transferred into tubes and mixed on a roller at 4°C for 30 minutes. The cell lysate was centrifuged at 15000 rcf

for 30 minutes at 4°C (Labnet International, NJ07095, USA). The supernatant collected, and the protein concentration of supernatant measured using the Pierce protein assay kit (Thermo Scientific, Rockford, USA.) (Appendix 7).

The gels were placed in an electrophoresis tank (Bio-Rad mini protean tetra system) which was filled with running buffer. The loading samples were prepared with 40 µg of the proteins lysate were loaded (the loading concentration of the protein were optimized in this study) and electrophoresed on 8-12% SDS-polyacrylamide gel using mini-protein tetra cell system (Bio-Rad, SA) at 150 V for 90 minutes. The proteins were transferred from the gel onto polyvinylidene fluoride (PVDF) transfer membrane (Immuno-Blot PVDF Membrane for Protein Blotting, Bio-Rad, SA), using a semi-dry transfer unit (Trans-Blot Turbo Transfer system, Bio-Rad, SA). After transfer, the membranes were blocked with 5% non-fat milk in 1x PBS with 0.1% tween-20 (PBS-T) for 1hour at room temperature. The membranes were incubated with primary antibodies against proteins of interest (Table). The membranes were washed with PBS-T and incubated with horseradish peroxidase (HRP) conjugated secondary antibody (Goat Anti-Mouse IgG HRP conjugate) (1:5000-1:8000) in 5% non-fat milk in PBS-T for 2 hours at room temperature. The membranes were then incubated with enhanced chemiluminescence (ECL) detection solution (Clarity Western ECL Substrate, Cat.170-5060, Bio-Rad, SA) then exposed to x-ray film (Agfar Healthcare, SA) in dark room.

The membranes were then stripped for housekeeping protein incubation. The membranes washed with distilled water, stripped with 8% NaOH, and blocked with 5% non-fat milk in PBS-T for 1 hour. The membranes were incubated with housekeeping protein primary antibody (Monoclonal anti-beat actin antibody produced in mouse) at dilution of 1:5000 in 5% non-fat milk in PBS-T overnight at 4°C. The membranes were then washed with distilled water and incubated with horseradish peroxidase (HRP) conjugated secondary antibody (Goat Anti-Mouse IgG (H+L)-HRP), at dilution of 1:10000 in 5% non-fat milk in PBS-T for 2 hours at room temperature. The membranes were then washed, incubated with ECL, and detected as above. The x-ray films were scanned and analysed using Image J software

(Image J, NIH, USA). The density of each band was expressed as a percentage of the mean density of all the bands. The percentage of each band was then normalised to the percentage density of it is respective housekeeping protein bands (Appendix 8).

2.10 Statistical analysis

In this study, data were presented as either the mean and standard error of the mean or as box and whisker plots. The statistical analysis was performed by using Statistica (version 13, USA) and Microcal Origin Lab programmes (Microcal Software, USA). Shapiro–Wilk test for normality test was used to test the distribution of variables. The comparison between the two glucose groups were done using an unpaired *t*-test for parametric data or Mann-Whitney *U* test for non-parametric data from multiple groups with normal distribution were compared using one-way analysis of variance (ANOVA) followed by appropriate Tukey's post-hoc test. A p-value of < 0.05 was regarded as statistically significant, n: represents the number of replicates.

Chapter 3: Results

3.1 Validation of stem cell culture model

3.1.1 Pluripotency of undifferentiated mESCs

3.1.1.1 Growth pattern and expression of master transcription factors

For growth pattern characteristics, Figure 2 shows typical mESCs seeded onto feeder layers of iMEFs. Generally, colonies of mESCs used in this study had well-defined borders and a high nuclei-to-cytoplasm volume ratios, thereby making them distinguishable from the underlying feeder layer of iMEFs, which consists of spindle-shaped fibroblasts (Figure 2). The colonies were formed within 24 hours of cell seeding. This pattern of growth was taken to be a sign of healthy proliferation of undifferentiated mESCs.

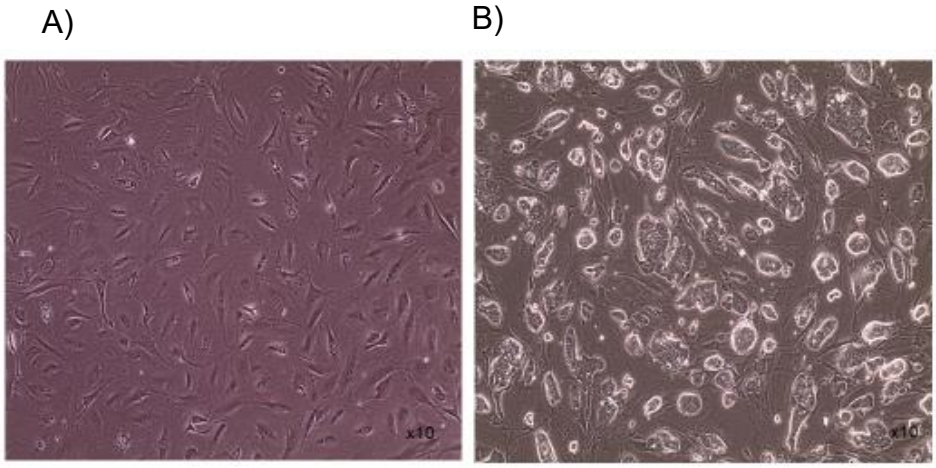

Figure 2: Mouse embryonic stem cell culture. A: Feeder layer of iMEFs. B: a co-culture of mESCs colonies on a feeder layer. iMEFs: inactivated primary mouse embryonic fibroblast.

Undifferentiated mESCs immunostained positively for Nanog (Figure 3.A) and Oct3/4 (Figure 3.B) nuclear transcription factors. The staining was observed in the mESC colonies but not in the nuclei of the iMEFs as indicated by arrowheads in Figure 3.

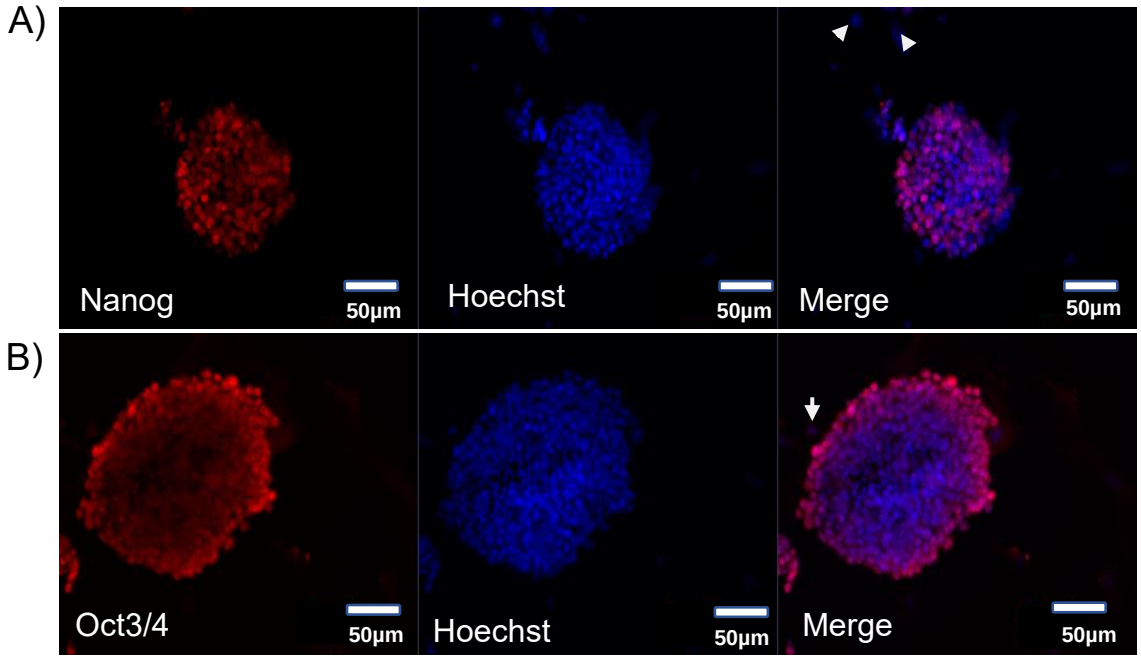

Figure 3: Expression of pluripotent biomarkers of mESCs. A- B: Representative fluorescence microscope images of Nanog (A), Oct3/4 (B), Hoechst, and merged images. Scale bar = 50 µm. Magnification x 40. n = 3 replicates. Arrowheads indicate nuclei of iMEFs. Scale bar = 50 µm.

3.1.1.2 *In-vitro* stem cell differentiation into three germ layers

The capacity of mESC to differentiate into multipotent cells was estimated using protocols of *in-vitro* differentiation into each of the three primary germ layers. mESCs induced into ectoderm were positive for βIII-tubulin (Figure 4.A), those induced into mesoderm were positive for α-SMA (Figure 4.B), whereas those induced into endoderm were positive for α1-fetoprotein (Figure 4.C).

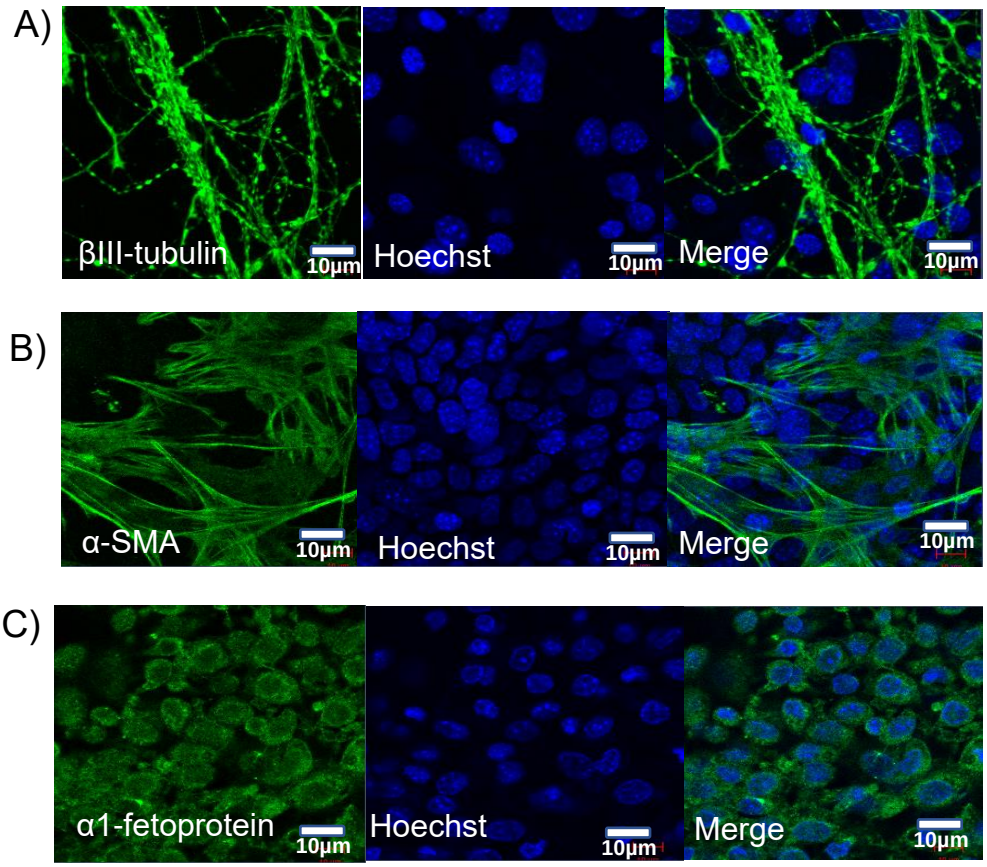

Figure 4: Expression of markers of mESC differentiation into the three germ layers. A: Ectoderm layer marker (βIII-tubulin), Hoechst, and merged images. B: Mesoderm marker (alpha smooth muscle actin), Hoechst, and merged images. C: Endoderm marker (alpha-1 fetoprotein), Hoechst, and merged images. Scale bar = 10μm. Magnification x 40. n = 3 replicates for each germ layer.

3.1.2 mESC differentiation into pulsatile cardiac-like cells via embryoid bodies

EBs were formed using the hanging drop method for 3 days then cultured in suspension for 3 days before attachment. Figure 5 shows the typical microscopic images of EB growth pattern over time. In the early stages (day 3), the EBs looked like bright spherical balls (simple EBs) with sharp distinct outlines (Figure 5.A). After a further 2-4 days in suspension, the EBs increased in size and most of them had formed darkened, cystic, centres (Figure 5.B and C). After 7 days in suspension culture, EBs were adhered onto gelatine-coated coverslips in tissue culture dishes. At that point, outgrowths started emerging from the EB 2 days later and the EBs started losing their regular spherical shape over the next week (Figure 5.D-F).

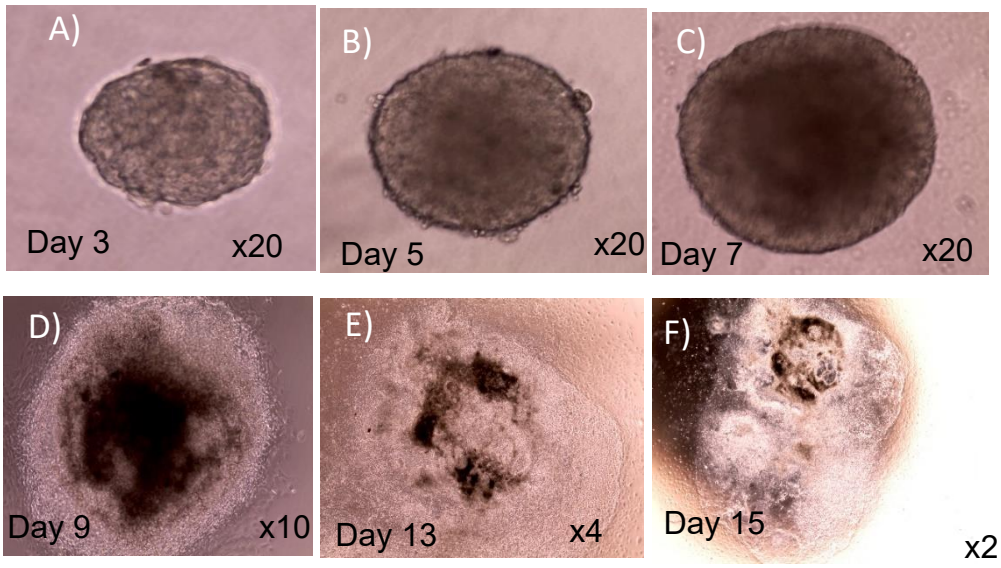

Figure 5: Embryoid body growth: A: Day 3 of differentiation. B: Day 5 of differentiation. C: Day 7 of differentiation. D: Day 9 of differentiation. E: Day 13 of differentiation. F: Day 15 of differentiation. Magnification of the microscope: x20 (B, C), x10 (D), X4 (E) and x2 (F). n = 5 replicates.

The onset of spontaneous beating of the EBs started at around day 9 post-induction of differentiation which was the second day after the EBs were adhered onto coverslips. The EBs continued to grow and differentiate into a heterogeneous mass

of cells including beating cells. Foci of beating cells appeared as clusters of cells of variable sizes.

3.1.2.1 Pulsatile characteristics of cardiac-like cells derived from stem cells

To determine the beating pattern of the pulsatile EB, an analysis of the contractile waveform was performed using the Myocyter software. Figure 6 shows one example of several tracings of the beating pattern of EBs, for which the analysis of the amplitudes and kinetics is shown in Figure 13 below. The beating patterns generally showed regular contractions of uniform amplitudes (Figure 6.A). The acute application of isoprenaline (1 µM) induced a significant increase in the EB beating rate of almost double the baseline value ($P < 0.05$ vs baseline for each condition, Figure 6.B).

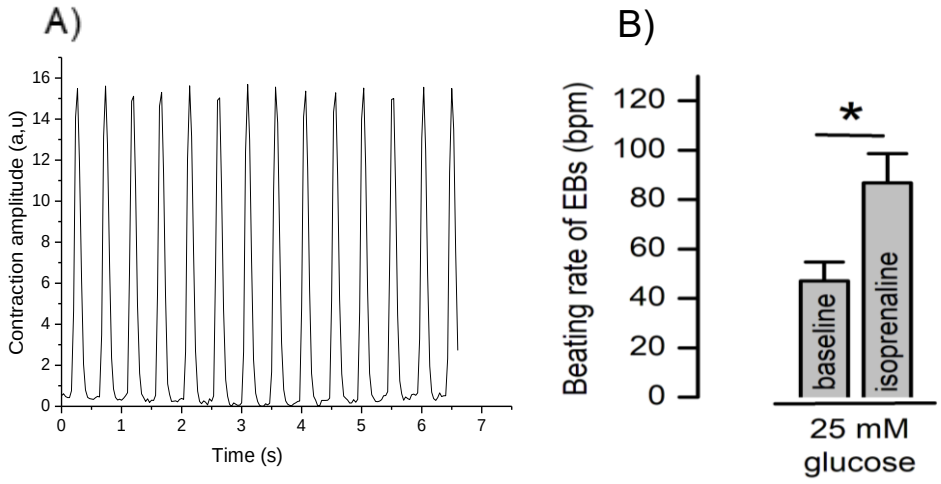

Figure 6: Cellular contractile activity. A: Representative tracings of the contractile activity of spontaneously beating EB derived from the Myocyter programme, with the amplitude expressed as arbitrary units (a.u.). The detailed analysis of contractile parameters is shown in figure 13 below. B: Response of EB beating rate to isoprenaline (* $P < 0.05$; $n = 4$). EBs: embryoid bodies.

3.1.2.2 Molecular biomarkers of stem cells derived cardiac-like cells

The beating EBs stained positive for cardiac troponin T (Figure 7.A), α-actinin 2 (Figure 7.B), which showed up as striated bands, MHC (α and β isoforms; Figure 7.C), which showed up in the cytoplasmic area around the nucleus, and connexin 43 (Figure 7.D), which showed up at the edges of the cells.

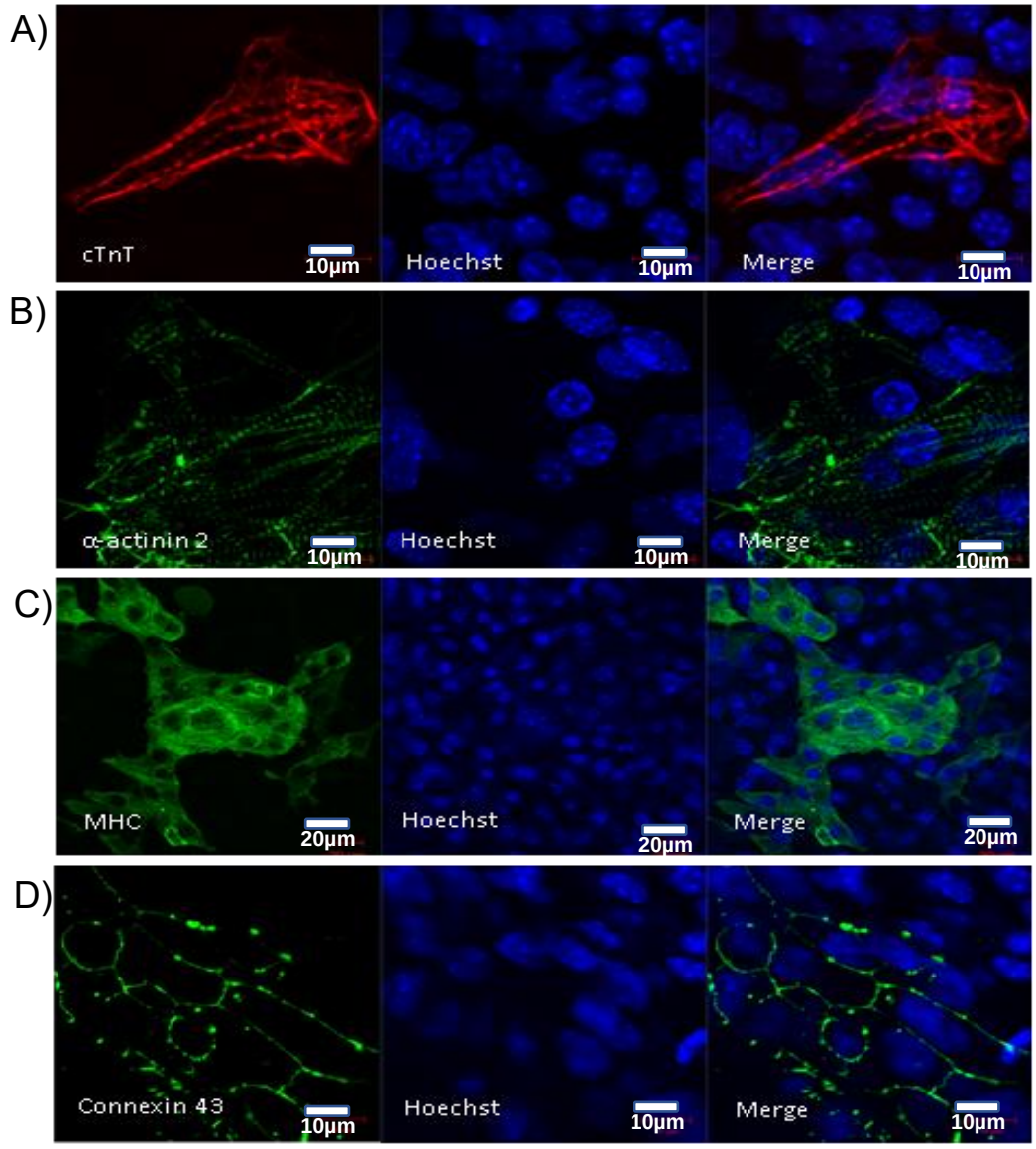

Figure 7: Detection of cardiac specific proteins. A-D: Representative confocal microscopy images of cardiac troponin T (cTnT) (A), α-actinin 2 (B), myosin heavy chain (MHC) (α and β isoforms). (C), connexin 43 (D), Hoechst, and merged images. Scale bar = 10 µm (A, B and D) and 20 µm (C). Magnification x 40. n = ≥ 3 replicates for each protein.

3.1.2.3 Optimal glucose concentration for differentiation of stem cells into cardiac-like cells

The glucose concentration of 25 mM has been used as the default optimal level in *in-vitro* mESCs culture and differentiation into functional, catecholamine-sensitive cardiomyocytes (Ali et al. 2004). In addition, 25 mM glucose has been shown to enhance mESC differentiation into cardiomyocytes (Crespo et al. 2010). Given that the normal plasma glucose concentration is about 5.5 mM, we evaluated whether the glucose of 5.5 mM would provide a superior cardiac phenotype compared the default condition of 25 mM glucose.

The EB size was measured to evaluate EB growth and maturation under both glucose concentration 5.5- and 25-mM glucose. The mean EB diameter on day 3 for 5.5 mM glucose was 304 ±13 µm, and for 25 mM glucose was 278 ± 11 µm ($P > 0.05$ and for 25-mM glucose versus 5.5-mM glucose) (Figure 8.A). The mean EB diameter on day 7 for 5.5 mM glucose was 453 ± 20 µm, and for 25 mM glucose 492 ±16 µm ($P > 0.05$ for 25 mM glucose versus 5.5-mM glucose) (Figure 8.B). Therefore, under the two glucose concentrations (25 mM and 5.5 mM), the EB diameter on day 3 and on day 7 was not significantly different.

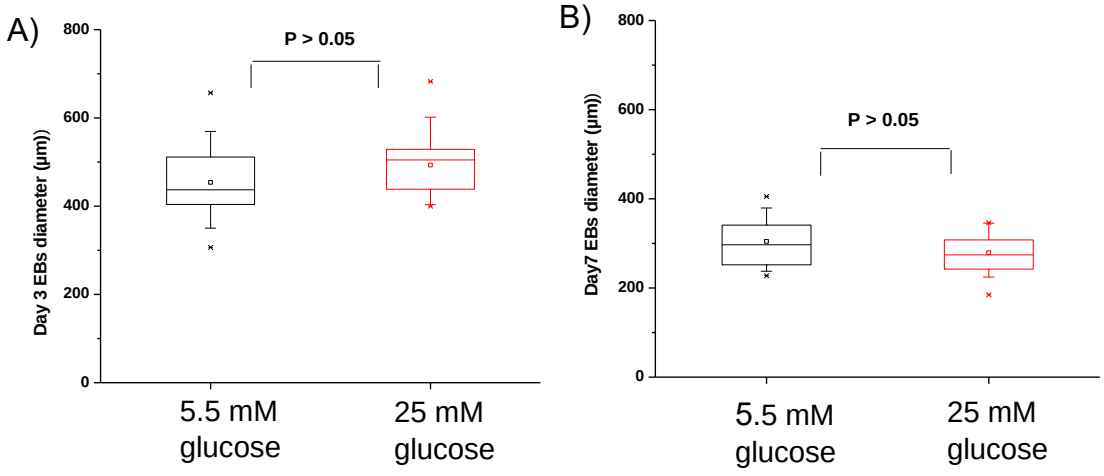

Figure 8: Effects of glucose levels on EBs diameter. A: Quantitative analysis of EBs diameter on day 3 of differentiation. B: Quantitative analysis of EBs diameter on day 7 of differentiation. n ≥ 11 EBs per group. Data are shown as box plot and the mean (■). EBs: embryoid body.

Overall, the 25 mM glucose group showed a higher percentage of beating EBs among the total number of EBs. However, there were no statistically significant differences between the two glucose groups (P > 0.05 for 25 mM glucose versus 5.5 mM glucose), except for day 13 of differentiation when the percentage of beating EBs was significantly higher for 25 mM glucose compared to 5.5 mM glucose (39% for 5.5 mM and 55% for 25 mM glucose group, P < 0.05 for 25 mM glucose versus 5.5 mM glucose) (Figure 9).

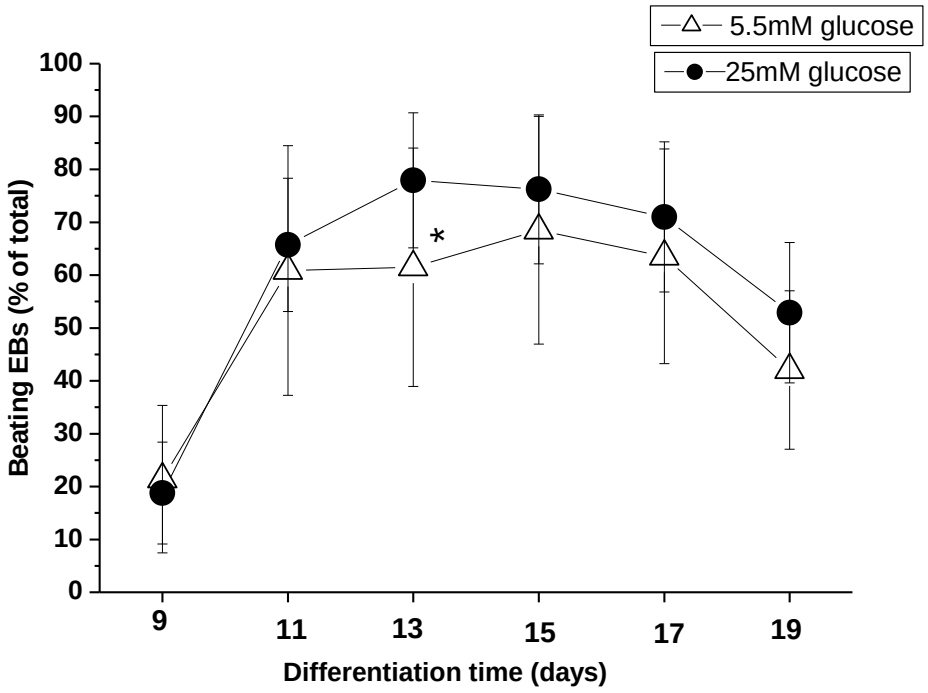

Figure 9: Percentage of beating EBs under 25 mM glucose and 5.5 mM glucose concentrations. Beating EBs expressed relative to total EBs in 25 mM glucose or 5.5 mM glucose, n = 6-7 experiments. * P < 0.05 for 5.5 mM glucose group versus 25 mM glucose group.

The beating rate on day 9 of differentiation was 34±6 beats /minute for the 25 mM glucose group, and 32±7 beats /minute for the 5.5 mM glucose group. The beating rate was increased with time to steady-state levels, and then started to decrease from approximately day 19. There was no significant difference in the average beating rate between the two groups ($P > 0.05$ for 25 mM glucose versus 5.5 mM glucose, Figure 10).

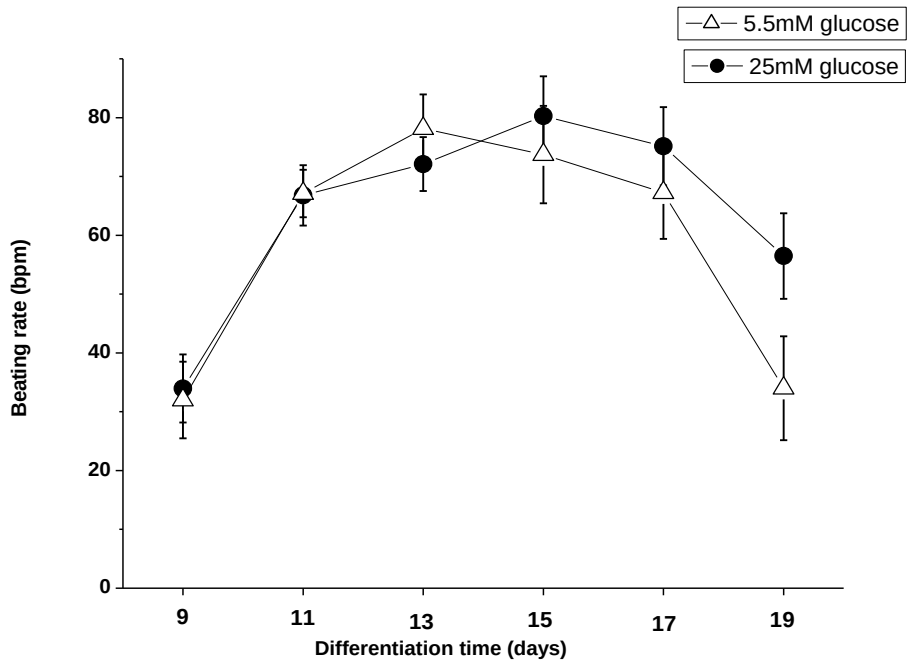

Figure 10: Beating rate of EBs under 25 mM glucose and 5.5 mM glucose concentrations. Beating rate calculated as beat per minute. n = 6-7 experiments.

3.2 Effects of hyperglycaemia on the differentiation of mESC into a cardiac-like model

3.2.1 Effect of hyperglycaemia on the percentage of beating embryoid bodies

The mESCs were differentiated under high glucose (50 mM) or baseline (25 mM) glucose levels. The percentage of beating EBs among total number of EBs formed was significantly lower in 50 mM glucose from day 9 to day 17 of differentiation ($P = 0.01$ for 50 mM glucose group versus 25 mM glucose group on day 9; $P < 0.01$ for days up to day 15 of differentiation, and $P = 0.02$ on day 17 of differentiation), while there were no statistically significant differences on day 19 of differentiation ($P > 0.05$ for 50 mM glucose group versus 25 mM glucose group) (Figure 11).

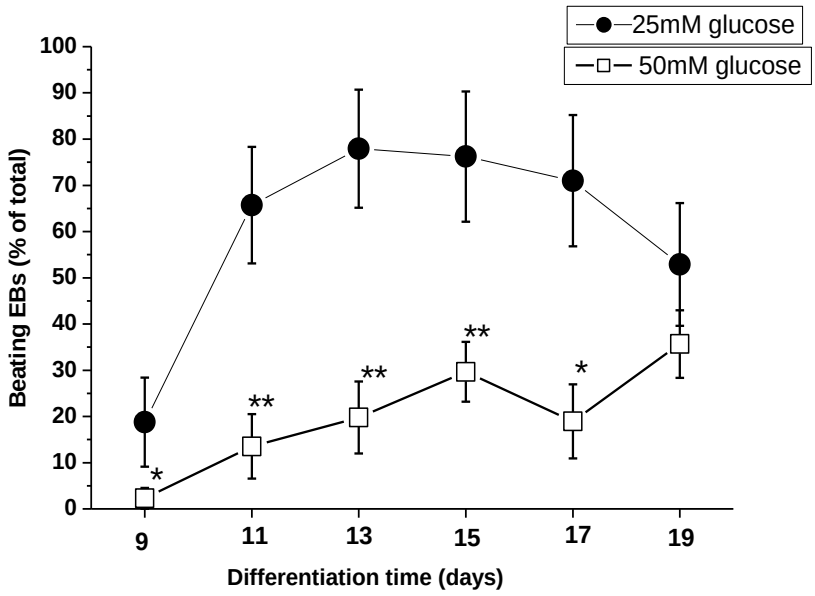

Figure 11: Effect of hyperglycaemia on the percentage of beating EBs. Quantitative analyses of the percentage of beating EBs (expressed relative to the total number of EBs) in the 25- and 50-mM glucose groups. n = 6–9 independent cell-culture batches for each glucose group and ≥ 14 EBs for each group. Data are shown as mean ± SEM. * $P < 0.05$ and ** $P < 0.01$ for 50 mM glucose group versus 25 mM glucose group.

3.2.2 Effect of hyperglycaemia on the beating rate of embryoid bodies

The EB beating rate was statistically significantly lower in the 50 mM glucose group in comparison to the 25 mM glucose group from day 9 to day 17 of differentiation, ($P < 0.05$ for 50 mM glucose group versus 25 mM glucose group) (Figure 12).

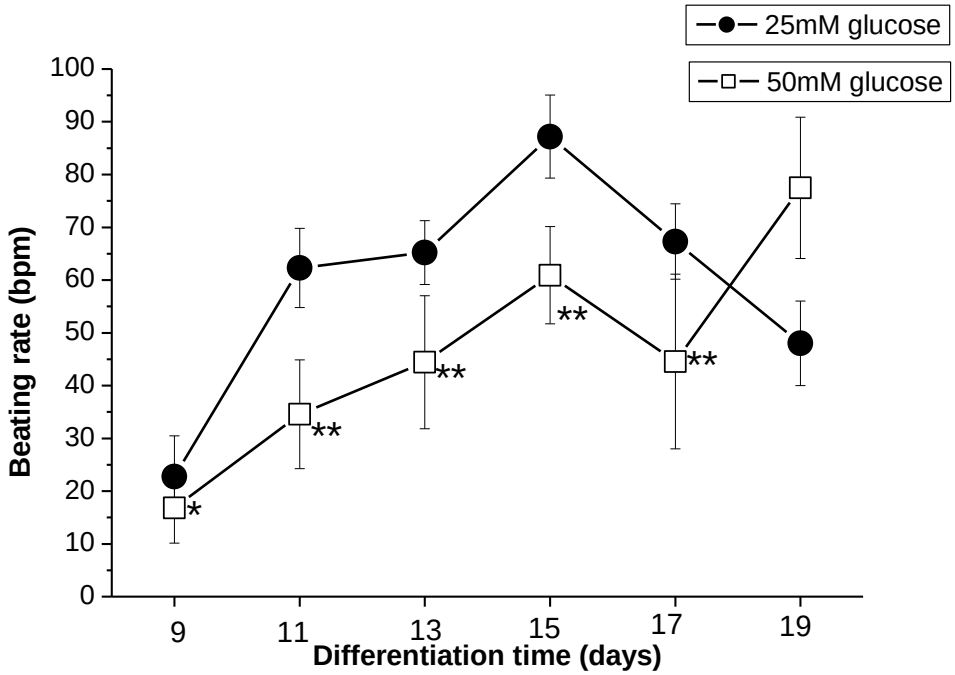

Figure 12: Effect of hyperglycaemia on the beating rate of pulsatile EBs. Quantitative analyses of the beating rate of EBs during differentiation. n = 6–9 independent cell-culture batches for each glucose concentration and ≥ 14 EBs for each time point. Data are shown as mean ± SEM; *P < 0.05 and **P < 0.01 for 50 mM glucose versus 25 mM glucose group.

3.3 Effects of hyperglycaemia on excitation-contraction coupling of mESC derived cardiac-like cells

3.3.1 Effects of hyperglycaemia on the EB contractile features

To evaluate the effect of hyperglycaemia on the contractile parameters of mESCs derived cardiac-like cells, the Myocyter analysis was performed. The 25 mM glucose group showed strong amplitudes of contraction at about 15 ± 1 a.u (Figure 13.A), whereas the 50 mM glucose group showed decreased amplitudes of contraction at about 10 ± 1 a.u (Figure 13.B). Therefore, hyperglycaemia (50 mM glucose)-induced a 30% reduction in the contraction amplitude that was statistically significant ($P < 0.00$ for 50 mM glucose group versus 25 mM glucose; Figure 13.C). In addition, high glucose 50 mM glucose decreased the maximal rate of change of amplitude upstroke [+d(Amplitude/dt); $P < 0.001$ for 50 mM glucose group versus 25 mM glucose; Figure 13.D] and the maximal rate of change of amplitude downstroke [-d(Amplitude/dt); $P = 0.001$ for 50 mM glucose group versus 25 mM glucose; Figure 13.E].

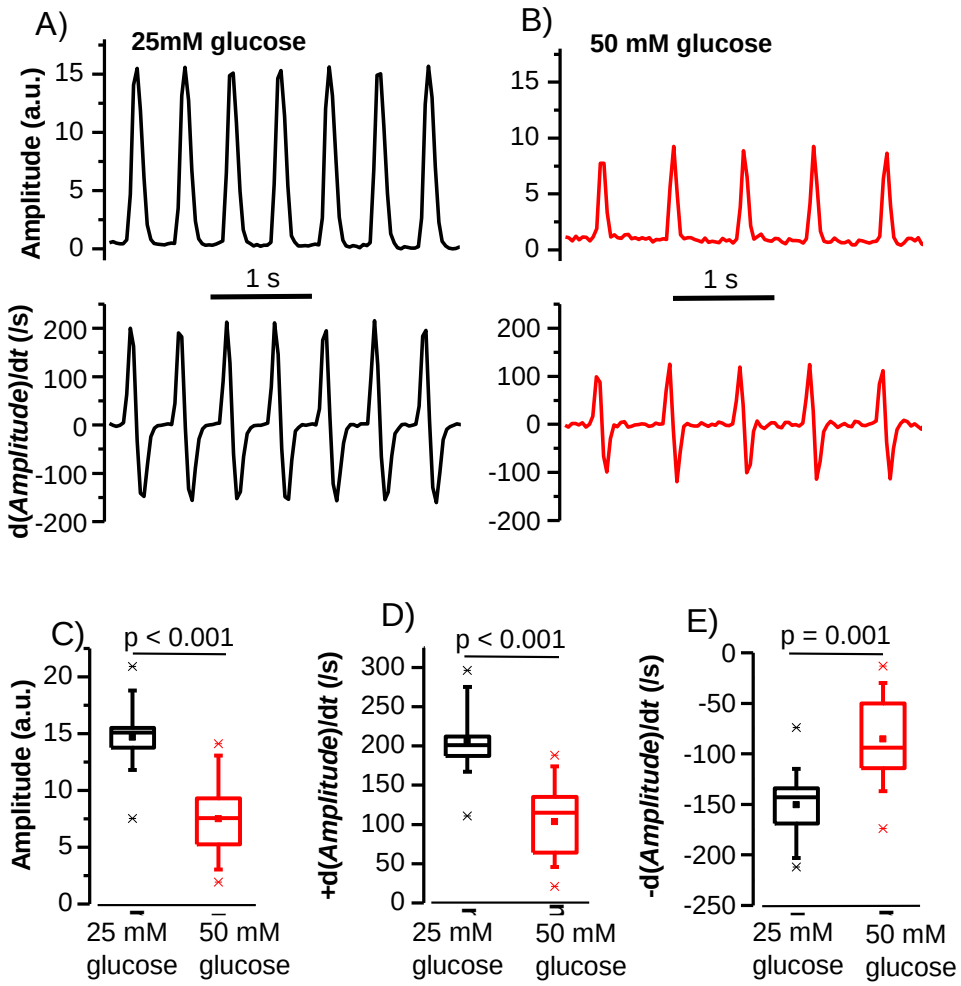

Figure 13: Effects of hyperglycaemia on the cellular contractile activity. A-B: Representative contraction tracing of beating embryoid bodies (EBs). Upper panel: the amplitude expressed as arbitrary units (a.u.). Lower panels show the corresponding tracings of the rate of change of amplitude over time [d(Amplitude/dt)]. C-E: Quantitative analysis of the cardiac contractility parameters. C: Contraction amplitude. D: The maximal rate of change of amplitude upstroke (+d (amplitude/dt). E: The maximal rate of change of amplitude downstroke (-d(Amplitude/dt). (n = 12 EBs per group). Data are shown as box plot and the mean (■). * P < 0.05 and ** P < 0.001 for 50 mM glucose versus 25 mM glucose group.

3.3.2 Effects of hyperglycaemia on Ca^{2+} transients and Ca^{2+} handling proteins of the pulsatile EBs

3.3.2.1 Effects of hyperglycaemia on the Ca^{2+} transients

Since 50 mM glucose induced changes in the EBs contractile parameters, we investigated whether Ca^{2+} signalling was also impacted. The Ca^{2+} transient was

recorded for both groups; high glucose significantly decreased the Ca^{2+} transient amplitude ($P = 0.004$ for 50 mM glucose group versus 25 mM glucose) (Figure 14.A-C). There were no statistically significant differences between the two groups in the Ca^{2+} transient duration ($P = 0.69$ for 50 mM glucose group versus 25 mM glucose, Figure 14.D), attack time ($P = 0.22$ for 50 mM glucose group versus 25 mM glucose, Figure 14.E), or decay time ($P = 0.26$ for 50 mM glucose group versus 25 mM glucose, Figure 14.F).

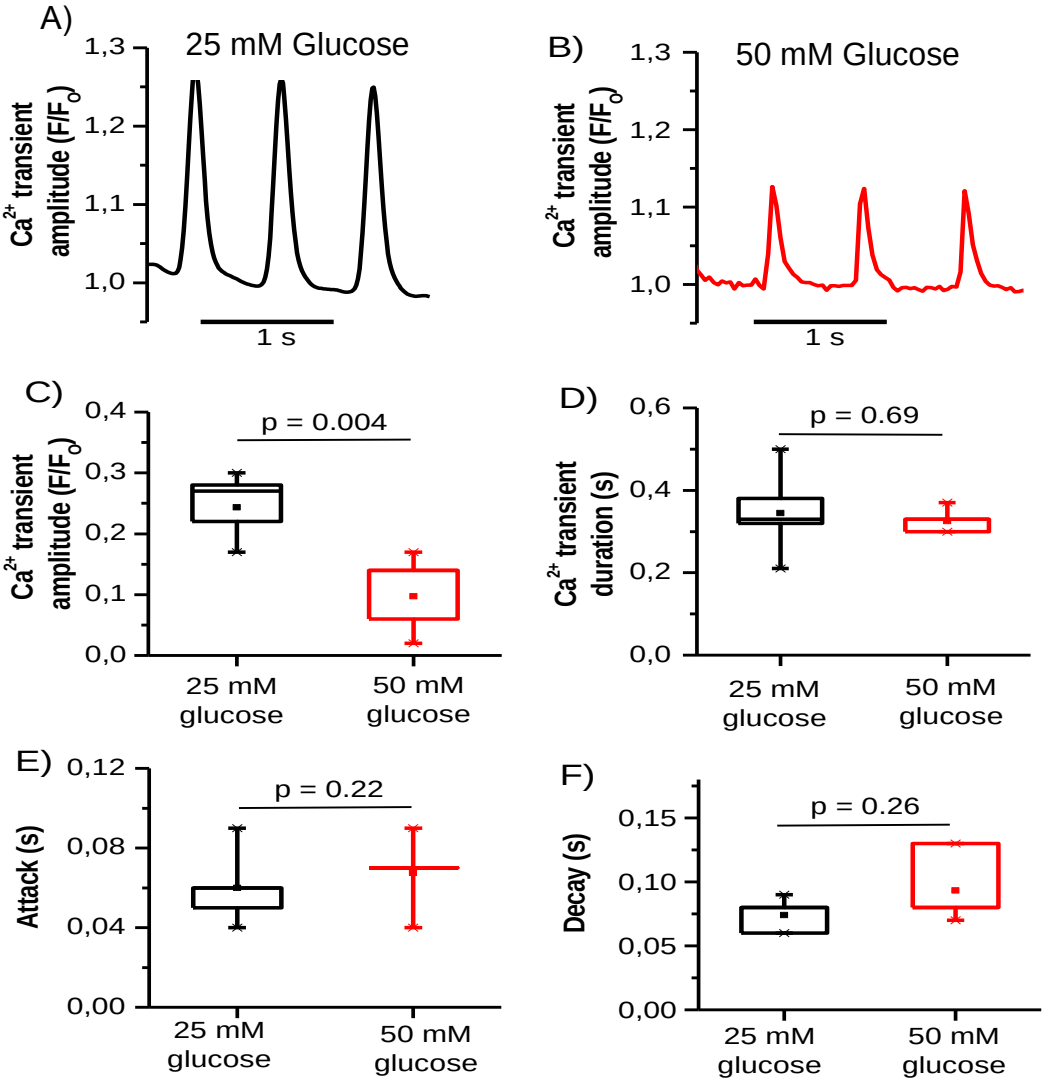

Figure 14: Effects of hyperglycaemia on the Ca^{2+} transient tracing. A–B: Representative tracings of Ca^{2+} transients recorded using Fluo-4 for 25 mM glucose (A) and 50 mM glucose (B) groups. C-F: Quantitative analysis of Ca^{2+} transient amplitude (C), duration (D), attack (E) and decay (F) under both glucose conditions. n = 4–6 EBs per group. Data are shown as box plot and the mean (■).

3.3.2.2 Effects of high glucose on Ca^{2+}handling proteins

To explore the role of key Ca^{2+} handling proteins, the ryanodine receptor and SERCA2 were evaluated. The ryanodine receptor was evaluated through caffeine stimulation (1 mM) and recording of the contractile activity on the baseline and on the

caffeine application. The amplitude of the contraction was increased by about 50% for the 25 mM glucose group in relation to the baseline amplitude while the contraction amplitude for 50 mM glucose group was increased by only about 10% for caffeine stimulation relative to baseline amplitude. Therefore, high glucose significantly decreased the caffeine-induced change in the amplitude of cellular contraction (P = 0.02 for 50 mM glucose versus 25 mM glucose group, Figure 15).

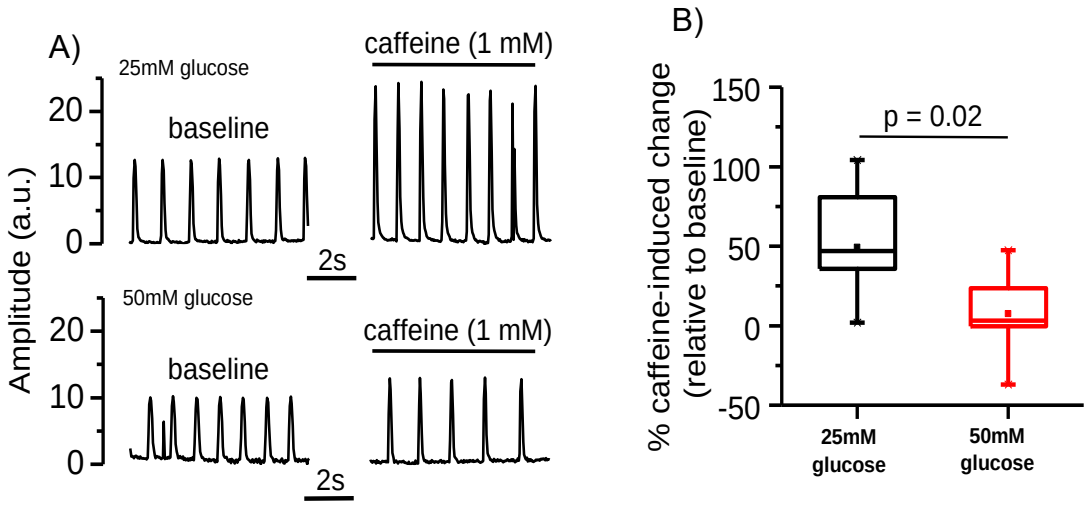

Figure 15: Effects of caffeine on contractile activity of pulsatile embryoid bodies in both glucose groups. A: Tracings of the contractile activity of pulsatile EBs before and during caffeine application, with the amplitude expressed as arbitrary units (a.u.) for 25 mM glucose (upper panel) and 50 mM glucose (lower panel). B: Quantitative analysis of the percentage of the changes in the amplitude of contraction in response to caffeine (n = 7 EBs per group). Data are shown as box plot and the mean.

The expression of SERCA 2 was evaluated via immunostaining and western blot analysis. Immunostaining showed the expression of SERCA 2 in both glucose groups. Both groups stained positive for SERCA 2, and it is well localized with α-actinin 2 (Figure 16.A). In addition, western blot analysis showed the expression of SERCA 2 in both groups. There was no significant difference in the expression of SERCA 2 (normalised to that of β-actin) between the two glucose groups (P =0.89, 50 mM glucose versus 25 mM glucose group, Figure 16.B).

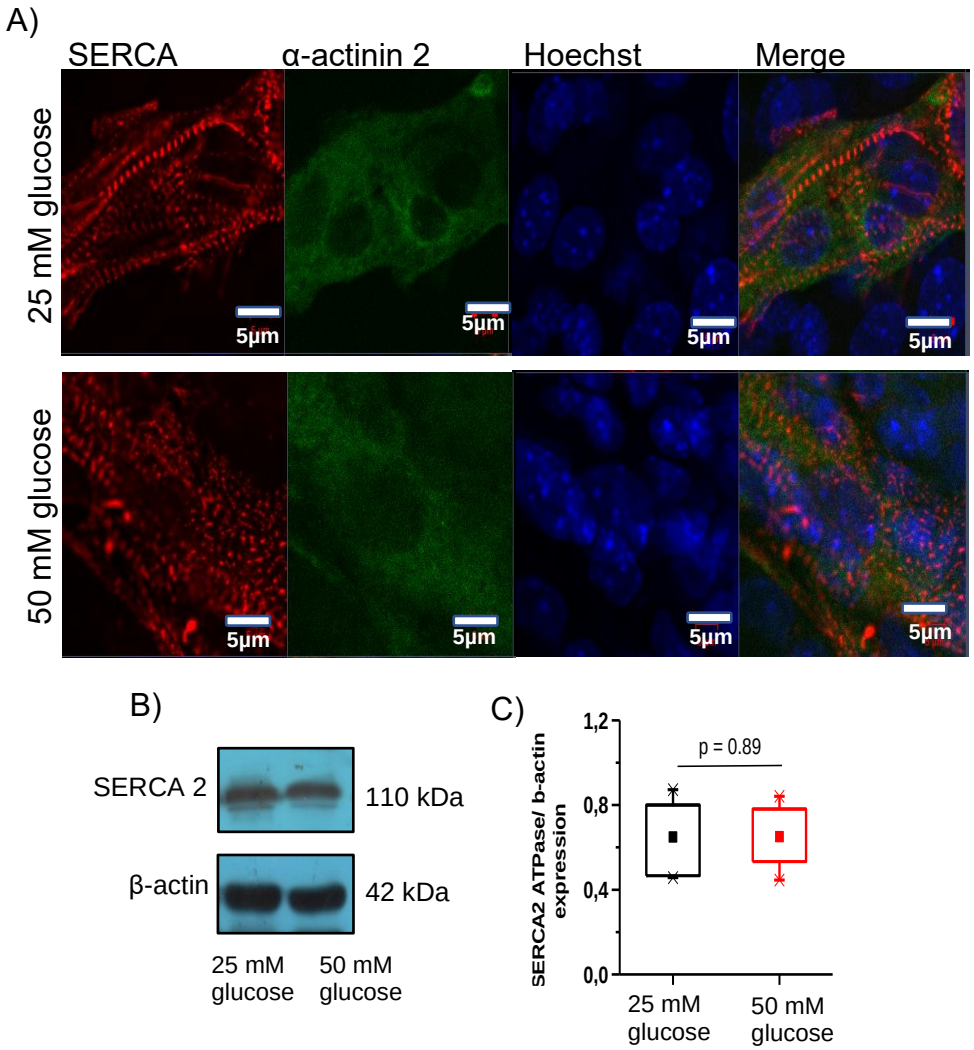

Figure 16: Effects of hyperglycaemia on sarcoplasmic reticulum Ca^{2+} handling proteins. A: Representative confocal microscopy images of SERCA 2, α-actinin 2, Hoechst, and merged images for both 25 mM and 50 mM glucose conditions. Scale bar = 5 µm. Magnification x 40. n = 3 replicates. B: Western blot images of SERCA2 and β-actin. C: Quantitative analysis of the SERCA 2 expression (normalised to that of β-actin) between the two glucose groups actin. n = 4 replicates. Data are shown as box plot and the mean. SERCA, sarco-endoplasmic reticulum calcium transport ATPase.

3.3.3 Effects of hyperglycaemia on the action potential parameters

The AP was recorded in both glucose groups using a voltage-sensitive dye (di-4 ANEPPS). Both glucose groups showed AP tracings with rapid depolarisation and

rapid depolarisation without a detectable plateau phase (Figure 17.A and B). There were no statistically significant differences in the action potential amplitude between the groups (Figure 17.C) for action potential durations at 50% and 90% repolarisation, nor in the ratio of ADP_{50}/ADP_{90} (Figure 17.D).

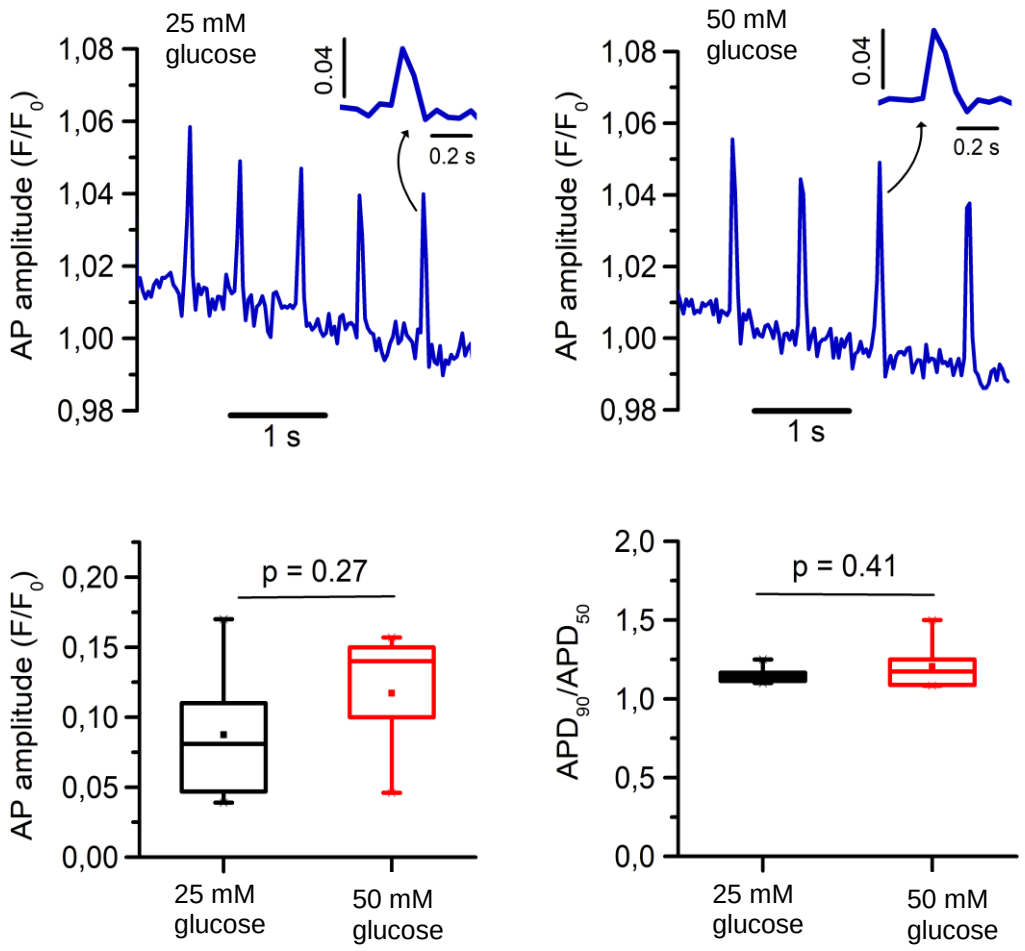

Figure 17: Effects of hyperglycaemia on action potential parameters of pulsatile EBs. A-B: Representative tracing of action potential amplitude for 25 mM glucose (A) and 50 mM glucose (B) groups. C and D: Quantitative analysis of action potential amplitude (C), APD90/ADP50 under different glucose conditions (n = 6 EBs per group). Data are shown as box plot and the mean (■). AP: action potential. The AP data were obtained using the output of the LC_Pro programme. The LC_Pro software computed an average of several APs over 6 seconds for each AP parameter value.

3.4 Effects of hyperglycaemia on structural changes of mESCs into cardiac-like cells

3.4.1 Effects of hyperglycaemia on embryoid body growth

To access the effect of high glucose on EB growth, the EB diameter was measured on day 3 and day 7 of differentiation. On day 3, the EB diameter in the 50 mM glucose group was 223 ± 13 µm compared to the 25 mM glucose group 278 ± 11 µm (P=0.01, 50 mM glucose group versus 25 mM glucose group) (Figure 18.C). The EB diameter on day 7 was 492 ± 16 µm for the 25 mM glucose group and 489 ± 20 µm for the 50 mM (P < 0.05, 50 mM glucose group versus 25 mM glucose group, Figure 18.D).

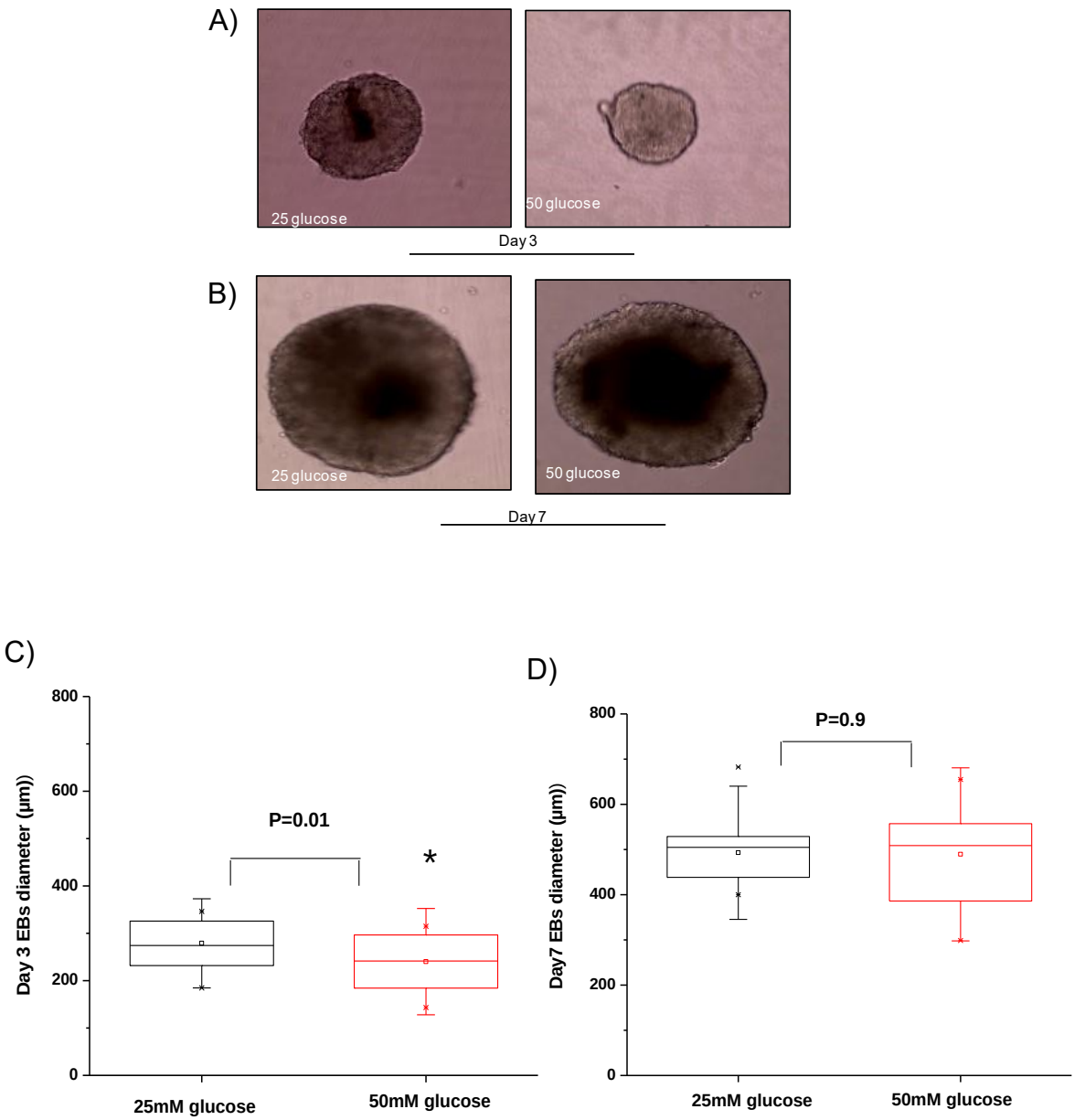

Figure 18: Effects of hyperglycaemia on the embryoid body diameter. A, B: Representative transmitted-light microscopy images of individual EBs on day 3 (A) and day 7 (B) of differentiation cultured under the two different glucose conditions, microscope objective x10. C, D: Quantitative analysis of EB diameter Day 3 (C), Day 7 (D) of differentiation. *P < 0.05 for 50 mM glucose versus 25 mM glucose group. n = 5 independent cell culture batches for both glucose groups and ≥ 16 EBs for each group. Data are shown as box plot and the mean (■).

3.4.2 Effects of hyperglycaemia on the expression of cardiac specific proteins

To evaluate effects of the 50 mM glucose on the expression of cardiac contractile proteins, beating EBs (day 12–15) co-stained positive for α-actinin 2 and cTnT. Both glucose groups showed cardiac myofilament proteins with spatial distribution appearing as alternating striations of myofibrillar assembles. The high 50 mM glucose significantly reduced the fluorescence intensity of both α-actinin 2 and cTnT relative to that of the Hoechst-stained nuclei ($P < 0.05$ for 50 mM glucose versus 25 mM glucose group for each protein, Figure 19).

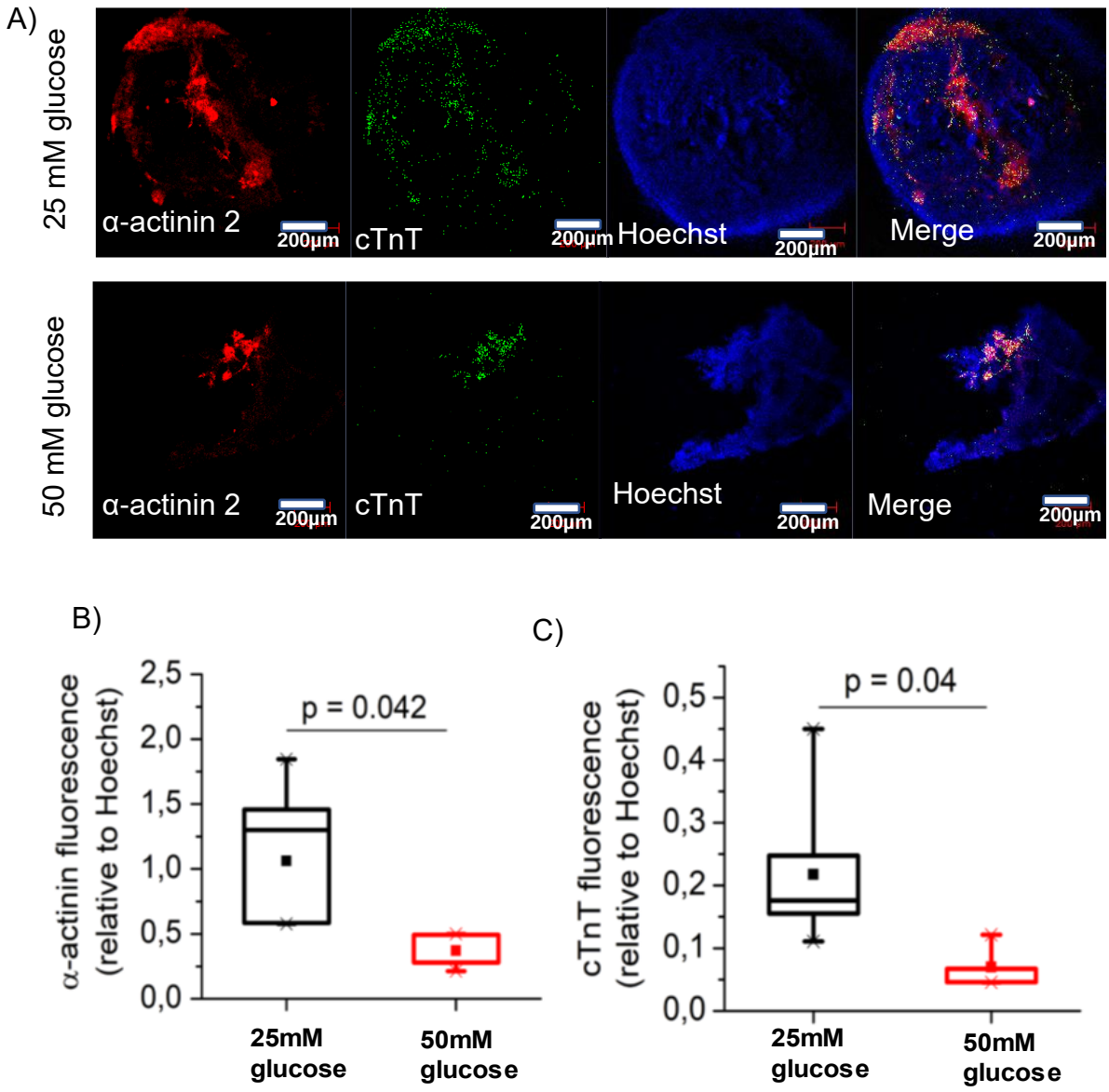

Figure 19: Effects of hyperglycaemia on the expression of cardiac contractile proteins. A: Low-magnification (10x) confocal microscopy images of EBs showing α-actinin 2, cTnT, Hoechst, and merged images for 25 mM glucose (upper panel), and 50 mM glucose (lower panel). Scale bar = 200 µm. Magnification x 10. B-C: Quantitative analysis of the fluorescence intensity of α-actinin 2 (B) or cTnT(C), comparative to that of the Hoechst (n = 4-6 EBs per group). Data are shown as box plot and the mean (■). cTnT: cardiac troponin T.

3.4.3 Effects of hyperglycaemia on cardiac sarcomeric organization

To evaluate the effect of high glucose on sarcomeric organization, beating EBs were immunostained with α-actinin 2 and MHC (α and β isoforms), which are the most abundant contractile sarcomeric proteins. High glucose (50 mM) substantially disrupted the α-actinin 2 striated organization pattern and generated a more mottled appearance (P = 0.04 for 50 mM glucose versus 25 mM glucose group, Figure 20.A and C). In addition, high glucose transformed the bands of MHC and induced an amorphous sarcomeric distribution (Figure 20.B). Qualitatively, high glucose reduced the number of fluorescence-stained MHC cells.

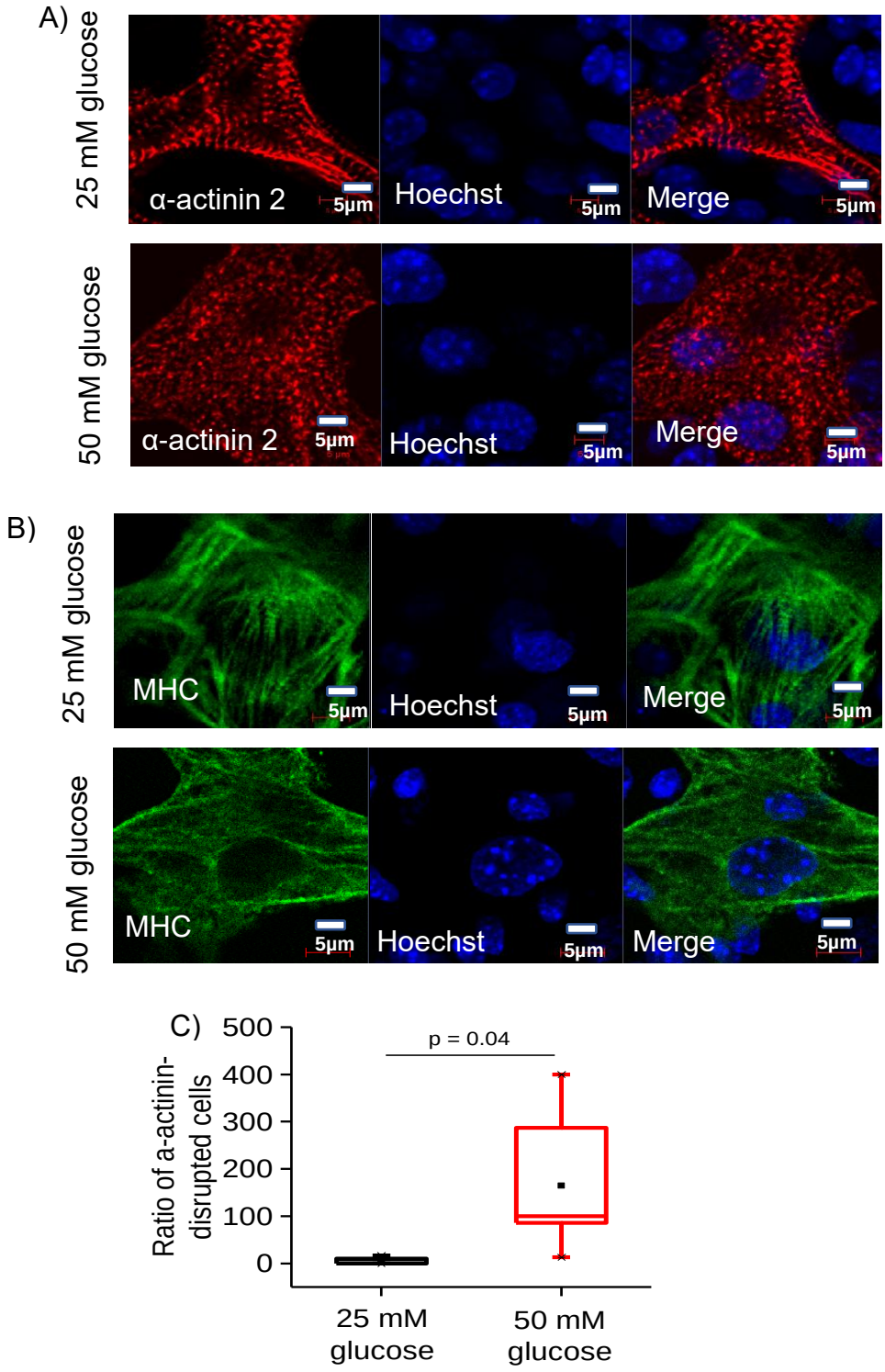

Figure 20: Effects of hyperglycaemia on the sarcomeric organization of cardiac contractile proteins. A: Representative confocal microscopy images of α-actinin 2, Hoechst, and merged images of 25 mM glucose (upper panel), and 50 mM glucose (lower panel). B: Representative confocal microscopy images of MHC, Hoechst, and merged images of 25 mM glucose (upper panel), and 50 mM glucose (lower panel). Scale bar = 5 µm. Magnification x 40. C: Quantitative analysis of the fraction of α-actinin-disrupted cells, relative to total cells. (n = 5–6 EBs per group). Data are shown as box plot and the mean (■). MHC: myosin heavy chain (α and β isoforms).

3.4.4 Effect of hyperglycaemia on cell proliferation

To determine the effects of hyperglycaemia on cell proliferation, adhered EBs were stained with Click-iT EdU. Both glucose groups stained positive for EdU (Figure 21.A). Quantitative analysis of the EdU stained nuclei relative to the total nuclei in the α-actinin stained area showed no significant differences between the 2 groups ($P > 0.05$ for 50 mM glucose versus 25 mM glucose group, Figure 21.B).

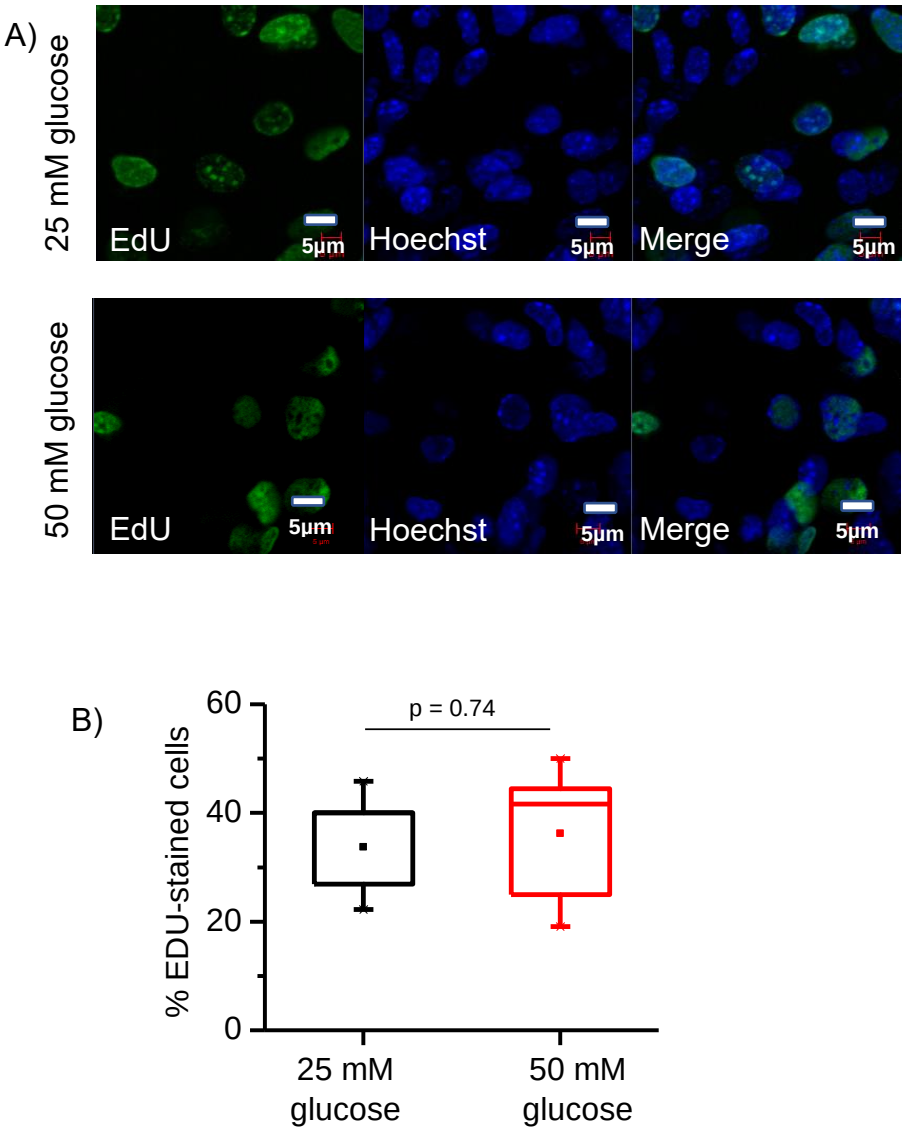

Figure 21: Effect of hyperglycaemia on cell proliferation. A: Confocal microscopy images of 5-ethynyl-2-deoxyuridine (EdU), Hoechst, and merged images for 25 mM glucose (upper panel) and 50 mM glucose (lower panel) groups. Scale bar =5 µm. Magnification x 40. B: Quantitative analysis of % EdU-positive nuclei relative to total (n = 4–6 EBs per group). Data are shown as box plot and the mean (■).

In addition, we evaluated the changes in the expression of RAGE, which is one of the key factors that mediate degenerative myocardial inflammatory responses and fibrosis (Bangert et al. 2016). The western blot results showed a positive expression of RAGE in both glucose conditions (Figure 22.A), but there was no statistically

significant difference in the RAGE expression between 25 mM and 50 mM glucose groups (P > 0.05 for 50 mM glucose versus 25 mM glucose group, Figure 22.B).

Furthermore, we tested whether there is a change in the TGF-β1, which is known to induce interstitial fibrosis (Rosenkranz et al. 2002). The western blot images showed a positive baseline expression of TGF-β1 in both glucose conditions (Figure 22.C), but there was no statistically significant difference in the TGF-β1 expression between the baseline- and high glucose groups (P > 0.05 for 50 mM glucose versus 25 mM glucose group, Figure 22.C).

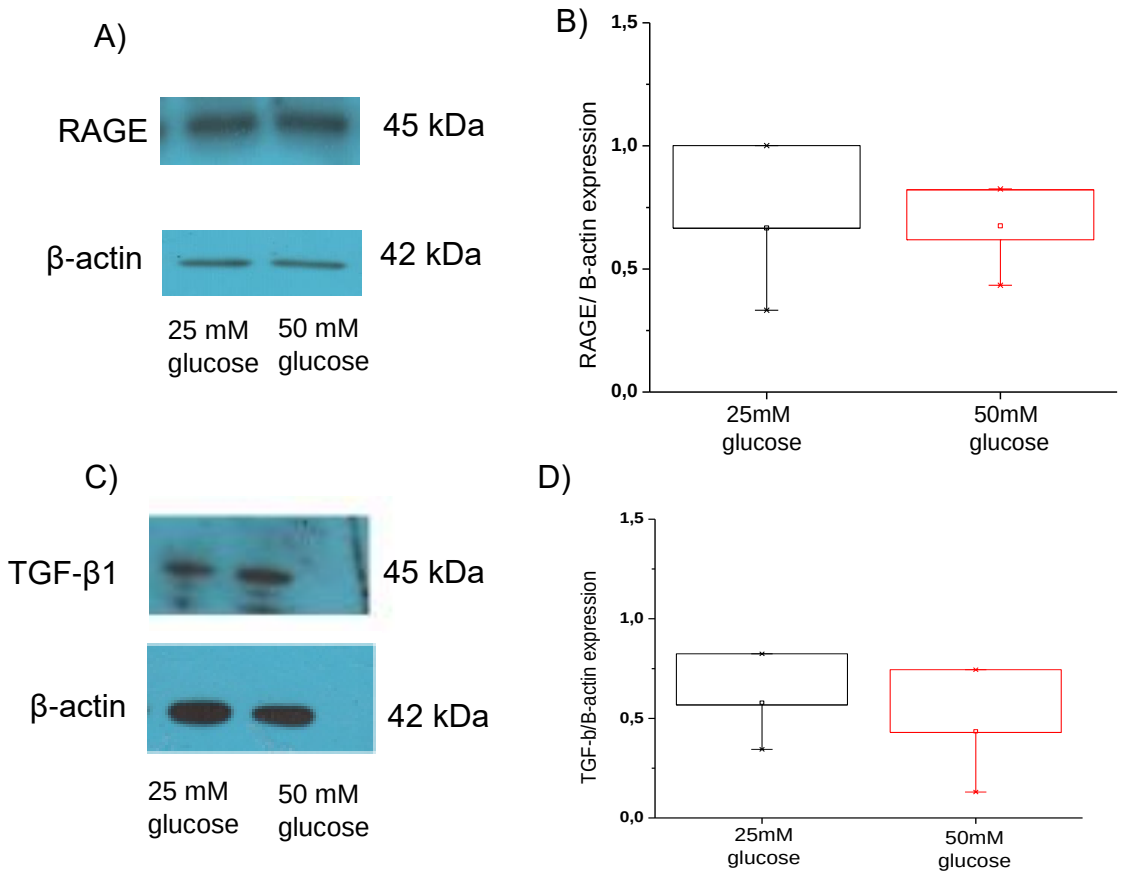

Figure 22: Effect of hyperglycaemia on the expression of fibrotic markers. A: Western blot images of the receptor of advanced glycation end-product (RAGE) and β-actin. B: Quantitative analysis of RAGE expression, relative to that of β-actin (n = 3 replicates). C: Western blot images of transforming growth factor-β (TGF-β1) and β-actin. D: Quantitative analysis of TGF-β1expression, relative to that of β-actin (n = 3 replicates). Data are shown as box plot and the mean (■).

3.4.5 Effects of hyperglycaemia on cardiac cellular degenerative changes

3.4.5.1 TUNEL assay analysis

Since hyperglycaemia induced changes in morphological and functional characteristics of the beating EBs, we investigated the role of apoptosis as the underlying factor causing such effects. The TUNEL assay was performed to detect the apoptotic cells. In cells co-stained with TUNEL and α-actinin 2, the TUNEL-positive nuclei and Hoechst-stained nuclei within the regions positive for α-actinin were counted in both 50 mM glucose and 25 mM glucose. The fraction of TUNEL-positive nuclei in α-actinin-positive cells was statistically significantly higher in 50 mM glucose ($P = 0.03$ for 50 mM glucose versus 25 mM glucose, Figure 23).

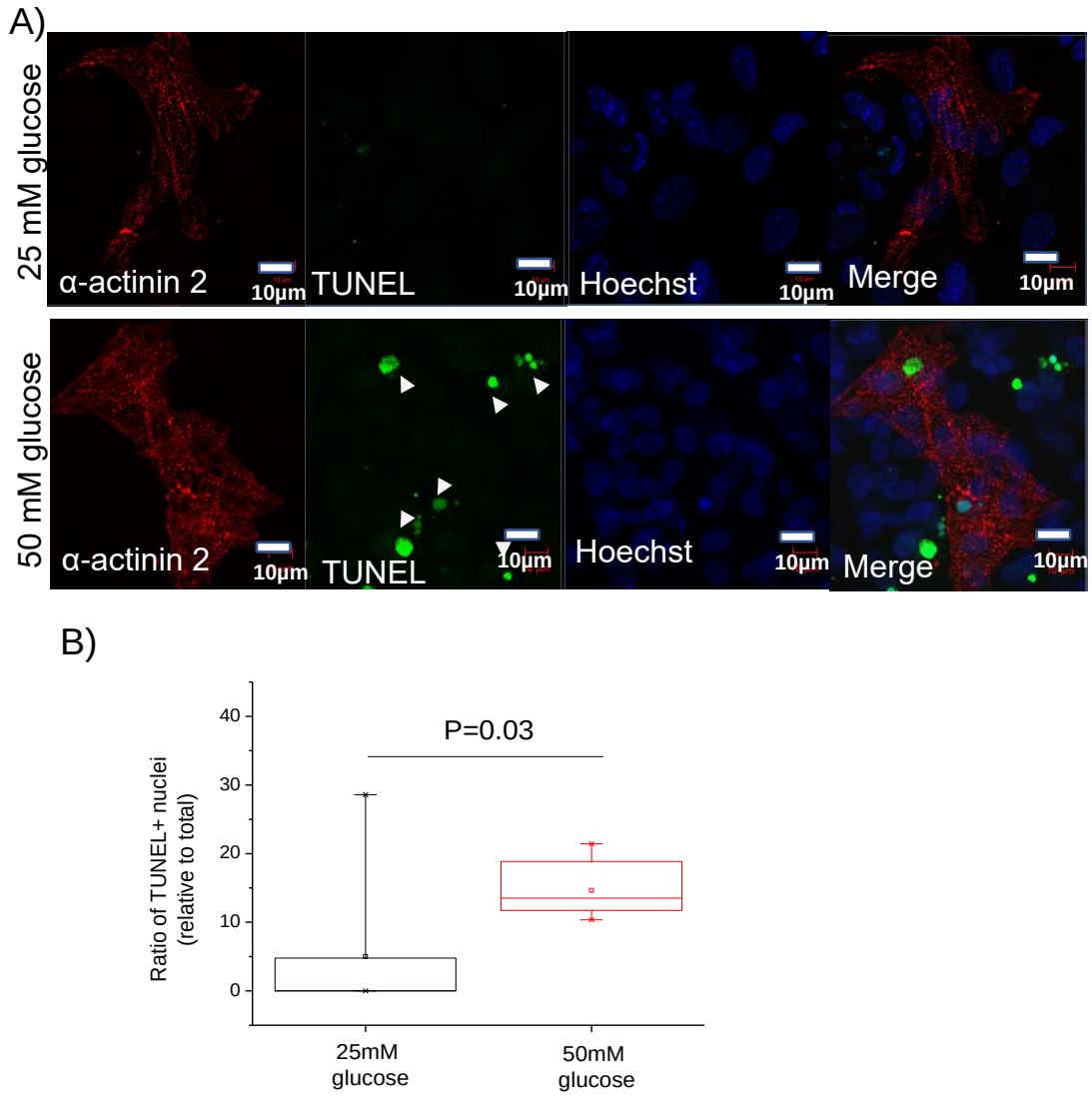

Figure 23: Hyperglycaemia-induced cellular apoptosis in mESCs derived cardiac-like cells. A: Representative confocal microscopy images of α-actinin 2, TUNEL, Hoechst and merged images for 25 mM glucose (upper panel) and 50 mM glucose (lower panel) groups. TUNEL-positive nuclei in α-actinin-positive areas are indicated by white arrowheads. Scale bar = 10 µm. Magnification x 40. B: Quantitative analysis of TUNEL-positive nuclei in α-actinin-positive cells, n = 5 replicates per group. TUNEL: terminal deoxynucleotidyl transferase dUTP nick-end labelling. Data are shown as box plot and the mean (■).

3.4.5.2 Effects of hyperglycaemia on mitochondrial components

Since mitochondria play a vital role in the process of cell death, we next evaluated the mitochondrial status and mitochondrial specific proteins, which could mediate the cellular apoptosis processes. The mitochondrial status of the EBs was assessed

using Mitotracker Green staining. The images were taken from beating areas of EBs. There was uptake of Mitotracker Green in the areas around the Hoechst-positive nuclei (equivalent to cytoplasmic regions) of beating EBs in both glucose groups (Figure 24.A). There were no statistically significant differences in the Mitotracker Green fluorescent intensity between 50 mM- and 25 mM glucose groups (P = 0.76 for 50 mM glucose versus 25 mM glucose, Figure 24.B).

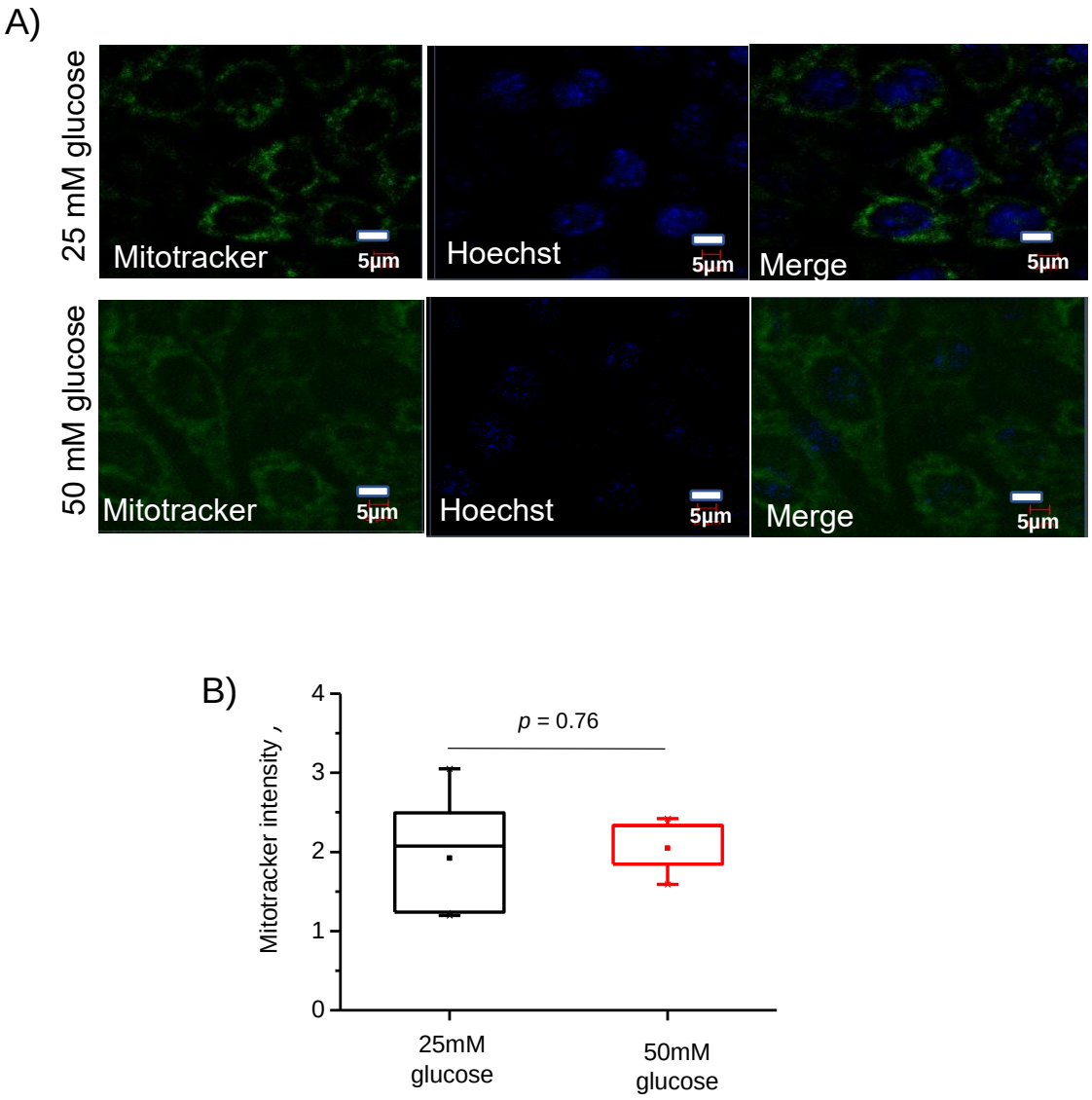

Figure 24: Effect of hyperglycaemia on the mitochondrial mass of mESCs derived cardiac-like cells. A: Representative confocal microscopy images of Mitotracker Green and merged images of Mitotracker Green and Hoechst for 25 mM glucose (upper panel) and 50 mM glucose (lower panel) groups. Magnification 20x. Scale bar = 5 µm. B: Quantitative analysis of the cellular Mitotracker Green fluorescence intensity. n = 4–6 replicates per group. Data are shown as box plot and the mean (■).

In order to test whether the mitochondria specific proteins were implicated in apoptosis, we performed immunoblotting for cytochrome c, which is the main component of the electron transport chain within the mitochondria. The result showed that the expression of cytochrome c in the 50 mM glucose group was significantly increased compared to that in 25 mM glucose group (P = 0.02 for 50 mM glucose group versus 25 mM glucose group, Figure 25).

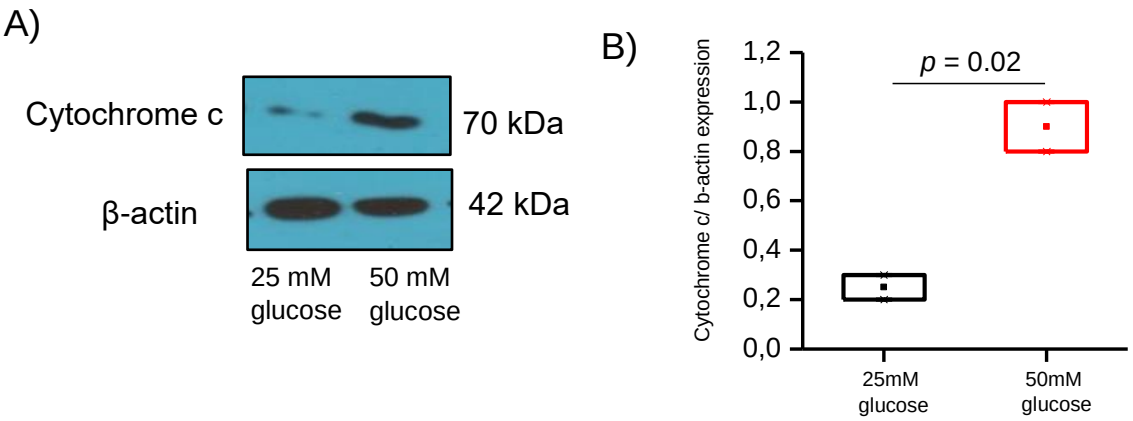

Figure 25: Effect of hyperglycaemia on mitochondrial proteins of mESCs derived cardiac-like cells. A: Western blot images of cytochrome c and β-actin. B: Quantitative analysis of cytochrome c expression (relative to that of β-actin). n = 3 replicates. Data are shown as box plot and the mean (■).

We further evaluated whether there was mitochondrial dysregulation via OPA1, which plays a key role in normal mitochondrial fusion structure and function and implicated in cardiac apoptosis (Chen et al. 2009). There was no statistically significant difference in the expression of OPA1 in the 50 mM glucose group compared to that in the 25 mM glucose group (P = 0.8 for 50 mM glucose group versus 25 mM glucose group, Figure 26).

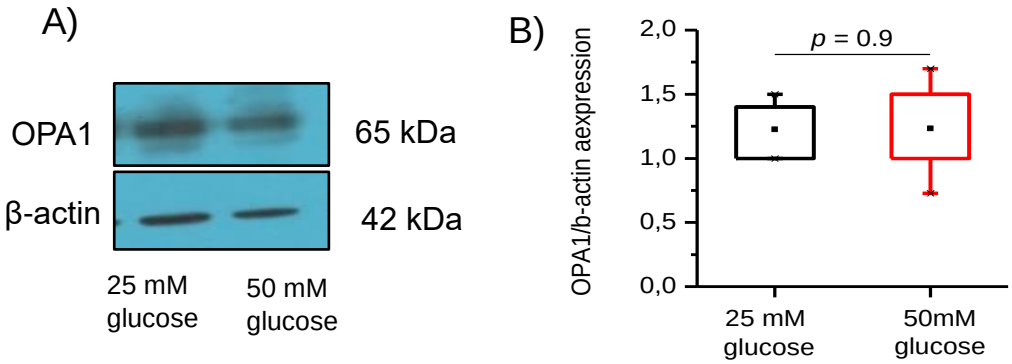

Figure 26: Effect of hyperglycaemia on the expression of mitochondria fusion protein of mESCs derived cardiac-like cells. A: Western blot images of OPA1 and β-actin. B: Quantitative analysis of the protein expression (relative to that of β-actin) of OPA1. n = 4 replicates. Data are shown as box plot and the mean (■). OPA1: the optic atrophy protein 1.

In addition, the anti-apoptotic protein Bcl-2, and pro-apoptotic Bax proteins were also immunoblotted. The expression of Bcl-2 was decreased (P= 0.014, 50 mM glucose versus 25 mM glucose group, Figure 27.A and B), whereas there were no significant differences in Bax expression between the two glucose groups (P > 0.05 for 50 mM glucose versus 25 mM glucose group, Figure 27.C, and D).

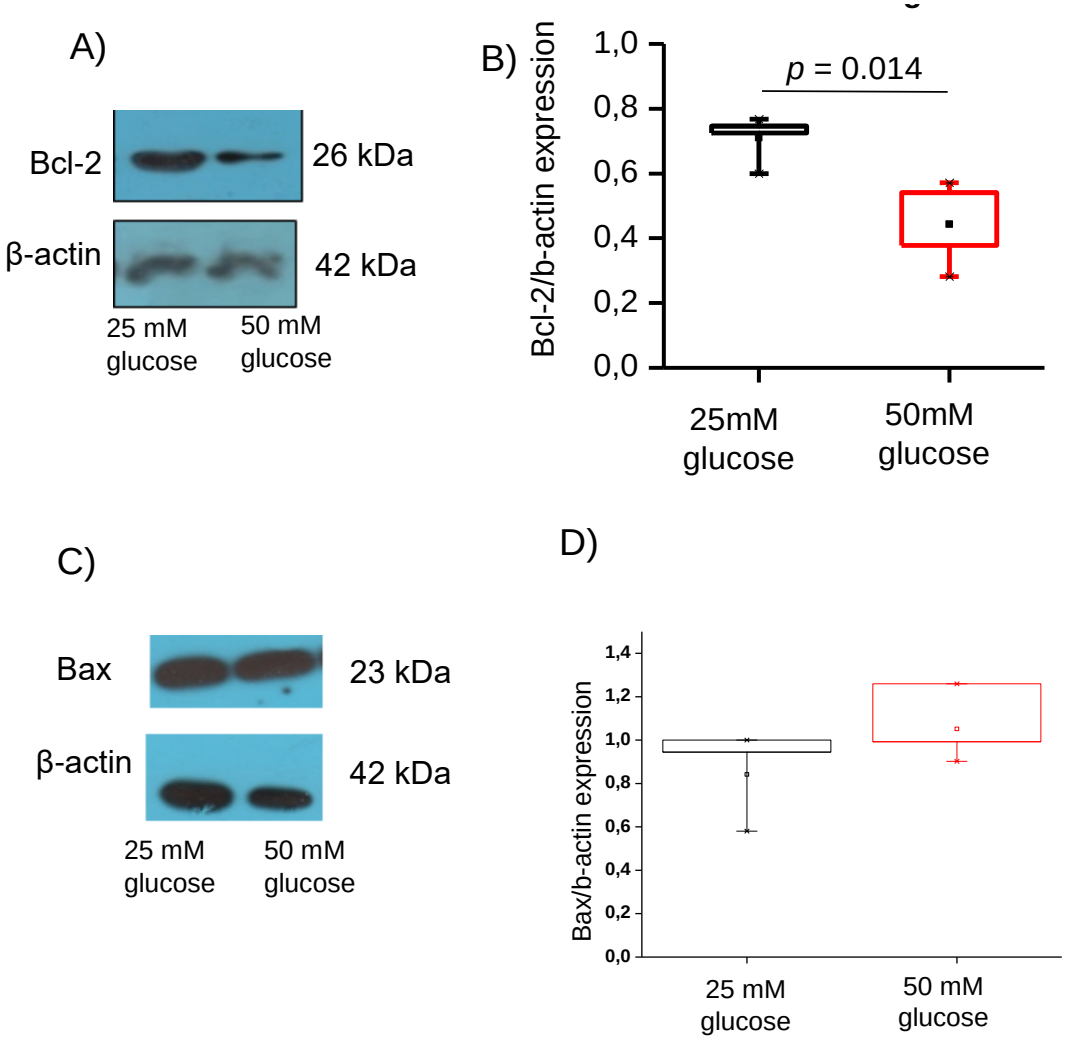

Figure 27: Effects of hyperglycaemia on the expression of the anti/pro-apoptotic proteins of mESCs derived cardiac-like cells. A: Western blot images of Bcl-2 and β-actin. B: Quantitative analysis of the Bcl-2 protein expression (relative to that of β-actin). n = 4 replicates. C: Western blot images of Bax and β-actin. D: Quantitative analysis of the Bax protein expression (relative to that of β-actin). n = 3 replicates. Data are shown as box plot and the mean (■).

3.4.5.3 Contributions of oxidative stress

To evaluate for the possible contribution of hyperglycaemia-induced oxidative stress, we assessed the presence of the oxidative stress marker nitrotyrosine (Ceriello et al. 2001). The beating EBs in 25 mM and 50 mM glucose groups were co-stained for α-actinin 2 and nitrotyrosine. The confocal microscope images showed relatively higher fluorescence signals of nitrotyrosine in high glucose compared to baseline glucose conditions (Figure 28.A). High glucose induced a statistically significant increase in the expression of nitrotyrosine in α-actinin 2 positive cardiac-like cells ($P = 0.044$ for 50 mM glucose versus 25 mM group, Figure 28.B).

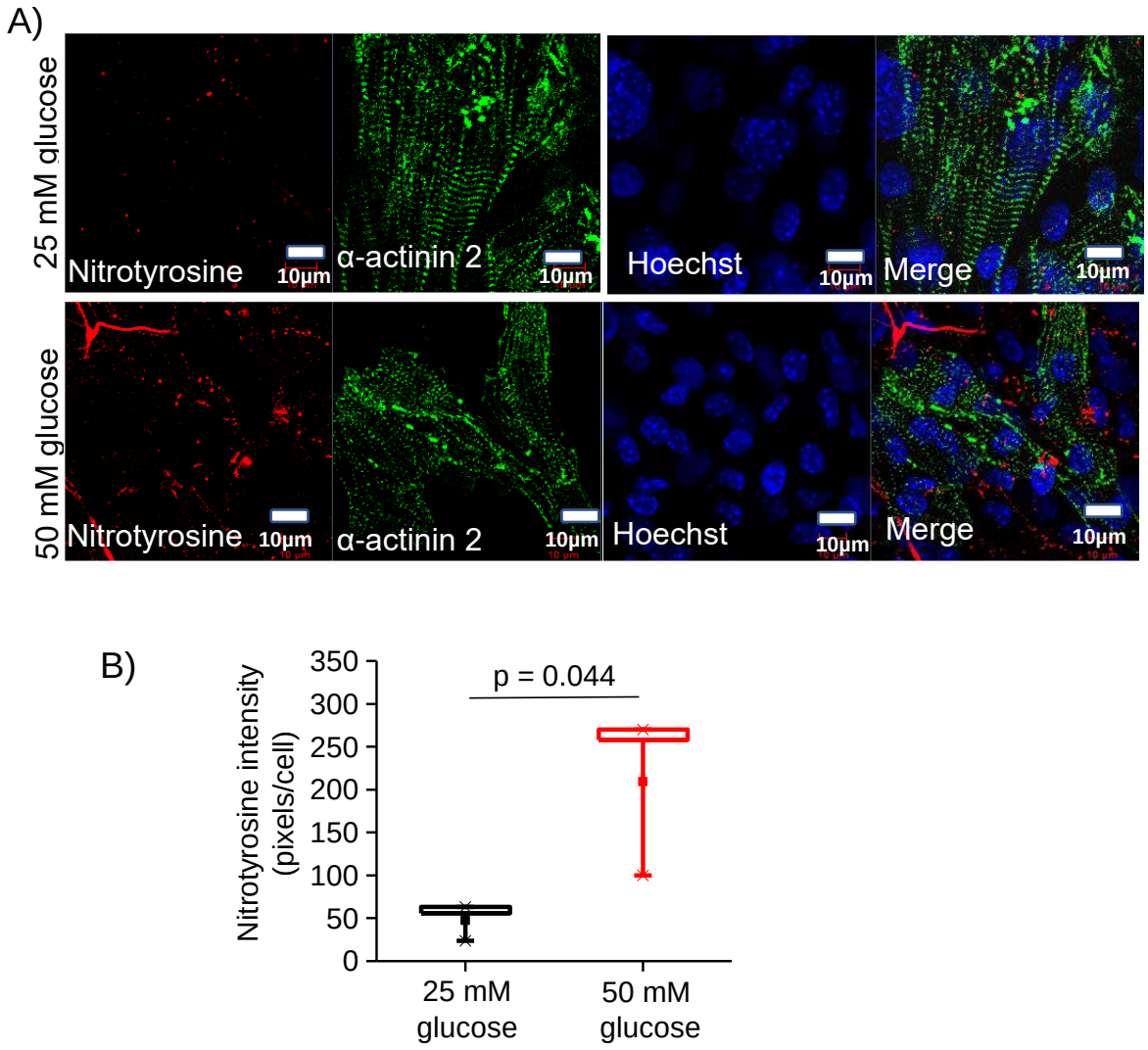

Figure 28: Hyperglycaemia-induced oxidative stress of mESCs derived cardiac-like cells. A: Confocal microscopy images of nitrotyrosine, α-actinin 2, Hoechst, and merged images for 25 mM glucose (upper panel) and 50 mM glucose (lower panel) groups. Scale bar = 10 µm. Magnification 40x. B: Quantitative analysis of the nitrotyrosine fluorescence intensity, relative to the number of nuclei in α-actinin 2 positive cells (n = 3 EBs per group). Data are shown as box plot and the mean (■).

We further evaluated the effect of the treatment with the antioxidant NAC. In EBs cultured under 25 mM glucose conditions, there was a minimal number of TUNEL-stained nuclei in α-actinin 2 positive cells, while those cultured in 50 mM glucose had numerous TUNEL-stained nuclei (Figure 29.A). Therefore, high glucose statistically significantly augmented the number of TUNEL-stained nuclei ($P < 0.05$, 50 mM glucose versus 25 mM glucose group). Treatment with NAC significantly reduced the

number of TUNEL-stained nuclei in EBs cultured under high glucose conditions ($P < 0.05$ for 50 mM glucose versus 25 mM glucose group, Figure 29.B). In addition, NAC treatment significantly decreased the number of cells with a disrupted striated pattern of α-actinin 2 compared to those cultured under high glucose alone ($P < 0.05$ for 50 mM glucose with NAC treatment versus 50 mM glucose group without NAC treatment, Figure 29.C).

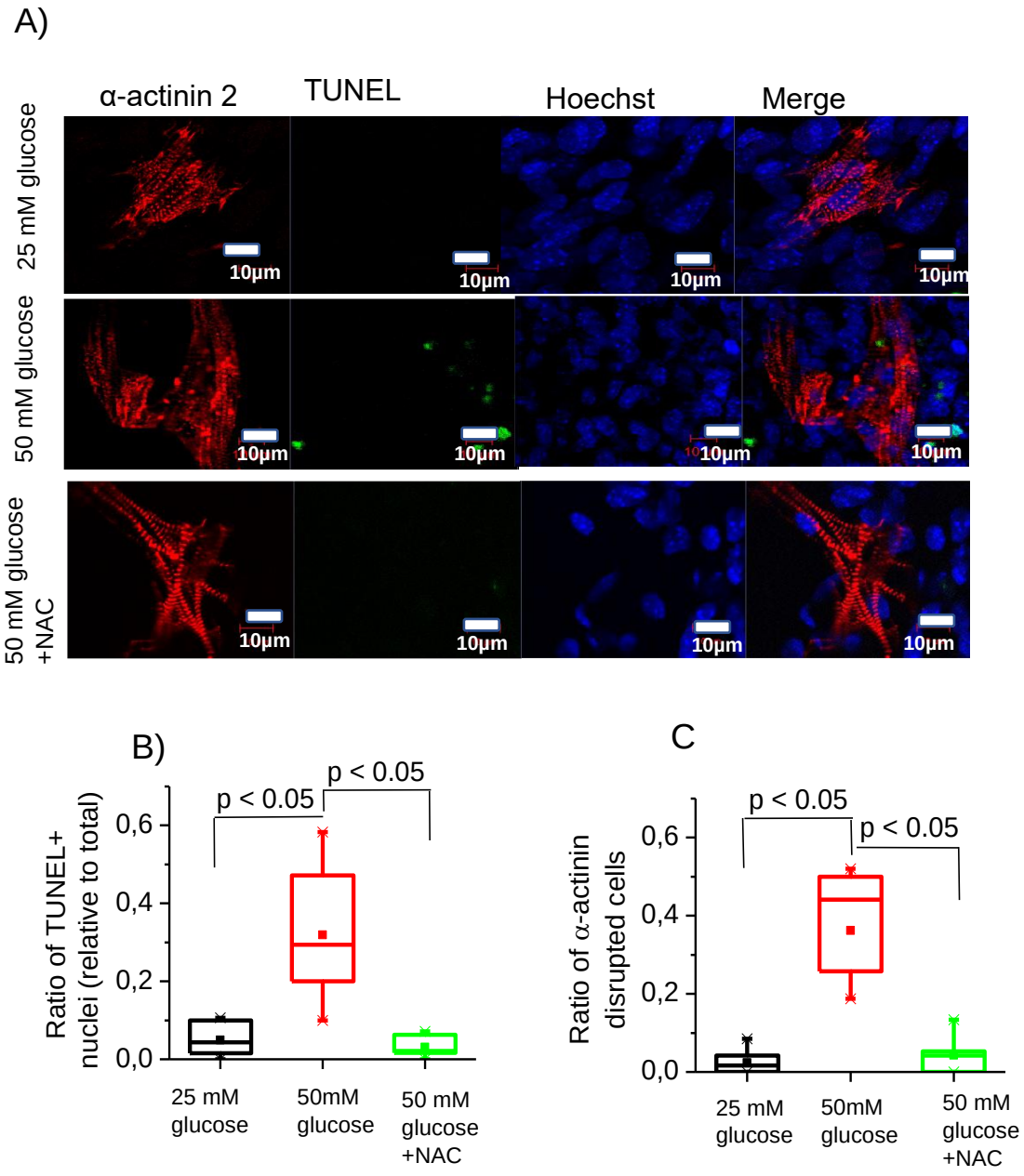

Figure 29: Effects of antioxidant treatment. A: Confocal microscopy images of actinin 2, TUNEL, Hoechst, and merged images for 25 mM glucose (upper panel) and 50 mM glucose (middle panel) and 50 mM treated with NAC groups. Scale bar = 10 µm. Magnification 40x. B: Quantitative analysis of the fraction of TUNEL-positive nuclei relative to total nuclei. C: Quantitative analysis of the fraction of α-actinin-disrupted cells, relative to total (n ≥ 6 EBs per group). Data are shown as box plot and the mean (■). TUNEL, terminal deoxynucleotidyl transferase dUTP nick-end labelling, NAC: N-acetyl cysteine.

Chapter 4: Discussion

This study showed that hyperglycaemia suppressed mESC differentiation into cardiac-like cells and induced contractile dysfunction of spontaneously-pulsatile cells. In addition, hyperglycaemia impaired the myofibrillar organization and decreased the expression of the cardiac myofilament proteins. These suppressive effects of hyperglycaemia on mESC cardiac differentiation were likely mediated by mitochondrial-dependent apoptosis and triggered by oxidative stress as well as by abnormal Ca^{2+} signalling.

4.1 Mouse embryonic stem cell differentiation into cardiac-like cells

In this study, mESCs were successfully differentiated into cardiac-like cells as was indicated by the presence of spontaneous, cardiac-like pulsatile characteristics and the expression of cardiac-specific biomarkers. The use of pluripotent mESCs was essential in the present study for establishing the basis of *in-vitro* differentiation. The evidence for the pluripotency was supported by the expression of the master transcription factors such as Nanog and Oct3/4 in mESC, which are important regulators of early development and stem cell identity (Boyer et al. 2005). In addition, the ability of mESC to differentiate into each of the three primary germ layers is taken as evidence of pluripotency (Wobus et al 2002). Maintaining the pluripotency of the stem cells is essential to ensure the ability of the stem cells to self-renew and to differentiate into specific cell types. The mESCs can maintain their ability to self-renew continuously for years if they are cultured in conditions that prevent their differentiation such as the presence of a feeder layer and growth factors like LIF (Burdon et al. 1999). In fundamental research, stem cells represent an effective system to investigate gene function and the physiological activities arising for the duration of development. In addition, a stem cell model will help to discover new diagnostic and prognostic biomarkers and to assess drugs discovery (Shi et al.

2020). However, although the mESC derived cardiac-like cells has been shown to recapitulate early cardiogenesis (Fijnvandraat et al. 2003), the resultant EB colonies include a variety of other non-cardiac cell types that interact via cell-cell contact and gap junctions (Lee, Cagavi Bozkulak, et al. 2011, Wobus et al. 2002). In this study, to overcome the alterations in cell proliferation and discrepancy in the composition of cells in EBs and the heterogeneity EB beating characteristics, the starting number of mESC seeded into hanging drops were fixed (Kowalski et al. 2012).

The mESC derived cardiac-like cells were characterized functionally and structurally. In the current study, the results showed that the spontaneous contraction of cell clusters started on day 9 of differentiation and increased gradually displaying functional properties consistent with early-stage cardiomyocytes (Zhang et al. 2012). In addition, the beating cell clusters showed spontaneous action potentials and Ca^{2+} transient signals. Furthermore, the beating cells showed a chronotropic response of to β-adrenergic stimulation using isoprenaline through the acute application of isoprenaline (1 µM), which induced a significant increase in the beating rate (Figure 6), thereby indicating physiological responses to catecholamine stimulation as expected in normal cardiac cells. For cardiac structural characteristics, the differentiated pulsatile mESCs expressed specific cardiac myofilament proteins such as α–actinin 2, cTnT, and cardiac MHC as well as gap junction protein Cx43. These findings confirm the cardiac like, functional and structural characteristics of the differentiated pulsatile cells.

There has been a lack of clarity in the literature regarding the optimal glucose concentration appropriate for mouse stem cell cardiac differentiation. Although *in-vivo* physiological glucose concentration is maintained at approximately 5.5 mM glucose, it has been shown that this glucose level does not promote embryonic stem cell differentiation into cardiac-like cells (Guan, Fürst, and Wobus 1999). In another study, Yang and colleagues showed that 5.5 mM glucose could produce superior cardiac differentiation of stem cells compared to 25 mM glucose levels (Yang et al. 2016). However, the results of the present study showed that the 5.5 mM did not generate a superior cardiac functional phenotype compared to 25 mM glucose.

Therefore, in this study, 25 mM glucose was used as the control glucose level and there was effective *in-vitro* differentiation of mESC into cardiac-like cells under such conditions. These findings were consistent with previous studies that reported enhanced *in-vitro* cardiac differentiation of stem cells in 25 mM glucose levels. A study by Crespo et al. (Crespo et al. 2010) observed that the 25 mM glucose concentration promotes mESC cardiac differentiation attributed to the production of stimulatory ROS. In addition, a study by Guan et al. (Guan, Fürst, and Wobus 1999) showed that the cardiac differentiation of mouse embryonic stem cells in medium with 25 mM glucose was significantly enhanced compared to 5.5 mM glucose conditions.

In the present study, the percentage of beating EBs was generally lower in 5.5 mM glucose than in 25 mM glucose conditions throughout the observation period (Figure 9). These results are consistent with those in a previous study by Mochizuki et al. (Mochizuki, Ohnuki, and Kurosawa 2011) who showed that the efficiency of mESC differentiation into cardiac-like cells was significantly higher in the 25 mM glucose than in the 5.5 mM glucose condition. Furthermore, the findings of the present study were consistent with those from a study by Crespo et al. (Crespo et al. 2010) in which the supraphysiological 25 mM glucose level was vital for cardiomyocyte generation. Consequently, it is likely that the optimal baseline glucose condition depends on the specific stem cell line studied and on the type of protocol used for the differentiation. In the present study, the mESC were spontaneously differentiated into pulsatile cardiac-like cells without additional modification such as glucose-adaptive protocols used in other studies (Yang et al. 2016).

4.2 Hyperglycaemia-induced structural and electrical alterations in stem cell derived cardiac like cells

The standard baseline glucose of 25 mM used in the present study was in accordance with that used in other mESC studies (Ali et al. 2004, Crespo et al. 2010, Guan, Fürst, and Wobus 1999). The model of hyperglycaemia of 50 mM glucose used in the present study has also been used by others in a hyperglycaemia model of a cardiac-like cell line, H9C2 (Du et al. 2018, Han et al. 2015, Xu et al. 2020), and in non-cardiac cells such as neuronal cells (Mohammadi-Farani, Ghazi-Khansari, and Sahebgharani 2014, Russell et al. 1999). This high glucose deviates substantially from clinical conditions, but in the present study, 50 mM glucose represents a doubling of baseline levels (25 mM), which is the same magnitude of change that takes place between physiological levels (5.5 mM) and the diabetic threshold (11 mM).

The present study showed that of 50 mM glucose impaired the EB development and maturation. The EB size on day 3 of differentiation was significantly lower in high glucose compared to standard glucose conditions, indicating that hyperglycaemia inhibited the EB growth. However, by day 7 of differentiation, the EB diameter was no different between the two glucose groups, possibly suggesting a greater sensitivity of mESC to glucotoxicity during the early stage of cellular growth (Kolwicz and Tian 2011). The results of the present study showed that hyperglycaemia reduced the total number of beating EBs and reduced their beating rate. Taken together, these findings suggest that the functionality of cardiomyocytes derived from mESC was impaired by hyperglycaemia. For the beating pattern, there was a decrease in beating rate with time, towards day 19 of differentiation creating a dome-shaped trend. This subsequent decrease in beating rate could be due to the maturation of the cardiac-like cells, with more cells becoming ventricular-like and therefore losing their intrinsic pacemaking ability (Guan, Fürst, and Wobus 1999). An alternative explanation could be that as the microtubular content of cells increases with maturation, the beating capacity is down-regulated, since a greater content of microtubules has been shown to suppress beating in cultured neonatal cardiac cells

(Webster and Patrick 2000). Another observation in this study is that the EBs in the high 50 mM glucose condition were less adherent on coverslips than those in 25 mM glucose conditions, suggesting that the cardiac-like cells were losing their property of adherence in hyperglycaemic conditions.

Hyperglycaemia significantly reduced the amplitude of cellular contraction, and the contractility parameters including decreasing the maximal rate of change of amplitude upstroke and downstroke (Figure 13). These results are consistent with our previous study where we observed a cardiac contractile dysfunction in a diabetic adult rat model (Aboalgasm, Petersen, and Gwanyanya 2021). In the developing heart cells, these results are consistent with those in another study where there was a cardiac dysfunction in foetal heart due to maternal hyperglycaemia (Han et al. 2015). The maximal rate of change of amplitude upstroke (+dP/dt) has been used generally as an index of cardiac contractility, while the maximum rate of change of amplitude downstroke (-dP/dt) is indicative of diastolic relaxation (Kass et al. 1987). In this study, hyperglycaemia decreased +dP/dt and elevated the -dP/dt, which both indicate contractile dysfunction.

The contractile dysfunction observed in the current study could be explained in part by abnormal changes in the cellular Ca^{2+} signalling. Hyperglycaemia significantly decreased Ca^{2+} transient amplitude without changes in Ca^{2+} transient decay time. It has also been shown that exposing cardiomyocytes to elevated extracellular glucose resulted in impaired cardiomyocyte contractility and Ca^{2+} flux (Ren et al. 1997). In addition, Belke et al. (Belke, Swanson, and Dillmann 2004) studied contractile performance and Ca^{2+} transients in Langendorff-perfused hearts and isolated cardiac myocytes. They demonstrated that in diabetic mouse hearts there was a reduction in the rate of contraction and relaxation. They further showed that the Ca^{2+} transients decay rate was significantly decreased in diabetic cardiomyocytes, indicating a reduced capacity for cytosolic Ca^{2+} removal not associated with a change in Na-Ca^{2+} exchange activity. In contrast, a study by Salem et al. (Salem et al. 2013) showed no substantial changes in Ca^{2+} transients and L-type Ca^{2+} current in diabetic cardiomyocyte. However, it is possible that the reduced Ca^{2+} transients detected in

this study might be due to the occurrence of cytosolic Ca^{2+} overload (Kumar, Kain, and Sitasawad 2012), an aspect that was not evaluated in the present study.

The implication of abnormalities in Ca^{2+} homeostasis in the present study led to the investigation of the integrity of the Ca^{2+} handling proteins SERCA and RyR, given that impaired Ca^{2+} handling proteins account for a compromised cardiac function (Hu et al. 2011). In some diabetic models, the SERCA expression is reduced (Choi et al. 2002, Zhang et al. 2008), whereas others studies reported a slight effect of SERCA on the sarcoplasmic Ca^{2+} content (Bode et al. 2011). The impairment of SERCA activity leads to contractile dysfunction as shown in a study in which the polyol pathway causes impairment of SERCA activity in hyperglycaemic conditions (Tang et al. 2010). The polyol pathway has been shown to be a main promoter of hyperglycaemia-induced oxidative stress in different tissues sensitive to hyperglycaemia-induced lesions (Chung and Chung 2005). In the present study, SERCA 2 expression was not changed suggesting that further evaluation of diastolic factors such as the Na^{+}/ Ca^{2+} exchange (Choi et al. 2002) could possibly play a role. In addition, Ca^{2+} overload results in the impairment of the Ca^{2+} transport system including the L-type Ca^{2+} channels, RyR, sarcoplasmic sodium-Ca^{2+} exchange, and the SERCA pump (Dhalla et al. 1985, Heyliger, Prakash, and McNeill 1987). However, in this study, the SERCA activity and Ca^{2+} level was not evaluated.

In addition, the peak of Ca^{2+} transients generated by caffeine stimulation may be utilized as an indirect indicator of sarcoplasmic releasable Ca^{2+} (Cheek et al. 1994, Dettbarn, Györke, and Palade 1994). The result of the present study showed that hyperglycaemia reduced the response to caffeine stimulation was evidenced by decreased the caffeine-induced change in the contraction amplitude in comparison to baseline glucose condition. The decrease in amplitude of Ca^{2+} transient due to hyperglycaemia could be due to a decrease in SR Ca^{2+} content or a defect in RyR -mediated Ca^{2+} release (Trafford et al. 2002). Since SERCA was normal and -d(Amplitude)/dt was elevated, it is likely that SR Ca^{2+} was normal and a defect in RyR-mediated Ca^{2+} release more likely. Support of this view is the decrease in

+d(Amplitude)/dt seen with hyperglycaemia (Figure13.D) and the observation that hyperglycaemia increased oxidative stress (Figure 28) since RyR is a redox sensitive ion channel (Turan and Vassort 2011). Therefore, the contractile dysfunction observed in the present study could be explained by the attenuation of both Ca^{2+} transient and RyR mediated Ca^{2+} release. The result of this study adds new knowledge in this research field, given that most of the findings reported in the literature are from adult cardiac cells compared to developing cardiac cells.

In the present study, hyperglycaemia decreased the expression of cardiac myofilament proteins α-actinin and cTnT. These results are consistent with a previous study in which adult rat cardiomyocytes exposed to high glucose showed decreased myofibril formation (Dyntar et al. 2006). The disruption of cardiac myofilament protein organization in the present study is also similar to that of a previous study which showed that the sarcomeric structure of the cells cultured under 25 mM glucose conditions were stable and had a well-organized pattern in comparison to other glucose concentrations (Guan, Fürst, and Wobus 1999). In addition, it has been shown in a study by Dyntar and colleagues (Dyntar et al. 2001) that the exposure of adult rat cardiomyocytes to high glucose concentration in the culture condition caused loss of myofibril organization and sarcomeric disarray. The loss of myofibrils is a common structural change in dilated cardiomyopathy (Mann et al. 1991), with sarcomeric disorganization being a specific feature of heart failure (Schaper et al. 1991). Furthermore, there is evidence that diabetes mellitus is associated with decreased cardiac myofilament function as evidenced by the altered Ca^{2+} induced contraction in human diabetes (Jweied et al. 2005). However, the finding in the present study cannot be attributed to alterations in the cell proliferation rate because there is no change in the pattern of cellular proliferation as indicated by nuclear EdU uptake. These findings are consistent with a previous study by Han et al. (Han et al. 2015) who showed that there was no difference in cell proliferation between cells cultured in 25- and 50-mM glucose conditions in cardiac-like H9C2 cells.

Moreover, in the current study, there was no change in the expression of RAGE, an important mediator of myocardial inflammation and fibrosis (Bangert et al. 2016). In contrast, a previous study showed that the intrauterine hyperglycaemia induced inflammatory signalling through RAGE in the cardiomyocytes of the infants of diabetic mother rats (Kawaharada et al. 2018). The increased RAGE expression occurs mainly under chronic hyperglycaemia conditions (Chandna et al. 2015). However, the result of the present study is specific to early cardiac cell development and to the duration of cells exposed to hyperglycaemia. In addition, the results of the present study showed no change in the expression of TGF-β1 expression between control and hyperglycaemia groups. In contrast to the present study, another study showed that maternal diabetes significantly decreased expression of TGF-β1 in the foetal heart (Wang, Reece, and Yang 2015). The findings of the current study therefore do not rule out the effect of hyperglycaemia on TGF-β since there are three isoforms of TGF-β, each of which all could play a role in cardiac remodelling due to hyperglycaemia.

4.3 Cellular apoptosis and oxidative stress as underlying mechanisms of hyperglycaemia-induced cellular alterations

The present study showed that hyperglycaemia induced cellular apoptosis as was evidenced by the presence of TUNEL-positive nuclei in cardiac-like cells, which is an indicator of DNA damage and cell death (Figure 23). These results were consistent with that of another study which showed increased apoptotic cells in the developing heart of embryos of diabetic mice (Kumar, Dheen, and Tay 2007). In addition, the increase in apoptotic cells have been reported in the hearts of the offspring of a diabetic mouse (Reinking et al. 2009). However, these studies did not indicate whether the apoptosis was linked to hyperglycaemia or not. Hyperglycaemia induced cardiac cell apoptosis has been also documented in H9C2 cell line (Han et al. 2015, Zhao et al. 2013), and in vascular endothelial cells (Hou et al. 2015). The present

study showed that cardiac cellular apoptosis could be implicated through mitochondrial-dependent pathway. The findings of this study indicates that there is an increase in the expression of cytochrome c in the cytoplasm of the cells cultured under hyperglycaemia conditions (50 mM glucose), and a decrease in the anti-apoptotic protein Bcl-2, without changes in the expression of the anti-apoptotic Bax protein. These results were consistent with a study by Cai et al. (Cai et al. 2002), which demonstrated that hyperglycaemia is directly linked with cardiac cellular apoptosis in a mouse model and in the H2C9 cardiac cell line. They also found that cellular apoptosis was mitochondrial dependent as evident by cytochrome c release and caspase-3 activation. The activation of caspase 3 can be stimulated by the pro-apoptotic Bax protein and inhibited by the antiapoptotic Bcl-2. Bax can counteract Bcl-2 actions through producing heterodimers with Bcl-2 (Reed et al. 1996). In addition, homodimers of Bax may separately activate additional downstream apoptotic signalling (Oltvai, Milliman, and Korsmeyer 1993). Thus, the effects of Bcl-2 and Bax on caspase 3 could be established by the comparative abundance of these two proteins. It has been described that the increased expression of Bcl-2 in the heart tissue without alterations in the expression of Bax, a condition that specifies protection from apoptosis (Raisova et al. 2001). So, it is consistent with the findings of this study as there is an increase in the expression of Bcl-2 in the control group in comparison to the hyperglycaemic group. The change in mitochondrial membrane potential could cause the mitochondria permeability transition pore to open. This may lead to swelling in the mitochondria, rupturing the outer membrane, and releasing cytochrome c into the cytoplasm (Vander Heiden et al. 1997). However, other studies showed that there is no change in the mitochondrial membrane potential with the release of cytochrome c into the cytoplasm (Green and Reed 1998). Indeed, cardiac cell death, as a comprehensive outcome of irregular cellular metabolism and gene expression at primary phase in response to hyperglycaemia, has been considered as a significant trigger of diabetic cardiomyopathy (Feuerstein and Young 2000). High glucose concentration in culture condition was also shown to induce cellular apoptosis in endothelial cells (Baumgartner-Parzer et al. 1995).

In the present study, the causes of mitochondria pathology were not obvious, given that there were no changes in one of the mitochondrial fusion regulatory proteins OPA1 which has been implicated in cellular apoptosis (Chen et al. 2009). OPA1 facilitates fusion of the inner mitochondrial membrane and is included in controlling mitochondrial membrane potential and regulating apoptosis. Downregulation of OPA1 leads to remodelling changes and to release of cytochrome c (Olichon et al. 2003). It has been shown in a previous study that OPA1 deficiency is associated with increased mitochondrial fragmentation which could be a primary cause of cardiac dysfunction in the streptozotocin-induced diabetic rat model (Ding et al. 2020). Also, there is evidence showing that hyperglycaemia causes dysfunction in cardiac progenitor cells through an increase in mitochondrial fission related proteins (Choi et al. 2016). However, the lack of changes in OPA1 observed in the present study do not rule out the changes in the mitochondrial fusion or fission process as there are several proteins responsible for this process. Apart from OPA1, the fusion process also depends on GTPase family members mitofusin 1, mitofusin 2. The present study, however, showed no change in the mitochondrial state as evidenced by unaltered Mitotracker cellular uptake.

This study also considered that oxidative stress is a trigger mechanism for cellular apoptosis. The results showed increased expression of the oxidative stress marker nitrotyrosine in the hyperglycaemia group, indicating the existence of oxidative stress (Figure 28). Nitrotyrosine is one of the oxidative stress markers that has been detected previously in a diabetic patient (Ceriello et al. 2001). The result of the present study is similar to findings in another study where there was an increase in the expression of nitrotyrosine in the diabetic rat heart model which was closely related to cardiomyocyte apoptosis (Zhang and Wei 2013). In addition, a study by Ho et al. (Ho et al. 2006) showed that exposure of vascular endothelial cells to high glucose levels induced significant ROS formation and apoptosis. Furthermore, oxidative stress induced apoptosis has been implicated in a study of diabetic induced embryopathy (Li et al. 2012). Therefore, the finding of the present study is novel regarding the link between hyperglycaemia with oxidative stress induced apoptosis in the early developing cardiac cell.

In the current study, the effect of treatment with NAC reduced the proportion of TUNEL-positive cells and improved α–actinin 2 organization in hyperglycaemia. NAC is recognised to act generally by neutralizing free radical-produced cellular injury and preventing excess ROS production (Sun 2010). The results of the present study were consistent with a previous study which showed that NAC treatments attenuate hyperglycaemia toxicity in H9C2 cardiac cell line (Dludla et al. 2019). In addition, NAC could also improve myocardial apoptosis by preventing excess mitochondrial ROS production in cultured neonatal rat cardiomyocytes (He et al. 2018). Moreover, NAC treatment has been shown to prevent congenital heart disease induced by pregestational diabetes in a diabetic model (Moazzen et al. 2014). Qualitatively, in this study the EBs cultured under hyperglycaemia conditions were less adherent on gelatine-coated coverslips. However, after NAC treatment the extent of EB adherence on the coverslips was improved. Overall, the results of the present study showed a role of oxidative stress in triggering cardiac cell apoptosis.

4.4 Study limitations and future prospective

Limitations of this study include the fact that *in-vitro* experiments, irrespective of mESCs being a good model to study cardiotoxicity (Shi et al. 2020), are not readily translatable to *in-vivo* conditions. This is because the standard baseline glucose of 25 mM used in mESC culture is a supraphysiological glucose level (Ali et al. 2004, Guan, Fürst, and Wobus 1999), therefore the hyperglycaemia model requires a higher glucose level such as 50 mM, therefore deviating significantly from clinical conditions. The 50 mM glucose level represents a doubling of the baseline glucose level (25 mM glucose), corresponding to the estimated doubling of normo-glycaemic blood levels at the clinical diabetes threshold. Interestingly, a previous study used 100 mM glucose in cell culture condition to mimic a diabetic condition (Chen et al. 2012). However, the high glucose concentrations (50 mM) used in the present study may hamper the direct clinical translation of the results, which making the clinical relevance of such levels of glucose remain unclear. In addition, the level of hyperglycaemia in GDM is comparable to that in ordinary diabetes mellitus, which is

outside the range used this study, so the findings of the present study still need to be validated in an *in-vivo* model.

Another limitation in the present study is the use of the EB model as a cardiac model because of the heterogeneity of cell types in the EB structure (Kowalski et al. 2012). Cardiomyocytes represent only 30-40% of the cells among the other types of cardiac cells (Zhou and Pu 2016). However, in this study, the heterogeneity of the EBs was reduced by using the hanging drop method, through which the defining number of mESC was seeded (Lee, Cagavi Bozkulak, et al. 2011, Wobus et al. 2002). In addition, in this study, the cardiac-like cells among the EBs were identified through co-staining with cardiac specific marker to evaluate the changes occurring among cardiac-like cells within the EB structure. However, further investigation is required to evaluate the other type of cells among the EB structure. The other limitation in this study is that the mechanisms through which antioxidant treatment reverse the occurrence of apoptosis is still unknown. Also, the effect of antioxidant treatment on functional alterations caused by hyperglycaemia has not been evaluated. Therefore, further investigation is required to evaluate the possible functional recovery with antioxidant treatments. In addition, the molecular changes associated with oxidative stress needs further evaluation.

4.5 Conclusion

In conclusion, the results of this study showed that hyperglycaemia suppressed the *in-vitro* differentiation of pluripotent mESC into cardiomyocyte-like cells and altered their contractile characteristics. Hyperglycaemia caused structural alterations in the growth and maturation of mESC derived cardiomyocyte-like cells and affected the expression and cellular organisation of cardiac myofilament proteins in mESC-derived cardiomyocytes, without inducing changes in the cellular proliferation rate, nor in the mediator for fibrosis. Hyperglycaemia also caused contractile dysfunction of mESC-derived cardiomyocytes, without altering cellular action potential parameters. These hyperglycaemic effects were possibly mediated by mitochondrial-

dependent cellular apoptosis and abnormalities in Ca^{2+} signalling, triggered by oxidative stress.

Clinical implications

The present study addressed the difficulty of studying the diabetic foetal cardiac disease in utero by establishing and validating an *in-vitro* stem cell cardiac hyperglycaemia model as a suitable- and stable disease model. The findings demonstrated the unique susceptibility of immature hearts to hyperglycaemia and identified molecular mechanistic pathways that could act as pharmacological targets for novel therapeutic approaches in the prevention- and management of the foetal heart disease in diabetic mothers. Therefore, the results of the present study create a platform for further translational studies on the often-overlooked but detrimental foetal diabetic cardiac disease.

References

2017. "International Diabetes Federation." *IDF Diabetes Atlas, 8th ed.; IDFBrussels, Belgium*.

Aboalgasm, H., M. Petersen, and A. Gwanyanya. 2021. "Improvement of cardiac ventricular function by magnesium treatment in chronic streptozotocin-induced diabetic rat heart." *Cardiovasc J Afr* 32 (3):141-148. doi: 10.5830/cvja-2020-054.

Aggarwal, S., S. Czaplicki, and K. Chintala. 2009. "Hemodynamic effect of fetal supraventricular tachycardia on the unaffected twin." *Prenat Diagn* 29 (3):292-3. doi: 10.1002/pd.2136.

Al Ghafli, M. H., R. Padmanabhan, H. H. Kataya, and B. Berg. 2004. "Effects of alpha-lipoic acid supplementation on maternal diabetes-induced growth retardation and congenital anomalies in rat fetuses." *Mol Cell Biochem* 261 (1-2):123-35. doi: 10.1023/b:mcbi.0000028747.92084.42.

Ali, N. N., X. Xu, M. Brito-Martins, P. A. Poole-Wilson, S. E. Harding, and S. J. Fuller. 2004. "Beta-adrenoceptor subtype dependence of chronotropy in mouse embryonic stem cell-derived cardiomyocytes." *Basic research in cardiology* 99 (6):382-391. doi: 10.1007/s00395-004-0484-5.

Almli, L. M., C. C. Alter, R. B. Russell, S. C. Tinker, P. P. Howards, J. Cragan, E. Petersen, G. E. Carrino, and J. Reefhuis. 2017. "Association Between Infant Mortality Attributable to Birth Defects and Payment Source for Delivery - United States, 2011-2013." *MMWR Morb Mortal Wkly Rep* 66 (3):84-87. doi: 10.15585/mmwr.mm6603a4.

Alyousif, S. M. M., F. T. Aldokhel, O. K. Alkhanbashi, M. H. A. Alqahtani, A. M. M. Aladawi, A. A. Ashmawi, A. Al-Qunaibet, and E. Masuadi. 2021. "The Incidence of Congenital Heart Defects in Offspring Among Women With Diabetes in Saudi Arabia." *Cureus* 13 (3):e14225. doi: 10.7759/cureus.14225.

Anversa, P., R. Ricci, and G. Olivetti. 1986. "Quantitative structural analysis of the myocardium during physiologic growth and induced cardiac hypertrophy: a review." *J Am Coll Cardiol* 7 (5):1140-9.

Aoyagi, T., and T. Matsui. 2011. "Phosphoinositide-3 kinase signaling in cardiac hypertrophy and heart failure." *Curr Pharm Des* 17 (18):1818-24.

Aragno, M., R. Mastrocola, C. Medana, M. G. Catalano, I. Vercellinatto, O. Danni, and G. Boccuzzi. 2006. "Oxidative stress-dependent impairment of cardiac-specific

transcription factors in experimental diabetes." *Endocrinology* 147 (12):5967-74. doi: 10.1210/en.2006-0728.

Arai, M. 2002. "Advanced glycation endproducts and their receptor: do they play a role in diabetic cardiomyopathy?" *J Mol Cell Cardiol* 34 (10):1305-8.

Axe, E. L., S. A. Walker, M. Manifava, P. Chandra, H. L. Roderick, A. Habermann, G. Griffiths, and N. T. Ktistakis. 2008. "Autophagosome formation from membrane compartments enriched in phosphatidylinositol 3-phosphate and dynamically connected to the endoplasmic reticulum." *J Cell Biol* 182 (4):685-701. doi: 10.1083/jcb.200803137.

Baker, L., R. Piddington, A. Goldman, J. Egler, and J. Moehring. 1990. "Myo-inositol and prostaglandins reverse the glucose inhibition of neural tube fusion in cultured mouse embryos." *Diabetologia* 33 (10):593-6. doi: 10.1007/bf00400202.

Ballo, R., L. J. Greenberg, and S. H. Kidson. 2012. "A new class of stem cells in South Africa: iPS cells." *S Afr Med J* 103 (1):16-7. doi: 10.7196/samj.6604.

Bangert, A., M. Andrassy, A. M. Müller, M. Bockstahler, A. Fischer, C. H. Volz, C. Leib, S. Göser, S. Korkmaz-Icöz, S. Zittrich, A. Jungmann, F. Lasitschka, G. Pfitzer, O. J. Müller, H. A. Katus, and Z. Kaya. 2016. "Critical role of RAGE and HMGB1 in inflammatory heart disease." *Proc Natl Acad Sci U S A* 113 (2):E155-64. doi: 10.1073/pnas.1522288113.

Barger, P. M., and D. P. Kelly. 2000. "PPAR signaling in the control of cardiac energy metabolism." *Trends Cardiovasc Med* 10 (6):238-45. doi: 10.1016/s1050-1738(00)00077-3.

Bartram, U., D. G. Molin, L. J. Wisse, A. Mohamad, L. P. Sanford, T. Doetschman, C. P. Speer, R. E. Poelmann, and A. C. Gittenberger-de Groot. 2001. "Double-outlet right ventricle and overriding tricuspid valve reflect disturbances of looping, myocardialization, endocardial cushion differentiation, and apoptosis in TGF-beta(2)-knockout mice." *Circulation* 103 (22):2745-52. doi: 10.1161/01.cir.103.22.2745.

Bassani, J. W., R. A. Bassani, and D. M. Bers. 1994. "Relaxation in rabbit and rat cardiac cells: species-dependent differences in cellular mechanisms." *J Physiol* 476 (2):279-93. doi: 10.1113/jphysiol.1994.sp020130.

Basta, G., A. M. Schmidt, and R. De Caterina. 2004. "Advanced glycation end products and vascular inflammation: implications for accelerated atherosclerosis in diabetes." *Cardiovasc Res* 63 (4):582-92. doi: 10.1016/j.cardiores.2004.05.001.

Baumgartner-Parzer, S. M., L. Wagner, M. Pettermann, J. Grillari, A. Gessl, and W. Waldhäusl. 1995. "High-glucose--triggered apoptosis in cultured endothelial cells." *Diabetes* 44 (11):1323-7. doi: 10.2337/diab.44.11.1323.

Belke, D. D., E. A. Swanson, and W. H. Dillmann. 2004. "Decreased sarcoplasmic reticulum activity and contractility in diabetic db/db mouse heart." *Diabetes* 53 (12):3201-8. doi: 10.2337/diabetes.53.12.3201.

Berg, T. J., K. Dahl-Jorgensen, P. A. Torjesen, and K. F. Hanssen. 1997. "Increased serum levels of advanced glycation end products (AGEs) in children and adolescents with IDDM." *Diabetes Care* 20 (6):1006-8.

Bertram, M. Y., A. V. Jaswal, V. P. Van Wyk, N. S. Levitt, and K. J. Hofman. 2013. "The non-fatal disease burden caused by type 2 diabetes in South Africa, 2009." *Glob Health Action* 6:19244. doi: 10.3402/gha.v6i0.19244.

Bhorat, I., M. Pillay, and T. Reddy. 2018. "Determination of the fetal myocardial performance index in women with gestational impaired glucose tolerance and to assess whether this parameter is a possible prognostic indicator of adverse fetal outcome." *J Matern Fetal Neonatal Med* 31 (15):2019-2026. doi: 10.1080/14767058.2017.1334047.

Bidasee, K. R., Y. Zhang, C. H. Shao, M. Wang, K. P. Patel, U. D. Dincer, and H. R. Besch, Jr. 2004. "Diabetes increases formation of advanced glycation end products on Sarco(endo)plasmic reticulum Ca2+-ATPase." *Diabetes* 53 (2):463-73.

Bode, E. F., S. J. Briston, C. L. Overend, S. C. O'Neill, A. W. Trafford, and D. A. Eisner. 2011. "Changes of SERCA activity have only modest effects on sarcoplasmic reticulum Ca2+ content in rat ventricular myocytes." *J Physiol* 589 (Pt 19):4723-9. doi: 10.1113/jphysiol.2011.211052.

Bootman, M. D., and M. J. Berridge. 1995. "The elemental principles of calcium signaling." *Cell* 83 (5):675-8. doi: 10.1016/0092-8674(95)90179-5.

Bos, M., and C. Agyemang. 2013. "Prevalence and complications of diabetes mellitus in Northern Africa, a systematic review." *BMC Public Health* 13:387. doi: 10.1186/1471-2458-13-387.

Boucher, J., A. Kleinridders, and C. R. Kahn. 2014. "Insulin receptor signaling in normal and insulin-resistant states." *Cold Spring Harb Perspect Biol* 6 (1). doi: 10.1101/cshperspect.a009191.

Boyer, L. A., T. I. Lee, M. F. Cole, S. E. Johnstone, S. S. Levine, J. P. Zucker, M. G. Guenther, R. M. Kumar, H. L. Murray, R. G. Jenner, D. K. Gifford, D. A. Melton, R.

Jaenisch, and R. A. Young. 2005. "Core transcriptional regulatory circuitry in human embryonic stem cells." *Cell* 122 (6):947-56. doi: 10.1016/j.cell.2005.08.020.

Brade, T., L. S. Pane, A. Moretti, K. R. Chien, and K. L. Laugwitz. 2013. "Embryonic heart progenitors and cardiogenesis." *Cold Spring Harb Perspect Med* 3 (10):a013847. doi: 10.1101/cshperspect.a013847.

Bradshaw, D., R. Norman, D. Pieterse, and N. S. Levitt. 2007. "Estimating the burden of disease attributable to diabetes in South Africa in 2000." *S Afr Med J* 97 (8 Pt 2):700-6.

Brett, J., A. M. Schmidt, S. D. Yan, Y. S. Zou, E. Weidman, D. Pinsky, R. Nowygrod, M. Neeper, C. Przysiecki, A. Shaw, and et al. 1993. "Survey of the distribution of a newly characterized receptor for advanced glycation end products in tissues." *Am J Pathol* 143 (6):1699-712.

Buchanan, T. A., and J. L. Kitzmiller. 1994. "Metabolic interactions of diabetes and pregnancy." *Annu Rev Med* 45:245-60. doi: 10.1146/annurev.med.45.1.245.

Burdon, T., I. Chambers, C. Stracey, H. Niwa, and A. Smith. 1999. "Signaling mechanisms regulating self-renewal and differentiation of pluripotent embryonic stem cells." *Cells Tissues Organs* 165 (3-4):131-43. doi: 10.1159/000016693.

Buse, M. G. 2006. "Hexosamines, insulin resistance, and the complications of diabetes: current status." *Am J Physiol Endocrinol Metab* 290 (1):E1-e8. doi: 10.1152/ajpendo.00329.2005.

Cade, W. T., P. T. Levy, R. A. Tinius, M. D. Patel, S. Choudhry, M. R. Holland, G. K. Singh, and A. G. Cahill. 2017. "Markers of maternal and infant metabolism are associated with ventricular dysfunction in infants of obese women with type 2 diabetes." *Pediatr Res* 82 (5):768-775. doi: 10.1038/pr.2017.140.

Cai, L., W. Li, G. Wang, L. Guo, Y. Jiang, and Y. J. Kang. 2002. "Hyperglycemia-induced apoptosis in mouse myocardium: mitochondrial cytochrome C-mediated caspase-3 activation pathway." *Diabetes* 51 (6):1938-48.

Cai, L., Y. Wang, G. Zhou, T. Chen, Y. Song, X. Li, and Y. J. Kang. 2006. "Attenuation by metallothionein of early cardiac cell death via suppression of mitochondrial oxidative stress results in a prevention of diabetic cardiomyopathy." *J Am Coll Cardiol* 48 (8):1688-97. doi: 10.1016/j.jacc.2006.07.022.

Cassidy-Stone, A., J. E. Chipuk, E. Ingerman, C. Song, C. Yoo, T. Kuwana, M. J. Kurth, J. T. Shaw, J. E. Hinshaw, D. R. Green, and J. Nunnari. 2008. "Chemical inhibition of the mitochondrial division dynamin reveals its role in Bax/Bak-dependent mitochondrial

outer membrane permeabilization." *Dev Cell* 14 (2):193-204. doi: 10.1016/j.devcel.2007.11.019.

Ceriello, A., F. Mercuri, L. Quagliaro, R. Assaloni, E. Motz, L. Tonutti, and C. Taboga. 2001. "Detection of nitrotyrosine in the diabetic plasma: evidence of oxidative stress." *Diabetologia* 44 (7):834-8. doi: 10.1007/s001250100529.

Chambers, I., D. Colby, M. Robertson, J. Nichols, S. Lee, S. Tweedie, and A. Smith. 2003. "Functional expression cloning of Nanog, a pluripotency sustaining factor in embryonic stem cells." *Cell* 113 (5):643-55. doi: 10.1016/s0092-8674(03)00392-1.

Chan, T. O., S. E. Rittenhouse, and P. N. Tsichlis. 1999. "AKT/PKB and other D3 phosphoinositide-regulated kinases: kinase activation by phosphoinositide-dependent phosphorylation." *Annu Rev Biochem* 68:965-1014. doi: 10.1146/annurev.biochem.68.1.965.

Chandna, A. R., N. Kuhlmann, C. A. Bryce, Q. Greba, V. A. Campanucci, and J. G. Howland. 2015. "Chronic maternal hyperglycemia induced during mid-pregnancy in rats increases RAGE expression, augments hippocampal excitability, and alters behavior of the offspring." *Neuroscience* 303:241-60. doi: 10.1016/j.neuroscience.2015.06.063.

Chang, T. I., M. Horal, S. K. Jain, F. Wang, R. Patel, and M. R. Loeken. 2003. "Oxidant regulation of gene expression and neural tube development: Insights gained from diabetic pregnancy on molecular causes of neural tube defects." *Diabetologia* 46 (4):538-45. doi: 10.1007/s00125-003-1063-2.

Cheek, T. R., M. J. Berridge, R. B. Moreton, K. A. Stauderman, M. M. Murawsky, and M. D. Bootman. 1994. "Quantal Ca2+ mobilization by ryanodine receptors is due to all-or-none release from functionally discrete intracellular stores." *Biochem J* 301 (Pt 3) (Pt 3):879-83. doi: 10.1042/bj3010879.

Chen, K., G. Li, F. Geng, Z. Zhang, J. Li, M. Yang, L. Dong, and F. Gao. 2014. "Berberine reduces ischemia/reperfusion-induced myocardial apoptosis via activating AMPK and PI3K-Akt signaling in diabetic rats." *Apoptosis* 19 (6):946-57. doi: 10.1007/s10495-014-0977-0.

Chen, L., Q. Gong, J. P. Stice, and A. A. Knowlton. 2009. "Mitochondrial OPA1, apoptosis, and heart failure." *Cardiovasc Res* 84 (1):91-9. doi: 10.1093/cvr/cvp181.

Chen, Y. H., J. Y. Chen, Y. W. Chen, S. T. Lin, and H. L. Chan. 2012. "High glucose-induced proteome alterations in retinal pigmented epithelium cells and its possible relevance to diabetic retinopathy." *Mol Biosyst* 8 (12):3107-24. doi: 10.1039/c2mb25331c.

Cheng, T. H., N. L. Shih, C. H. Chen, H. Lin, J. C. Liu, H. H. Chao, J. Y. Liou, Y. L. Chen, H. W. Tsai, Y. S. Chen, C. F. Cheng, and J. J. Chen. 2005. "Role of mitogen-activated protein kinase pathway in reactive oxygen species-mediated endothelin-1-induced beta-myosin heavy chain gene expression and cardiomyocyte hypertrophy." *J Biomed Sci* 12 (1):123-33. doi: 10.1007/s11373-004-8168-6.

Cheng, T. H., N. L. Shih, S. Y. Chen, D. L. Wang, and J. J. Chen. 1999. "Reactive oxygen species modulate endothelin-I-induced c-fos gene expression in cardiomyocytes." *Cardiovasc Res* 41 (3):654-62.

Choi, H. Y., J. H. Park, W. B. Jang, S. T. Ji, S. Y. Jung, Y. Kim da, S. Kang, Y. J. Kim, J. Yun, J. H. Kim, S. H. Baek, and S. M. Kwon. 2016. "High Glucose Causes Human Cardiac Progenitor Cell Dysfunction by Promoting Mitochondrial Fission: Role of a GLUT1 Blocker." *Biomol Ther (Seoul)* 24 (4):363-70. doi: 10.4062/biomolther.2016.097.

Choi, K. M., Y. Zhong, B. D. Hoit, I. L. Grupp, H. Hahn, K. W. Dilly, S. Guatimosim, W. J. Lederer, and M. A. Matlib. 2002. "Defective intracellular Ca(2+) signaling contributes to cardiomyopathy in Type 1 diabetic rats." *Am J Physiol Heart Circ Physiol* 283 (4):H1398-408. doi: 10.1152/ajpheart.00313.2002.

Chung, S. S., and S. K. Chung. 2005. "Aldose reductase in diabetic microvascular complications." *Curr Drug Targets* 6 (4):475-86. doi: 10.2174/1389450054021891.

Costa, V. N., R. M. Nomura, K. S. Reynolds, S. Miyadahira, and M. Zugaib. 2009. "Effects of maternal glycemia on fetal heart rate in pregnancies complicated by pregestational diabetes mellitus." *Eur J Obstet Gynecol Reprod Biol* 143 (1):14-7. doi: 10.1016/j.ejogrb.2008.10.019.

Coumel, P. 1993. "Cardiac arrhythmias and the autonomic nervous system." *J Cardiovasc Electrophysiol* 4 (3):338-55. doi: 10.1111/j.1540-8167.1993.tb01235.x.

Crespo, F. L., V. R. Sobrado, L. Gomez, A. M. Cervera, and K. J. McCreath. 2010. "Mitochondrial reactive oxygen species mediate cardiomyocyte formation from embryonic stem cells in high glucose." *Stem Cells* 28 (7):1132-42. doi: 10.1002/stem.441.

Dabelea, D., and D. J. Pettitt. 2001. "Intrauterine diabetic environment confers risks for type 2 diabetes mellitus and obesity in the offspring, in addition to genetic susceptibility." *J Pediatr Endocrinol Metab* 14 (8):1085-91. doi: 10.1515/jpem-2001-0803.

Davies, M. P., R. H. An, P. Doevendans, S. Kubalak, K. R. Chien, and R. S. Kass. 1996. "Developmental changes in ionic channel activity in the embryonic murine heart." *Circ Res* 78 (1):15-25. doi: 10.1161/01.res.78.1.15.

Deluyker, D., L. Evens, and V. Bito. 2017. "Advanced glycation end products (AGEs) and cardiovascular dysfunction: focus on high molecular weight AGEs." *Amino Acids*. doi: 10.1007/s00726-017-2464-8.

Depla, A. L., L. De Wit, T. J. Steenhuis, M. G. Slieker, D. N. Voormolen, P. G. Scheffer, R. De Heus, B. B. Van Rijn, and M. N. Bekker. 2021. "Effect of maternal diabetes on fetal heart function on echocardiography: systematic review and meta-analysis." *Ultrasound Obstet Gynecol* 57 (4):539-550. doi: 10.1002/uog.22163.

Depre, C., M. E. Young, J. Ying, H. S. Ahuja, Q. Han, N. Garza, P. J. Davies, and H. Taegtmeyer. 2000. "Streptozotocin-induced changes in cardiac gene expression in the absence of severe contractile dysfunction." *J Mol Cell Cardiol* 32 (6):985-96. doi: 10.1006/jmcc.2000.1139.

Desouza, C., H. Salazar, B. Cheong, J. Murgo, and V. Fonseca. 2003. "Association of hypoglycemia and cardiac ischemia: a study based on continuous monitoring." *Diabetes Care* 26 (5):1485-9. doi: 10.2337/diacare.26.5.1485.

Dettbarn, C., S. Györke, and P. Palade. 1994. "Many agonists induce "quantal" Ca2+ release or adaptive behavior in muscle ryanodine receptors." *Mol Pharmacol* 46 (3):502-7.

Devendra, D., E. Liu, and G. S. Eisenbarth. 2004. "Type 1 diabetes: recent developments." *Bmj* 328 (7442):750-4. doi: 10.1136/bmj.328.7442.750.

Devereux, R. B., M. J. Roman, M. Paranicas, M. J. O'Grady, E. T. Lee, T. K. Welty, R. R. Fabsitz, D. Robbins, E. R. Rhoades, and B. V. Howard. 2000. "Impact of diabetes on cardiac structure and function: the strong heart study." *Circulation* 101 (19):2271-6.

Dhalla, N. S., G. N. Pierce, I. R. Innes, and R. E. Beamish. 1985. "Pathogenesis of cardiac dysfunction in diabetes mellitus." *Can J Cardiol* 1 (4):263-81.

Di Cianni, G., R. Miccoli, L. Volpe, C. Lencioni, and S. Del Prato. 2003. "Intermediate metabolism in normal pregnancy and in gestational diabetes." *Diabetes Metab Res Rev* 19 (4):259-70. doi: 10.1002/dmrr.390.

Dillmann, W. H. 1980. "Diabetes mellitus induces changes in cardiac myosin of the rat." *Diabetes* 29 (7):579-82.

Ding, M., C. Liu, R. Shi, M. Yu, K. Zeng, J. Kang, F. Fu, and M. Mi. 2020. "Mitochondrial fusion promoter restores mitochondrial dynamics balance and ameliorates diabetic

cardiomyopathy in an optic atrophy 1-dependent way." *Acta Physiol (Oxf)* 229 (1):e13428. doi: 10.1111/apha.13428.

Dludla, P. V., P. Orlando, S. Silvestri, S. E. Mazibuko-Mbeje, R. Johnson, F. Marcheggiani, I. Cirilli, C. J. F. Muller, J. Louw, N. Obonye, T. Nyawo, B. B. Nkambule, and L. Tiano. 2019. "N-Acetyl cysteine ameliorates hyperglycemia-induced cardiomyocyte toxicity by improving mitochondrial energetics and enhancing endogenous Coenzyme Q(9/10) levels." *Toxicol Rep* 6:1240-1245. doi: 10.1016/j.toxrep.2019.11.004.

Dornhorst, A., J. S. Nicholls, K. Ali, C. Andres, D. L. Adamson, L. F. Kelly, R. Niththyananthan, R. W. Beard, and I. P. Gray. 1994. "Fetal proinsulin and birth weight." *Diabet Med* 11 (2):177-81. doi: 10.1111/j.1464-5491.1994.tb02016.x.

Dowling, D., N. Corrigan, S. Horgan, C. J. Watson, J. Baugh, P. Downey, and F. M. McAuliffe. 2014. "Cardiomyopathy in offspring of pregestational diabetic mouse pregnancy." *J Diabetes Res* 2014:624939. doi: 10.1155/2014/624939.

Druet, C., N. Tubiana-Rufi, D. Chevenne, O. Rigal, M. Polak, and C. Levy-Marchal. 2006. "Characterization of insulin secretion and resistance in type 2 diabetes of adolescents." *J Clin Endocrinol Metab* 91 (2):401-4. doi: 10.1210/jc.2005-1672.

Du, Q., S. Jovanović, A. Sukhodub, Y. S. Ngoi, A. Lal, M. Zheleva, and A. Jovanović. 2018. "Insulin down-regulates cardioprotective SUR2A in the heart-derived H9c2 cells: A possible explanation for some adverse effects of insulin therapy." *Biochem Biophys Rep* 16:12-18. doi: 10.1016/j.bbrep.2018.08.005.

Du, X. L., D. Edelstein, S. Dimmeler, Q. Ju, C. Sui, and M. Brownlee. 2001. "Hyperglycemia inhibits endothelial nitric oxide synthase activity by posttranslational modification at the Akt site." *J Clin Invest* 108 (9):1341-8. doi: 10.1172/jci11235.

Dyntar, D., M. Eppenberger-Eberhardt, K. Maedler, M. Pruschy, H. M. Eppenberger, G. A. Spinas, and M. Y. Donath. 2001. "Glucose and palmitic acid induce degeneration of myofibrils and modulate apoptosis in rat adult cardiomyocytes." *Diabetes* 50 (9):2105-13. doi: 10.2337/diabetes.50.9.2105.

Dyntar, D., P. Sergeev, J. Klisic, P. Ambühl, M. C. Schaub, and M. Y. Donath. 2006. "High glucose alters cardiomyocyte contacts and inhibits myofibrillar formation." *J Clin Endocrinol Metab* 91 (5):1961-7. doi: 10.1210/jc.2005-1904.

El-Bassiouni, E. A., M. H. Helmy, N. Abou Rawash, S. M. El-Zoghby, M. A. Kamel, and A. N. Abou Rayah. 2005. "Embryopathy in experimental diabetic gestation: assessment of oxidative stress and antioxidant defence." *Br J Biomed Sci* 62 (2):71-6. doi: 10.1080/09674845.2005.11732688.

El-Ganzoury, M. M., S. A. El-Masry, R. A. El-Farrash, M. Anwar, and R. Z. Abd Ellatife. 2012. "Infants of diabetic mothers: echocardiographic measurements and cord blood IGF-I and IGFBP-1." *Pediatr Diabetes* 13 (2):189-96. doi: 10.1111/j.1399-5448.2011.00811.x.

Elmore, S. 2007. "Apoptosis: a review of programmed cell death." *Toxicol Pathol* 35 (4):495-516. doi: 10.1080/01926230701320337.

Engelhardt, S., P. Boknik, U. Keller, J. Neumann, M. J. Lohse, and L. Hein. 2001. "Early impairment of calcium handling and altered expression of junctin in hearts of mice overexpressing the beta1-adrenergic receptor." *Faseb j* 15 (14):2718-20. doi: 10.1096/fj.01-0107fje.

Ericsson, A., K. Säljö, E. Sjöstrand, N. Jansson, P. D. Prasad, T. L. Powell, and T. Jansson. 2007. "Brief hyperglycaemia in the early pregnant rat increases fetal weight at term by stimulating placental growth and affecting placental nutrient transport." *J Physiol* 581 (Pt 3):1323-32. doi: 10.1113/jphysiol.2007.131185.

Eriksson, U. J., and L. A. Borg. 1993. "Diabetes and embryonic malformations. Role of substrate-induced free-oxygen radical production for dysmorphogenesis in cultured rat embryos." *Diabetes* 42 (3):411-9. doi: 10.2337/diab.42.3.411.

Eslamian, L., S. Akbari, V. Marsoosi, and A. Jamal. 2013. "Association between fetal overgrowth and metabolic parameters in cord blood of newborns of women with GDM." *Minerva Med* 104 (3):317-24.

Evers, I. M., H. W. de Valk, and G. H. Visser. 2004. "Risk of complications of pregnancy in women with type 1 diabetes: nationwide prospective study in the Netherlands." *Bmj* 328 (7445):915. doi: 10.1136/bmj.38043.583160.EE.

Fava, S., J. Azzopardi, H. A. Muscat, and F. F. Fenech. 1993. "Factors that influence outcome in diabetic subjects with myocardial infarction." *Diabetes Care* 16 (12):1615-8.

Feng, C. C., S. Pandey, C. Y. Lin, C. Y. Shen, R. L. Chang, T. T. Chang, R. J. Chen, V. P. Viswanadha, Y. M. Lin, and C. Y. Huang. 2018. "Cardiac apoptosis induced under high glucose condition involves activation of IGF2R signaling in H9c2 cardiomyoblasts and streptozotocin-induced diabetic rat hearts." *Biomed Pharmacother* 97:880-885. doi: 10.1016/j.biopha.2017.11.020.

Ferencz, C., J. D. Rubin, R. J. McCarter, and E. B. Clark. 1990. "Maternal diabetes and cardiovascular malformations: predominance of double outlet right ventricle and truncus arteriosus." *Teratology* 41 (3):319-26. doi: 10.1002/tera.1420410309.

Feuerstein, G. Z., and P. R. Young. 2000. "Apoptosis in cardiac diseases: stress- and mitogen-activated signaling pathways." *Cardiovasc Res* 45 (3):560-9. doi: 10.1016/s0008-6363(99)00372-7.

Fijnvandraat, A. C., A. C. van Ginneken, C. A. Schumacher, K. R. Boheler, R. H. Lekanne Deprez, V. M. Christoffels, and A. F. Moorman. 2003. "Cardiomyocytes purified from differentiated embryonic stem cells exhibit characteristics of early chamber myocardium." *J Mol Cell Cardiol* 35 (12):1461-72. doi: 10.1016/j.yjmcc.2003.09.011.

Floris, I., B. Descamps, A. Vardeu, T. Mitić, A. M. Posadino, S. Shantikumar, G. Sala-Newby, G. Capobianco, G. Mangialardi, L. Howard, S. Dessole, R. Urrutia, G. Pintus, and C. Emanueli. 2015. "Gestational diabetes mellitus impairs fetal endothelial cell functions through a mechanism involving microRNA-101 and histone methyltransferase enhancer of zester homolog-2." *Arterioscler Thromb Vasc Biol* 35 (3):664-74. doi: 10.1161/atvbaha.114.304730.

Fountoulaki, K., N. Dagres, and E. K. Iliodromitis. 2015. "Cellular Communications in the Heart." *Card Fail Rev* 1 (2):64-68. doi: 10.15420/cfr.2015.1.2.64.

Francis, M., X. Qian, C. Charbel, J. Ledoux, J. C. Parker, and M. S. Taylor. 2012. "Automated region of interest analysis of dynamic Ca^{2+} signals in image sequences." *Am J Physiol Cell Physiol* 303 (3):C236-43. doi: 10.1152/ajpcell.00016.2012.

Frezza, C., S. Cipolat, O. Martins de Brito, M. Micaroni, G. V. Beznoussenko, T. Rudka, D. Bartoli, R. S. Polishuck, N. N. Danial, B. De Strooper, and L. Scorrano. 2006. "OPA1 controls apoptotic cristae remodeling independently from mitochondrial fusion." *Cell* 126 (1):177-89. doi: 10.1016/j.cell.2006.06.025.

Frustaci, A., J. Kajstura, C. Chimenti, I. Jakoniuk, A. Leri, A. Maseri, B. Nadal-Ginard, and P. Anversa. 2000. "Myocardial cell death in human diabetes." *Circ Res* 87 (12):1123-32. doi: 10.1161/01.res.87.12.1123.

Galderisi, M., K. M. Anderson, P. W. Wilson, and D. Levy. 1991. "Echocardiographic evidence for the existence of a distinct diabetic cardiomyopathy (the Framingham Heart Study)." *Am J Cardiol* 68 (1):85-9. doi: 10.1016/0002-9149(91)90716-x.

Galtier, F. 2010. "Definition, epidemiology, risk factors." *Diabetes Metab* 36 (6 Pt 2):628-51. doi: 10.1016/j.diabet.2010.11.014.

Ganguly, P. K., G. N. Pierce, K. S. Dhalla, and N. S. Dhalla. 1983. "Defective sarcoplasmic reticular calcium transport in diabetic cardiomyopathy." *Am J Physiol* 244 (6):E528-35. doi: 10.1152/ajpendo.1983.244.6.E528.

Gardiner, H. M., L. Pasquini, J. Wolfenden, E. Kulinskaya, W. Li, and M. Henein. 2006. "Increased periconceptual maternal glycated haemoglobin in diabetic mothers reduces fetal long axis cardiac function." *Heart* 92 (8):1125-30. doi: 10.1136/hrt.2005.076885.

Garg, S., P. Sharma, D. Sharma, V. Behera, M. Durairaj, and A. Dhall. 2014. "Use of fetal echocardiography for characterization of fetal cardiac structure in women with normal pregnancies and gestational diabetes mellitus." *J Ultrasound Med* 33 (8):1365-9. doi: 10.7863/ultra.33.8.1365.

Ghosh, S., T. Pulinilkunnil, G. Yuen, G. Kewalramani, D. An, D. Qi, A. Abrahani, and B. Rodrigues. 2005. "Cardiomyocyte apoptosis induced by short-term diabetes requires mitochondrial GSH depletion." *Am J Physiol Heart Circ Physiol* 289 (2):H768-76. doi: 10.1152/ajpheart.00038.2005.

Gidh-Jain, M., B. Huang, P. Jain, G. Gick, and N. El-Sherif. 1998. "Alterations in cardiac gene expression during ventricular remodeling following experimental myocardial infarction." *J Mol Cell Cardiol* 30 (3):627-37. doi: 10.1006/jmcc.1997.0628.

Gong, H., F. Zolzer, G. von Recklinghausen, J. Rossler, S. Breit, W. Havers, T. Fotsis, and L. Schweigerer. 1999. "Arginine deiminase inhibits cell proliferation by arresting cell cycle and inducing apoptosis." *Biochem Biophys Res Commun* 261 (1):10-4. doi: 10.1006/bbrc.1999.1004.

Green, D. R., and J. C. Reed. 1998. "Mitochondria and apoptosis." *Science* 281 (5381):1309-12. doi: 10.1126/science.281.5381.1309.

Gregg, E. W., M. K. Sophiea, and M. Weldegiorgis. 2021. "Diabetes and COVID-19: Population Impact 18 Months Into the Pandemic." *Diabetes Care* 44 (9):1916-1923. doi: 10.2337/dci21-0001.

Grundy, S. M., I. J. Benjamin, G. L. Burke, A. Chait, R. H. Eckel, B. V. Howard, W. Mitch, S. C. Smith, Jr., and J. R. Sowers. 1999. "Diabetes and cardiovascular disease: a statement for healthcare professionals from the American Heart Association." *Circulation* 100 (10):1134-46.

Grune, T., C. Ott, S. Häseli, A. Höhn, and T. Jung. 2019. "The "MYOCYTER" - Convert cellular and cardiac contractions into numbers with ImageJ." *Sci Rep* 9 (1):15112. doi: 10.1038/s41598-019-51676-x.

Guan, K., D. O. Fürst, and A. M. Wobus. 1999. "Modulation of sarcomere organization during embryonic stem cell-derived cardiomyocyte differentiation." *Eur J Cell Biol* 78 (11):813-23. doi: 10.1016/s0171-9335(99)80032-6.

Guasch, G., and E. Fuchs. 2005. "Mice in the world of stem cell biology." *Nat Genet* 37 (11):1201-6. doi: 10.1038/ng1667.

Hagemann, L. L., and P. Zielinsky. 1996. "[Prenatal study of hypertrophic cardiomyopathy and its association with insulin levels in fetuses of diabetic mothers]." *Arq Bras Cardiol* 66 (4):193-8.

Hall, B. K. 2008. "The neural crest and neural crest cells: discovery and significance for theories of embryonic organization." *J Biosci* 33 (5):781-93. doi: 10.1007/s12038-008-0098-4.

Hall, V., R. W. Thomsen, O. Henriksen, and N. Lohse. 2011. "Diabetes in Sub Saharan Africa 1999-2011: epidemiology and public health implications. A systematic review." *BMC Public Health* 11:564. doi: 10.1186/1471-2458-11-564.

Han, S. S., G. Wang, Y. Jin, Z. L. Ma, W. J. Jia, X. Wu, X. Y. Wang, M. Y. He, X. Cheng, W. J. Li, X. Yang, and G. S. Liu. 2015. "Investigating the Mechanism of Hyperglycemia-Induced Fetal Cardiac Hypertrophy." *PLoS One* 10 (9):e0139141. doi: 10.1371/journal.pone.0139141.

Hatém, M. A., P. Zielinsky, D. M. Hatém, L. H. Nicoloso, J. L. Manica, A. L. Piccoli, J. Zanettini, V. Oliveira, F. Scarpa, and R. Petracco. 2008. "Assessment of diastolic ventricular function in fetuses of diabetic mothers using tissue Doppler." *Cardiol Young* 18 (3):297-302. doi: 10.1017/s1047951108002138.

Hattori, Y., N. Matsuda, J. Kimura, T. Ishitani, A. Tamada, S. Gando, O. Kemmotsu, and M. Kanno. 2000. "Diminished function and expression of the cardiac Na+-Ca2+ exchanger in diabetic rats: implication in Ca2+ overload." *J Physiol* 527 Pt 1 (Pt 1):85-94. doi: 10.1111/j.1469-7793.2000.00085.x.

Hayat, S. A., B. Patel, R. S. Khattar, and R. A. Malik. 2004. "Diabetic cardiomyopathy: mechanisms, diagnosis and treatment." *Clin Sci (Lond)* 107 (6):539-57. doi: 10.1042/cs20040057.

He, Y., L. Zhou, Z. Fan, S. Liu, and W. Fang. 2018. "Palmitic acid, but not high-glucose, induced myocardial apoptosis is alleviated by N-acetylcysteine due to attenuated mitochondrial-derived ROS accumulation-induced endoplasmic reticulum stress." *Cell Death Dis* 9 (5):568. doi: 10.1038/s41419-018-0593-y.

Heineke, J., and J. D. Molkentin. 2006. "Regulation of cardiac hypertrophy by intracellular signalling pathways." *Nat Rev Mol Cell Biol* 7 (8):589-600. doi: 10.1038/nrm1983.

Henderson, C. J., E. Aleo, A. Fontanini, R. Maestro, G. Paroni, and C. Brancolini. 2005. "Caspase activation and apoptosis in response to proteasome inhibitors." *Cell Death Differ* 12 (9):1240-54. doi: 10.1038/sj.cdd.4401729.

Hengartner, M. O. 2000. "The biochemistry of apoptosis." *Nature* 407 (6805):770-6. doi: 10.1038/35037710.

Hescheler, J., B. K. Fleischmann, S. Lentini, V. A. Maltsev, J. Rohwedel, A. M. Wobus, and K. Addicks. 1997. "Embryonic stem cells: a model to study structural and functional properties in cardiomyogenesis." *Cardiovasc Res* 36 (2):149-62.

Heyliger, C. E., A. Prakash, and J. H. McNeill. 1987. "Alterations in cardiac sarcolemmal Ca2+ pump activity during diabetes mellitus." *Am J Physiol* 252 (3 Pt 2):H540-4. doi: 10.1152/ajpheart.1987.252.3.H540.

Hink, U., H. Li, H. Mollnau, M. Oelze, E. Matheis, M. Hartmann, M. Skatchkov, F. Thaiss, R. A. Stahl, A. Warnholtz, T. Meinertz, K. Griendling, D. G. Harrison, U. Forstermann, and T. Munzel. 2001. "Mechanisms underlying endothelial dysfunction in diabetes mellitus." *Circ Res* 88 (2):E14-22.

Ho, F. M., W. W. Lin, B. C. Chen, C. M. Chao, C. R. Yang, L. Y. Lin, C. C. Lai, S. H. Liu, and C. S. Liau. 2006. "High glucose-induced apoptosis in human vascular endothelial cells is mediated through NF-kappaB and c-Jun NH2-terminal kinase pathway and prevented by PI3K/Akt/eNOS pathway." *Cell Signal* 18 (3):391-9. doi: 10.1016/j.cellsig.2005.05.009.

Hoodbhoy, Z., N. Mohammed, N. Aslam, U. Fatima, S. Ashiqali, A. Rizvi, C. Pascua, D. Chowdhury, and B. S. Hasan. 2019. "Is the child at risk? Cardiovascular remodelling in children born to diabetic mothers." *Cardiol Young* 29 (4):467-474. doi: 10.1017/s1047951119000040.

Hou, Q., M. Lei, K. Hu, and M. Wang. 2015. "The effects of high glucose levels on reactive oxygen species-induced apoptosis and involved signaling in human vascular endothelial cells." *Cardiovasc Toxicol* 15 (2):140-6. doi: 10.1007/s12012-014-9276-9.

Howarth, F. C., R. Al-Sharhan, A. Al-Hammadi, and M. A. Qureshi. 2007. "Effects of streptozotocin-induced diabetes on action potentials in the sinoatrial node compared with other regions of the rat heart." *Mol Cell Biochem* 300 (1-2):39-46. doi: 10.1007/s11010-006-9366-5.

Howarth, F. C., N. J. Chandler, S. Kharche, J. O. Tellez, I. D. Greener, T. T. Yamanushi, R. Billeter, M. R. Boyett, H. Zhang, and H. Dobrzynski. 2008. "Effects of streptozotocin-

induced diabetes on connexin43 mRNA and protein expression in ventricular muscle." *Mol Cell Biochem* 319 (1-2):105-14. doi: 10.1007/s11010-008-9883-5.

Howarth, F. C., N. Nowotny, E. Zilahi, M. A. El Haj, and M. Lei. 2007. "Altered expression of gap junction connexin proteins may partly underlie heart rhythm disturbances in the streptozotocin-induced diabetic rat heart." *Mol Cell Biochem* 305 (1-2):145-51. doi: 10.1007/s11010-007-9537-z.

Hu, S. T., G. S. Liu, Y. F. Shen, Y. L. Wang, Y. Tang, and Y. J. Yang. 2011. "Defective Ca(2+) handling proteins regulation during heart failure." *Physiol Res* 60 (1):27-37. doi: 10.33549/physiolres.931948.

Ishii, Y. 1981. "Nature of the mitomycin-C induced lesion causing sister-chromatid exchange." *Mutat Res* 91 (1):51-5. doi: 10.1016/0165-7992(81)90070-1.

Itskovitz-Eldor, J., M. Schuldiner, D. Karsenti, A. Eden, O. Yanuka, M. Amit, H. Soreq, and N. Benvenisty. 2000. "Differentiation of human embryonic stem cells into embryoid bodies compromising the three embryonic germ layers." *Mol Med* 6 (2):88-95.

Jaeggi, E. T., J. C. Fouron, and F. Proulx. 2001. "Fetal cardiac performance in uncomplicated and well-controlled maternal type I diabetes." *Ultrasound Obstet Gynecol* 17 (4):311-5. doi: 10.1046/j.1469-0705.2001.00365.x.

Jandeleit-Dahm, K., and M. E. Cooper. 2008. "The role of AGEs in cardiovascular disease." *Curr Pharm Des* 14 (10):979-86. doi: 10.2174/138161208784139684.

Ji, G. J., B. K. Fleischmann, W. Bloch, M. Feelisch, C. Andressen, K. Addicks, and J. Hescheler. 1999. "Regulation of the L-type Ca2+ channel during cardiomyogenesis: switch from NO to adenylyl cyclase-mediated inhibition." *Faseb j* 13 (2):313-24. doi: 10.1096/fasebj.13.2.313.

Jweied, E. E., R. D. McKinney, L. A. Walker, I. Brodsky, A. S. Geha, M. G. Massad, P. M. Buttrick, and P. P. de Tombe. 2005. "Depressed cardiac myofilament function in human diabetes mellitus." *Am J Physiol Heart Circ Physiol* 289 (6):H2478-83. doi: 10.1152/ajpheart.00638.2005.

Kang, Y. J. 2001. "Molecular and cellular mechanisms of cardiotoxicity." *Environ Health Perspect* 109 Suppl 1 (Suppl 1):27-34. doi: 10.1289/ehp.01109s127.

Karamitsos, T. D., H. I. Karvounis, E. G. Dalamanga, C. E. Papadopoulos, T. P. Didangellos, D. T. Karamitsos, G. E. Parharidis, and G. E. Louridas. 2007. "Early diastolic impairment of diabetic heart: the significance of right ventricle." *Int J Cardiol* 114 (2):218-23. doi: 10.1016/j.ijcard.2006.02.003.

Kass, D. A., W. L. Maughan, Z. M. Guo, A. Kono, K. Sunagawa, and K. Sagawa. 1987. "Comparative influence of load versus inotropic states on indexes of ventricular contractility: experimental and theoretical analysis based on pressure-volume relationships." *Circulation* 76 (6):1422-36. doi: 10.1161/01.cir.76.6.1422.

Kawaharada, R., H. Masuda, Z. Chen, E. Blough, T. Kohama, and A. Nakamura. 2018. "Intrauterine hyperglycemia-induced inflammatory signalling via the receptor for advanced glycation end products in the cardiac muscle of the infants of diabetic mother rats." *Eur J Nutr* 57 (8):2701-2712. doi: 10.1007/s00394-017-1536-6.

Kawamura, M., J. W. Heinecke, and A. Chait. 1994. "Pathophysiological concentrations of glucose promote oxidative modification of low density lipoprotein by a superoxide-dependent pathway." *J Clin Invest* 94 (2):771-8. doi: 10.1172/jci117396.

Kelly, R. G., M. E. Buckingham, and A. F. Moorman. 2014. "Heart fields and cardiac morphogenesis." *Cold Spring Harb Perspect Med* 4 (10). doi: 10.1101/cshperspect.a015750.

Kim, E. C., B. S. Yun, I. J. Ryoo, J. K. Min, M. H. Won, K. S. Lee, Y. M. Kim, I. Yoo, and Y. G. Kwon. 2004. "Complestatin prevents apoptotic cell death: inhibition of a mitochondrial caspase pathway through AKT/PKB activation." *Biochem Biophys Res Commun* 313 (1):193-204. doi: 10.1016/j.bbrc.2003.11.104.

Kischkel, F. C., D. A. Lawrence, A. Tinel, H. LeBlanc, A. Virmani, P. Schow, A. Gazdar, J. Blenis, D. Arnott, and A. Ashkenazi. 2001. "Death receptor recruitment of endogenous caspase-10 and apoptosis initiation in the absence of caspase-8." *J Biol Chem* 276 (49):46639-46. doi: 10.1074/jbc.M105102200.

Kolm-Litty, V., U. Sauer, A. Nerlich, R. Lehmann, and E. D. Schleicher. 1998. "High glucose-induced transforming growth factor beta1 production is mediated by the hexosamine pathway in porcine glomerular mesangial cells." *J Clin Invest* 101 (1):160-9. doi: 10.1172/jci119875.

Kolwicz, S. C., Jr., and R. Tian. 2011. "Glucose metabolism and cardiac hypertrophy." *Cardiovasc Res* 90 (2):194-201. doi: 10.1093/cvr/cvr071.

Kowalski, M. P., A. Yoder, L. Liu, and L. Pajak. 2012. "Controlling embryonic stem cell growth and differentiation by automation: enhanced and more reliable differentiation for drug discovery." *J Biomol Screen* 17 (9):1171-9. doi: 10.1177/1087057112452783.

Krentz, A. J., G. Clough, and C. D. Byrne. 2007. "Interactions between microvascular and macrovascular disease in diabetes: pathophysiology and therapeutic implications." *Diabetes Obes Metab* 9 (6):781-91. doi: 10.1111/j.1463-1326.2007.00670.x.

Kulkarni, A., L. Li, M. Craft, M. Nanda, J. M. M. Lorenzo, D. Danford, and S. Kutty. 2017. "Fetal myocardial deformation in maternal diabetes mellitus and obesity." *Ultrasound Obstet Gynecol* 49 (5):630-636. doi: 10.1002/uog.15971.

Kumar, S. D., S. T. Dheen, and S. S. Tay. 2007. "Maternal diabetes induces congenital heart defects in mice by altering the expression of genes involved in cardiovascular development." *Cardiovasc Diabetol* 6:34. doi: 10.1186/1475-2840-6-34.

Kumar, S., V. Kain, and S. L. Sitasawad. 2012. "High glucose-induced Ca2+ overload and oxidative stress contribute to apoptosis of cardiac cells through mitochondrial dependent and independent pathways." *Biochim Biophys Acta* 1820 (7):907-20. doi: 10.1016/j.bbagen.2012.02.010.

Kurosawa, H. 2007. "Methods for inducing embryoid body formation: in vitro differentiation system of embryonic stem cells." *J Biosci Bioeng* 103 (5):389-98. doi: 10.1263/jbb.103.389.

Kwon, S. H., D. R. Pimentel, A. Remondino, D. B. Sawyer, and W. S. Colucci. 2003. "H(2)O(2) regulates cardiac myocyte phenotype via concentration-dependent activation of distinct kinase pathways." *J Mol Cell Cardiol* 35 (6):615-21.

Lauriol, J., K. Keith, F. Jaffré, A. Couvillon, A. Saci, S. A. Goonasekera, J. R. McCarthy, C. W. Kessinger, J. Wang, Q. Ke, P. M. Kang, J. D. Molkentin, C. Carpenter, and M. I. Kontaridis. 2014. "RhoA signaling in cardiomyocytes protects against stress-induced heart failure but facilitates cardiac fibrosis." *Sci Signal* 7 (348):ra100. doi: 10.1126/scisignal.2005262.

Lee, M. Y., E. Cagavi Bozkulak, S. Schliffke, P. J. Amos, Y. Ren, X. Ge, B. E. Ehrlich, and Y. Qyang. 2011. "High density cultures of embryoid bodies enhanced cardiac differentiation of murine embryonic stem cells." *Biochem Biophys Res Commun* 416 (1-2):51-7. doi: 10.1016/j.bbrc.2011.10.140.

Lee, T. I., Y. H. Kao, Y. C. Chen, N. H. Pan, Y. K. Lin, and Y. J. Chen. 2011. "Cardiac peroxisome-proliferator-activated receptor expression in hypertension co-existing with diabetes." *Clin Sci (Lond)* 121 (7):305-12. doi: 10.1042/cs20100529.

Lee, T. W., T. I. Lee, C. J. Chang, G. S. Lien, Y. H. Kao, T. F. Chao, and Y. J. Chen. 2015. "Potential of vitamin D in treating diabetic cardiomyopathy." *Nutr Res* 35 (4):269-79. doi: 10.1016/j.nutres.2015.02.005.

Lehman, J. J., and D. P. Kelly. 2002. "Transcriptional activation of energy metabolic switches in the developing and hypertrophied heart." *Clin Exp Pharmacol Physiol* 29 (4):339-45. doi: 10.1046/j.1440-1681.2002.03655.x.

Lehtoranta, L., O. Vuolteenaho, V. J. Laine, A. Koskinen, H. Soukka, V. Kytö, J. Määttä, M. Haapsamo, E. Ekholm, and J. Räsänen. 2013. "Maternal hyperglycemia leads to fetal cardiac hyperplasia and dysfunction in a rat model." *Am J Physiol Endocrinol Metab* 305 (5):E611-9. doi: 10.1152/ajpendo.00043.2013.

Li, X., H. Weng, E. A. Reece, and P. Yang. 2011. "SOD1 overexpression in vivo blocks hyperglycemia-induced specific PKC isoforms: substrate activation and consequent lipid peroxidation in diabetic embryopathy." *Am J Obstet Gynecol* 205 (1):84.e1-6. doi: 10.1016/j.ajog.2011.02.071.

Li, X., H. Weng, C. Xu, E. A. Reece, and P. Yang. 2012. "Oxidative stress-induced JNK1/2 activation triggers proapoptotic signaling and apoptosis that leads to diabetic embryopathy." *Diabetes* 61 (8):2084-92. doi: 10.2337/db11-1624.

Lin, H., K. Ogawa, I. Imanaga, and N. Tribulova. 2006. "Remodeling of connexin 43 in the diabetic rat heart." *Mol Cell Biochem* 290 (1-2):69-78. doi: 10.1007/s11010-006-9166-y.

Lin, L., L. Cui, W. Zhou, D. Dufort, X. Zhang, C. L. Cai, L. Bu, L. Yang, J. Martin, R. Kemler, M. G. Rosenfeld, J. Chen, and S. M. Evans. 2007. "Beta-catenin directly regulates Islet1 expression in cardiovascular progenitors and is required for multiple aspects of cardiogenesis." *Proc Natl Acad Sci U S A* 104 (22):9313-8. doi: 10.1073/pnas.0700923104.

Lindsay, R. S., J. D. Walker, I. Halsall, C. N. Hales, A. A. Calder, B. A. Hamilton, and F. D. Johnstone. 2003. "Insulin and insulin propeptides at birth in offspring of diabetic mothers." *J Clin Endocrinol Metab* 88 (4):1664-71. doi: 10.1210/jc.2002-021018.

Lipinski, B. 2001. "Pathophysiology of oxidative stress in diabetes mellitus." *J Diabetes Complications* 15 (4):203-10. doi: 10.1016/s1056-8727(01)00143-x.

Liu, X., N. Takeda, and N. S. Dhalla. 1996. "Troponin I phosphorylation in heart homogenate from diabetic rat." *Biochim Biophys Acta* 1316 (2):78-84.

Liu, X., N. Takeda, and N. S. Dhalla. 1997. "Myosin light-chain phosphorylation in diabetic cardiomyopathy in rats." *Metabolism* 46 (1):71-5.

Lopaschuk, G. D., M. A. Spafford, and D. R. Marsh. 1991. "Glycolysis is predominant source of myocardial ATP production immediately after birth." *Am J Physiol* 261 (6 Pt 2):H1698-705. doi: 10.1152/ajpheart.1991.261.6.H1698.

Luo, M., and M. E. Anderson. 2013. "Mechanisms of altered Ca(2)(+) handling in heart failure." *Circ Res* 113 (6):690-708. doi: 10.1161/circresaha.113.301651.

Ma, H., S. Y. Li, P. Xu, S. A. Babcock, E. K. Dolence, M. Brownlee, J. Li, and J. Ren. 2009. "Advanced glycation endproduct (AGE) accumulation and AGE receptor (RAGE) up-regulation contribute to the onset of diabetic cardiomyopathy." *J Cell Mol Med* 13 (8b):1751-64. doi: 10.1111/j.1582-4934.2008.00547.x.

Maahs, D. M., N. A. West, J. M. Lawrence, and E. J. Mayer-Davis. 2010. "Epidemiology of type 1 diabetes." *Endocrinol Metab Clin North Am* 39 (3):481-97. doi: 10.1016/j.ecl.2010.05.011.

Madsen, N. L., S. M. Schwartz, M. B. Lewin, and B. A. Mueller. 2013. "Prepregnancy body mass index and congenital heart defects among offspring: a population-based study." *Congenit Heart Dis* 8 (2):131-41. doi: 10.1111/j.1747-0803.2012.00714.x.

Maltsev, V. A., A. M. Wobus, J. Rohwedel, M. Bader, and J. Hescheler. 1994. "Cardiomyocytes differentiated in vitro from embryonic stem cells developmentally express cardiac-specific genes and ionic currents." *Circ Res* 75 (2):233-44.

Mann, D. L., Y. Urabe, R. L. Kent, S. Vinciguerra, and G. th Cooper. 1991. "Cellular versus myocardial basis for the contractile dysfunction of hypertrophied myocardium." *Circ Res* 68 (2):402-15. doi: 10.1161/01.res.68.2.402.

Maritim, A. C., R. A. Sanders, and J. B. Watkins, 3rd. 2003. "Diabetes, oxidative stress, and antioxidants: a review." *J Biochem Mol Toxicol* 17 (1):24-38. doi: 10.1002/jbt.10058.

Marshall, S., V. Bacote, and R. R. Traxinger. 1991. "Discovery of a metabolic pathway mediating glucose-induced desensitization of the glucose transport system. Role of hexosamine biosynthesis in the induction of insulin resistance." *J Biol Chem* 266 (8):4706-12.

Martinvalet, D., P. Zhu, and J. Lieberman. 2005. "Granzyme A induces caspase-independent mitochondrial damage, a required first step for apoptosis." *Immunity* 22 (3):355-70. doi: 10.1016/j.immuni.2005.02.004.

Mayosi, B. M., A. J. Flisher, U. G. Lalloo, F. Sitas, S. M. Tollman, and D. Bradshaw. 2009. "The burden of non-communicable diseases in South Africa." *Lancet* 374 (9693):934-47. doi: 10.1016/s0140-6736(09)61087-4.

Maytin, M., J. Leopold, and J. Loscalzo. 1999. "Oxidant stress in the vasculature." *Curr Atheroscler Rep* 1 (2):156-64. doi: 10.1007/s11883-999-0012-z.

McLeod, L., and J. G. Ray. 2002. "Prevention and detection of diabetic embryopathy." *Community Genet* 5 (1):33-9. doi: 10.1159/000064629.

Meng, Y., W. Wang, J. Kang, X. Wang, and L. Sun. 2017. "Role of the PI3K/AKT signalling pathway in apoptotic cell death in the cerebral cortex of streptozotocin-induced diabetic rats." *Exp Ther Med* 13 (5):2417-2422. doi: 10.3892/etm.2017.4259.

Merzouk, H., S. Madani, N. Korso, M. Bouchenak, J. Prost, and J. Belleville. 2000. "Maternal and fetal serum lipid and lipoprotein concentrations and compositions in type 1 diabetic pregnancy: relationship with maternal glycemic control." *J Lab Clin Med* 136 (6):441-8. doi: 10.1067/mlc.2000.111004.

Miller-Hance, W. C., M. LaCorbiere, S. J. Fuller, S. M. Evans, G. Lyons, C. Schmidt, J. Robbins, and K. R. Chien. 1993. "In vitro chamber specification during embryonic stem cell cardiogenesis. Expression of the ventricular myosin light chain-2 gene is independent of heart tube formation." *J Biol Chem* 268 (33):25244-52.

Miragoli, M., G. Gaudesius, and S. Rohr. 2006. "Electrotonic modulation of cardiac impulse conduction by myofibroblasts." *Circ Res* 98 (6):801-10. doi: 10.1161/01.RES.0000214537.44195.a3.

Moazzen, H., X. Lu, N. L. Ma, T. J. Velenosi, B. L. Urquhart, L. J. Wisse, A. C. Gittenberger-de Groot, and Q. Feng. 2014. "N-Acetylcysteine prevents congenital heart defects induced by pregestational diabetes." *Cardiovasc Diabetol* 13:46. doi: 10.1186/1475-2840-13-46.

Moccia, F., F. Lodola, I. Stadiotti, C. A. Pilato, M. Bellin, S. Carugo, G. Pompilio, E. Sommariva, and A. S. Maione. 2019. "Calcium as a Key Player in Arrhythmogenic Cardiomyopathy: Adhesion Disorder or Intracellular Alteration?" *Int J Mol Sci* 20 (16). doi: 10.3390/ijms20163986.

Mochizuki, H., Y. Ohnuki, and H. Kurosawa. 2011. "Effect of glucose concentration during embryoid body (EB) formation from mouse embryonic stem cells on EB growth and cell differentiation." *J Biosci Bioeng* 111 (1):92-7. doi: 10.1016/j.jbiosc.2010.09.001.

Mohammadi-Farani, A., M. Ghazi-Khansari, and M. Sahebgharani. 2014. "Glucose concentration in culture medium affects mRNA expression of TRPV1 and CB1 receptors and changes capsaicin toxicity in PC12 cells." *Iran J Basic Med Sci* 17 (9):673-378.

Molkentin, J. D. 2004. "Calcineurin-NFAT signaling regulates the cardiac hypertrophic response in coordination with the MAPKs." *Cardiovasc Res* 63 (3):467-75. doi: 10.1016/j.cardiores.2004.01.021.

Nag, A. C., M. L. Lee, and F. H. Sarkar. 1996. "Remodelling of adult cardiac muscle cells in culture: dynamic process of disorganization and reorganization of myofibrils." *J Muscle Res Cell Motil* 17 (3):313-34. doi: 10.1007/bf00240929.

Nakano, H., I. Minami, D. Braas, H. Pappoe, X. Wu, A. Sagadevan, L. Vergnes, K. Fu, M. Morselli, C. Dunham, X. Ding, A. Z. Stieg, J. K. Gimzewski, M. Pellegrini, P. M. Clark, K. Reue, A. J. Lusis, B. Ribalet, S. K. Kurdistani, H. Christofk, N. Nakatsuji, and A. Nakano. 2017. "Glucose inhibits cardiac muscle maturation through nucleotide biosynthesis." *Elife* 6. doi: 10.7554/eLife.29330.

Nichols, J., B. Zevnik, K. Anastassiadis, H. Niwa, D. Klewe-Nebenius, I. Chambers, H. Schöler, and A. Smith. 1998. "Formation of pluripotent stem cells in the mammalian embryo depends on the POU transcription factor Oct4." *Cell* 95 (3):379-91. doi: 10.1016/s0092-8674(00)81769-9.

Nicholson, D. W., and N. A. Thornberry. 1997. "Caspases: killer proteases." *Trends Biochem Sci* 22 (8):299-306. doi: 10.1016/s0968-0004(97)01085-2.

Nikfarjam, L., and P. Farzaneh. 2012. "Prevention and detection of Mycoplasma contamination in cell culture." *Cell J* 13 (4):203-12.

Noble, J. A., A. M. Valdes, M. Cook, W. Klitz, G. Thomson, and H. A. Erlich. 1996. "The role of HLA class II genes in insulin-dependent diabetes mellitus: molecular analysis of 180 Caucasian, multiplex families." *Am J Hum Genet* 59 (5):1134-48.

Nordin, C., E. Gilat, and R. S. Aronson. 1985. "Delayed afterdepolarizations and triggered activity in ventricular muscle from rats with streptozotocin-induced diabetes." *Circ Res* 57 (1):28-34.

Nozynski, J., M. Zakliczynski, D. Konecka-Mrowka, B. Nikiel, J. Mlynarczyk-Liszka, E. Zembala-Nozynska, D. Lange, M. Maruszewski, and M. Zembala. 2009. "Advanced glycation end products in the development of ischemic and dilated cardiomyopathy in patients with diabetes mellitus type 2." *Transplant Proc* 41 (1):99-104. doi: 10.1016/j.transproceed.2008.09.065.

Obrosova, I. G., P. Pacher, C. Szabo, Z. Zsengeller, H. Hirooka, M. J. Stevens, and M. A. Yorek. 2005. "Aldose reductase inhibition counteracts oxidative-nitrosative stress and poly(ADP-ribose) polymerase activation in tissue sites for diabetes complications." *Diabetes* 54 (1):234-42.

Olichon, A., L. Baricault, N. Gas, E. Guillou, A. Valette, P. Belenguer, and G. Lenaers. 2003. "Loss of OPA1 perturbates the mitochondrial inner membrane structure and integrity,

leading to cytochrome c release and apoptosis." *J Biol Chem* 278 (10):7743-6. doi: 10.1074/jbc.C200677200.

Oltvai, Z. N., C. L. Milliman, and S. J. Korsmeyer. 1993. "Bcl-2 heterodimerizes in vivo with a conserved homolog, Bax, that accelerates programmed cell death." *Cell* 74 (4):609-19. doi: 10.1016/0092-8674(93)90509-o.

Paauw, N. D., R. Stegeman, Mamj de Vroede, J. U. M. Termote, M. W. Freund, and Jmpj Breur. 2020. "Neonatal cardiac hypertrophy: the role of hyperinsulinism-a review of literature." *Eur J Pediatr* 179 (1):39-50. doi: 10.1007/s00431-019-03521-6.

Pauliks, L. B. 2015. "The effect of pregestational diabetes on fetal heart function." *Expert Rev Cardiovasc Ther* 13 (1):67-74. doi: 10.1586/14779072.2015.988141.

Peer, N., A. P. Kengne, A. A. Motala, and J. C. Mbanya. 2014. "Diabetes in the Africa Region: an update." *Diabetes Res Clin Pract* 103 (2):197-205. doi: 10.1016/j.diabres.2013.11.006.

Peiró, C., N. Lafuente, N. Matesanz, E. Cercas, J. L. Llergo, S. Vallejo, L. Rodríguez-Mañas, and C. F. Sánchez-Ferrer. 2001. "High glucose induces cell death of cultured human aortic smooth muscle cells through the formation of hydrogen peroxide." *Br J Pharmacol* 133 (7):967-74. doi: 10.1038/sj.bjp.0704184.

Poon, I. K., C. D. Lucas, A. G. Rossi, and K. S. Ravichandran. 2014. "Apoptotic cell clearance: basic biology and therapeutic potential." *Nat Rev Immunol* 14 (3):166-80. doi: 10.1038/nri3607.

Porter, G. A., Jr., R. F. Makuck, and S. A. Rivkees. 2003. "Intracellular calcium plays an essential role in cardiac development." *Dev Dyn* 227 (2):280-90. doi: 10.1002/dvdy.10307.

Priest, J. R., W. Yang, G. Reaven, J. W. Knowles, and G. M. Shaw. 2015. "Maternal Midpregnancy Glucose Levels and Risk of Congenital Heart Disease in Offspring." *JAMA Pediatr* 169 (12):1112-6. doi: 10.1001/jamapediatrics.2015.2831.

Proskuryakov, S. Y., A. G. Konoplyannikov, and V. L. Gabai. 2003. "Necrosis: a specific form of programmed cell death?" *Exp Cell Res* 283 (1):1-16. doi: 10.1016/s0014-4827(02)00027-7.

Raisova, M., A. M. Hossini, J. Eberle, C. Riebeling, T. Wieder, I. Sturm, P. T. Daniel, C. E. Orfanos, and C. C. Geilen. 2001. "The Bax/Bcl-2 ratio determines the susceptibility of human melanoma cells to CD95/Fas-mediated apoptosis." *J Invest Dermatol* 117 (2):333-40. doi: 10.1046/j.0022-202x.2001.01409.x.

Ramachandran, A., C. Snehalatha, E. Latha, M. Manoharan, and V. Vijay. 1999. "Impacts of urbanisation on the lifestyle and on the prevalence of diabetes in native Asian Indian population." *Diabetes Res Clin Pract* 44 (3):207-13.

Rao Kondapally Seshasai, S., S. Kaptoge, A. Thompson, E. Di Angelantonio, P. Gao, N. Sarwar, P. H. Whincup, K. J. Mukamal, R. F. Gillum, I. Holme, I. Njolstad, A. Fletcher, P. Nilsson, S. Lewington, R. Collins, V. Gudnason, S. G. Thompson, N. Sattar, E. Selvin, F. B. Hu, and J. Danesh. 2011. "Diabetes mellitus, fasting glucose, and risk of cause-specific death." *N Engl J Med* 364 (9):829-841. doi: 10.1056/NEJMoa1008862.

Reece, E. A. 2012. "Diabetes-induced birth defects: what do we know? What can we do?" *Curr Diab Rep* 12 (1):24-32. doi: 10.1007/s11892-011-0251-6.

Reed, J. C., H. Zha, C. Aime-Sempe, S. Takayama, and H. G. Wang. 1996. "Structure-function analysis of Bcl-2 family proteins. Regulators of programmed cell death." *Adv Exp Med Biol* 406:99-112.

Reinking, B. E., E. W. Wedemeyer, R. M. Weiss, J. L. Segar, and T. D. Scholz. 2009. "Cardiomyopathy in offspring of diabetic rats is associated with activation of the MAPK and apoptotic pathways." *Cardiovasc Diabetol* 8:43. doi: 10.1186/1475-2840-8-43.

Ren, J., G. A. Gintant, R. E. Miller, and A. J. Davidoff. 1997. "High extracellular glucose impairs cardiac E-C coupling in a glycosylation-dependent manner." *Am J Physiol* 273 (6):H2876-83. doi: 10.1152/ajpheart.1997.273.6.H2876.

Rizzo, Giuseppe, Maria Pietrolucci, Ilenia Mappa, Victoria Bitsadze, Jamilya Khizroeva, and Alexander Makatsariya. 2020. "Fetal cardiac remodelling in pregnancies complicated by gestational diabetes mellitus: a prospective cohort study." (1):13-18. doi: 10.5114/pcard.2020.94558.

Robbins, J., J. Gulick, A. Sanchez, P. Howles, and T. Doetschman. 1990. "Mouse embryonic stem cells express the cardiac myosin heavy chain genes during development in vitro." *J Biol Chem* 265 (20):11905-9.

Roest, P. A., L. van Iperen, S. Vis, L. J. Wisse, R. E. Poelmann, R. P. Steegers-Theunissen, D. G. Molin, U. J. Eriksson, and A. C. Gittenberger-De Groot. 2007. "Exposure of neural crest cells to elevated glucose leads to congenital heart defects, an effect that can be prevented by N-acetylcysteine." *Birth Defects Res A Clin Mol Teratol* 79 (3):231-5. doi: 10.1002/bdra.20341.

Roglic, G., N. Unwin, P. H. Bennett, C. Mathers, J. Tuomilehto, S. Nag, V. Connolly, and H. King. 2005. "The burden of mortality attributable to diabetes: realistic estimates for the year 2000." *Diabetes Care* 28 (9):2130-5.

Rosenkranz, S., M. Flesch, K. Amann, C. Haeuseler, H. Kilter, U. Seeland, K. D. Schluter, and M. Bohm. 2002. "Alterations of beta-adrenergic signaling and cardiac hypertrophy in transgenic mice overexpressing TGF-beta(1)." *Am J Physiol Heart Circ Physiol* 283 (3):H1253-62. doi: 10.1152/ajpheart.00578.2001.

Rosenn, M. F. 1998. "Pregnancy outcomes in women with gestational diabetes compared with the general obstetric population." *Obstet Gynecol* 91 (4):638-9; author reply 639-40.

Rubler, S., J. Dlugash, Y. Z. Yuceoglu, T. Kumral, A. W. Branwood, and A. Grishman. 1972. "New type of cardiomyopathy associated with diabetic glomerulosclerosis." *Am J Cardiol* 30 (6):595-602. doi: 10.1016/0002-9149(72)90595-4.

Rupp, H., V. Elimban, and N. S. Dhalla. 1989. "Diabetes-like action of intermittent fasting on sarcoplasmic reticulum Ca2+-pump ATPase and myosin isoenzymes can be prevented by sucrose." *Biochem Biophys Res Commun* 164 (1):319-25.

Russell, J. W., K. A. Sullivan, A. J. Windebank, D. N. Herrmann, and E. L. Feldman. 1999. "Neurons undergo apoptosis in animal and cell culture models of diabetes." *Neurobiol Dis* 6 (5):347-63. doi: 10.1006/nbdi.1999.0254.

Russell, N. E., P. Holloway, S. Quinn, M. Foley, P. Kelehan, and F. M. McAuliffe. 2008. "Cardiomyopathy and cardiomegaly in stillborn infants of diabetic mothers." *Pediatr Dev Pathol* 11 (1):10-4. doi: 10.2350/07-05-0277.1.

Russell, R. R., 3rd, R. Yin, M. J. Caplan, X. Hu, J. Ren, G. I. Shulman, A. J. Sinusas, and L. H. Young. 1998. "Additive effects of hyperinsulinemia and ischemia on myocardial GLUT1 and GLUT4 translocation in vivo." *Circulation* 98 (20):2180-6.

Sadoshima, J., and S. Izumo. 1997. "The cellular and molecular response of cardiac myocytes to mechanical stress." *Annu Rev Physiol* 59:551-71. doi: 10.1146/annurev.physiol.59.1.551.

Salem, K. A., M. A. Qureshi, V. Sydorenko, K. Parekh, P. Jayaprakash, T. Iqbal, J. Singh, M. Oz, T. E. Adrian, and F. C. Howarth. 2013. "Effects of exercise training on excitation-contraction coupling and related mRNA expression in hearts of Goto-Kakizaki type 2 diabetic rats." *Mol Cell Biochem* 380 (1-2):83-96. doi: 10.1007/s11010-013-1662-2.

Salvesen, G. S., and V. M. Dixit. 1997. "Caspases: intracellular signaling by proteolysis." *Cell* 91 (4):443-6. doi: 10.1016/s0092-8674(00)80430-4.

Sauer, H., T. Theben, J. Hescheler, M. Lindner, M. C. Brandt, and M. Wartenberg. 2001. "Characteristics of calcium sparks in cardiomyocytes derived from embryonic stem cells." *Am J Physiol Heart Circ Physiol* 281 (1):H411-21. doi: 10.1152/ajpheart.2001.281.1.H411.

Schaper, J., R. Froede, S. Hein, A. Buck, H. Hashizume, B. Speiser, A. Friedl, and N. Bleese. 1991. "Impairment of the myocardial ultrastructure and changes of the cytoskeleton in dilated cardiomyopathy." *Circulation* 83 (2):504-14. doi: 10.1161/01.cir.83.2.504.

Schleich, J. M., T. Abdulla, R. Summers, and L. Houyel. 2013. "An overview of cardiac morphogenesis." *Arch Cardiovasc Dis* 106 (11):612-23. doi: 10.1016/j.acvd.2013.07.001.

Schleicher, E. D., and C. Weigert. 2000. "Role of the hexosamine biosynthetic pathway in diabetic nephropathy." *Kidney Int Suppl* 77:S13-8. doi: 10.1046/j.1523-1755.2000.07703.x.

Schleiffarth, J. R., A. D. Person, B. J. Martinsen, D. J. Sukovich, A. Neumann, C. V. Baker, J. L. Lohr, D. N. Cornfield, S. C. Ekker, and A. Petryk. 2007. "Wnt5a is required for cardiac outflow tract septation in mice." *Pediatr Res* 61 (4):386-91. doi: 10.1203/pdr.0b013e3180323810.

Sekaran, N. K., A. L. Crowley, F. R. de Souza, E. S. Resende, and S. V. Rao. 2017. "The Role for Cardiovascular Remodeling in Cardiovascular Outcomes." *Curr Atheroscler Rep* 19 (5):23. doi: 10.1007/s11883-017-0656-z.

Sesaki, H., and R. E. Jensen. 1999. "Division versus fusion: Dnm1p and Fzo1p antagonistically regulate mitochondrial shape." *J Cell Biol* 147 (4):699-706. doi: 10.1083/jcb.147.4.699.

Shaw, J. E., R. A. Sicree, and P. Z. Zimmet. 2010. "Global estimates of the prevalence of diabetes for 2010 and 2030." *Diabetes Res Clin Pract* 87 (1):4-14. doi: 10.1016/j.diabres.2009.10.007.

Shi, M., N. T. Tien, L. de Haan, J. Louisse, Imcm Rietjens, and H. Bouwmeester. 2020. "Evaluation of in vitro models of stem cell-derived cardiomyocytes to screen for potential cardiotoxicity of chemicals." *Toxicol In Vitro* 67:104891. doi: 10.1016/j.tiv.2020.104891.

Shizukuda, Y., M. E. Reyland, and P. M. Buttrick. 2002. "Protein kinase C-delta modulates apoptosis induced by hyperglycemia in adult ventricular myocytes." *Am J Physiol Heart Circ Physiol* 282 (5):H1625-34. doi: 10.1152/ajpheart.00783.2001.

Sinclair, A., P. Saeedi, A. Kaundal, S. Karuranga, B. Malanda, and R. Williams. 2020. "Diabetes and global ageing among 65-99-year-old adults: Findings from the International Diabetes Federation Diabetes Atlas, 9(th) edition." *Diabetes Res Clin Pract* 162:108078. doi: 10.1016/j.diabres.2020.108078.

Sivan, E., Y. C. Lee, Y. K. Wu, and E. A. Reece. 1997. "Free radical scavenging enzymes in fetal dysmorphogenesis among offspring of diabetic rats." *Teratology* 56 (6):343-9. doi: 10.1002/(sici)1096-9926(199712)56:6<343::Aid-tera1>3.0.Co;2-x.

Siwik, D. A., P. J. Pagano, and W. S. Colucci. 2001. "Oxidative stress regulates collagen synthesis and matrix metalloproteinase activity in cardiac fibroblasts." *Am J Physiol Cell Physiol* 280 (1):C53-60. doi: 10.1152/ajpcell.2001.280.1.C53.

Smith, A. G., J. K. Heath, D. D. Donaldson, G. G. Wong, J. Moreau, M. Stahl, and D. Rogers. 1988. "Inhibition of pluripotential embryonic stem cell differentiation by purified polypeptides." *Nature* 336 (6200):688-90. doi: 10.1038/336688a0.

Soedamah-Muthu, S. S., J. H. Fuller, H. E. Mulnier, V. S. Raleigh, R. A. Lawrenson, and H. M. Colhoun. 2006. "High risk of cardiovascular disease in patients with type 1 diabetes in the U.K.: a cohort study using the general practice research database." *Diabetes Care* 29 (4):798-804.

Soltysinska, E., T. Speerschneider, S. V. Winther, and M. B. Thomsen. 2014. "Sinoatrial node dysfunction induces cardiac arrhythmias in diabetic mice." *Cardiovasc Diabetol* 13:122. doi: 10.1186/s12933-014-0122-y.

Sprick, M. R., M. A. Weigand, E. Rieser, C. T. Rauch, P. Juo, J. Blenis, P. H. Krammer, and H. Walczak. 2000. "FADD/MORT1 and caspase-8 are recruited to TRAIL receptors 1 and 2 and are essential for apoptosis mediated by TRAIL receptor 2." *Immunity* 12 (6):599-609. doi: 10.1016/s1074-7613(00)80211-3.

Stanley, W. C., F. A. Recchia, and G. D. Lopaschuk. 2005. "Myocardial substrate metabolism in the normal and failing heart." *Physiol Rev* 85 (3):1093-129. doi: 10.1152/physrev.00006.2004.

Starikov, R., J. Bohrer, W. Goh, M. Kuwahara, E. K. Chien, V. Lopes, and D. Coustan. 2013. "Hemoglobin A1c in pregestational diabetic gravidas and the risk of congenital heart disease in the fetus." *Pediatr Cardiol* 34 (7):1716-22. doi: 10.1007/s00246-013-0704-6.

Steinhauser, M. L., and R. T. Lee. 2011. "Regeneration of the heart." *EMBO Mol Med* 3 (12):701-12. doi: 10.1002/emmm.201100175.

Striker, L. J., and G. E. Striker. 1996. "Administration of AGEs in vivo induces extracellular matrix gene expression." *Nephrol Dial Transplant* 11 Suppl 5:62-5.

Sun, S. Y. 2010. "N-acetylcysteine, reactive oxygen species and beyond." *Cancer Biol Ther* 9 (2):109-10. doi: 10.4161/cbt.9.2.10583.

Swynghedauw, B. 1999. "Molecular mechanisms of myocardial remodeling." *Physiol Rev* 79 (1):215-62. doi: 10.1152/physrev.1999.79.1.215.

Tang, W. H., W. T. Cheng, G. M. Kravtsov, X. Y. Tong, X. Y. Hou, S. K. Chung, and S. S. Chung. 2010. "Cardiac contractile dysfunction during acute hyperglycemia due to impairment of SERCA by polyol pathway-mediated oxidative stress." *Am J Physiol Cell Physiol* 299 (3):C643-53. doi: 10.1152/ajpcell.00137.2010.

Tang, W. H., K. A. Martin, and J. Hwa. 2012. "Aldose reductase, oxidative stress, and diabetic mellitus." *Front Pharmacol* 3:87. doi: 10.3389/fphar.2012.00087.

Tartaglia, L. A., M. Rothe, Y. F. Hu, and D. V. Goeddel. 1993. "Tumor necrosis factor's cytotoxic activity is signaled by the p55 TNF receptor." *Cell* 73 (2):213-6. doi: 10.1016/0092-8674(93)90222-c.

Teramo, K. A. 2010. "Obstetric problems in diabetic pregnancy - The role of fetal hypoxia." *Best Pract Res Clin Endocrinol Metab* 24 (4):663-71. doi: 10.1016/j.beem.2010.05.005.

Thomson, J. A., J. Itskovitz-Eldor, S. S. Shapiro, M. A. Waknitz, J. J. Swiergiel, V. S. Marshall, and J. M. Jones. 1998. "Embryonic stem cell lines derived from human blastocysts." *Science* 282 (5391):1145-7.

Toblli, J. E., G. Cao, G. DeRosa, and P. Forcada. 2005. "Reduced cardiac expression of plasminogen activator inhibitor 1 and transforming growth factor beta1 in obese Zucker rats by perindopril." *Heart* 91 (1):80-6. doi: 10.1136/hrt.2003.022707.

Toker, A., and L. C. Cantley. 1997. "Signalling through the lipid products of phosphoinositide-3-OH kinase." *Nature* 387 (6634):673-6. doi: 10.1038/42648.

Trafford, A. W., M. E. Díaz, S. C. O'Neill, and D. A. Eisner. 2002. "Integrative analysis of calcium signalling in cardiac muscle." *Front Biosci* 7:d843-52. doi: 10.2741/trafford.

Trump, B. F., I. K. Berezesky, S. H. Chang, and P. C. Phelps. 1997. "The pathways of cell death: oncosis, apoptosis, and necrosis." *Toxicol Pathol* 25 (1):82-8. doi: 10.1177/019262339702500116.

Tse, G., E. T. Lai, J. M. Yeo, and B. P. Yan. 2016. "Electrophysiological Mechanisms of Bayés Syndrome: Insights from Clinical and Mouse Studies." *Front Physiol* 7:188. doi: 10.3389/fphys.2016.00188.

Turan, B., and G. Vassort. 2011. "Ryanodine receptor: a new therapeutic target to control diabetic cardiomyopathy." *Antioxid Redox Signal* 15 (7):1847-61. doi: 10.1089/ars.2010.3725.

Tziakas, D. N., G. K. Chalikias, and J. C. Kaski. 2005. "Epidemiology of the diabetic heart." *Coron Artery Dis* 16 Suppl 1:S3-s10.

Uemura, S., H. Matsushita, W. Li, A. J. Glassford, T. Asagami, K. H. Lee, D. G. Harrison, and P. S. Tsao. 2001. "Diabetes mellitus enhances vascular matrix metalloproteinase activity: role of oxidative stress." *Circ Res* 88 (12):1291-8.

Ullmo, S., Y. Vial, S. Di Bernardo, M. Roth-Kleiner, Y. Mivelaz, N. Sekarski, J. Ruiz, and E. J. Meijboom. 2007. "Pathologic ventricular hypertrophy in the offspring of diabetic mothers: a retrospective study." *Eur Heart J* 28 (11):1319-25. doi: 10.1093/eurheartj/ehl416.

van Heerebeek, L., N. Hamdani, M. L. Handoko, I. Falcao-Pires, R. J. Musters, K. Kupreishvili, A. J. Ijsselmuiden, C. G. Schalkwijk, J. G. Bronzwaer, M. Diamant, A. Borbely, J. van der Velden, G. J. Stienen, G. J. Laarman, H. W. Niessen, and W. J. Paulus. 2008. "Diastolic stiffness of the failing diabetic heart: importance of fibrosis, advanced glycation end products, and myocyte resting tension." *Circulation* 117 (1):43-51. doi: 10.1161/circulationaha.107.728550.

van Kempen, M. J., C. Fromaget, D. Gros, A. F. Moorman, and W. H. Lamers. 1991. "Spatial distribution of connexin43, the major cardiac gap junction protein, in the developing and adult rat heart." *Circ Res* 68 (6):1638-51. doi: 10.1161/01.res.68.6.1638.

Vander Heiden, M. G., N. S. Chandel, E. K. Williamson, P. T. Schumacker, and C. B. Thompson. 1997. "Bcl-xL regulates the membrane potential and volume homeostasis of mitochondria." *Cell* 91 (5):627-37. doi: 10.1016/s0092-8674(00)80450-x.

Veille, J. C., R. Hanson, M. Sivakoff, H. Hoen, and M. Ben-Ami. 1993. "Fetal cardiac size in normal, intrauterine growth retarded, and diabetic pregnancies." *Am J Perinatol* 10 (4):275-9. doi: 10.1055/s-2007-994739.

Vermeulen, I., I. Weets, M. Asanghanwa, J. Ruige, L. Van Gaal, C. Mathieu, B. Keymeulen, V. Lampasona, J. M. Wenzlau, J. C. Hutton, D. G. Pipeleers, and F. K. Gorus. 2011. "Contribution of antibodies against IA-2β and zinc transporter 8 to classification of diabetes diagnosed under 40 years of age." *Diabetes Care* 34 (8):1760-5. doi: 10.2337/dc10-2268.

Viatchenko-Karpinski, S., B. K. Fleischmann, Q. Liu, H. Sauer, O. Gryshchenko, G. J. Ji, and J. Hescheler. 1999. "Intracellular Ca2+ oscillations drive spontaneous contractions in

cardiomyocytes during early development." *Proc Natl Acad Sci U S A* 96 (14):8259-64. doi: 10.1073/pnas.96.14.8259.

von Harsdorf, R., P. F. Li, and R. Dietz. 1999. "Signaling pathways in reactive oxygen species-induced cardiomyocyte apoptosis." *Circulation* 99 (22):2934-41.

Vural, M., L. Leke, H. Mahomedaly, Y. Maingourd, O. Kremp, and B. Risbourg. 1995. "Should an echocardiographic scan be done routinely for infants of diabetic mothers?" *Turk J Pediatr* 37 (4):351-6.

Wang, F., E. A. Reece, and P. Yang. 2015. "Oxidative stress is responsible for maternal diabetes-impaired transforming growth factor beta signaling in the developing mouse heart." *Am J Obstet Gynecol* 212 (5):650.e1-11. doi: 10.1016/j.ajog.2015.01.014.

Wang, X., J. Pan, D. Liu, M. Zhang, X. Li, J. Tian, M. Liu, T. Jin, and F. An. 2019. "Nicorandil alleviates apoptosis in diabetic cardiomyopathy through PI3K/Akt pathway." *J Cell Mol Med* 23 (8):5349-5359. doi: 10.1111/jcmm.14413.

Wang, Y., and J. A. Hill. 2010. "Electrophysiological remodeling in heart failure." *J Mol Cell Cardiol* 48 (4):619-32. doi: 10.1016/j.yjmcc.2010.01.009.

Way, K. J., K. Isshiki, K. Suzuma, T. Yokota, D. Zvagelsky, F. J. Schoen, G. E. Sandusky, P. A. Pechous, C. J. Vlahos, H. Wakasaki, and G. L. King. 2002. "Expression of connective tissue growth factor is increased in injured myocardium associated with protein kinase C beta2 activation and diabetes." *Diabetes* 51 (9):2709-18.

Weber, K. T. 1997. "Extracellular matrix remodeling in heart failure: a role for de novo angiotensin II generation." *Circulation* 96 (11):4065-82.

Webster, D. R., and D. L. Patrick. 2000. "Beating rate of isolated neonatal cardiomyocytes is regulated by the stable microtubule subset." *Am J Physiol Heart Circ Physiol* 278 (5):H1653-61. doi: 10.1152/ajpheart.2000.278.5.H1653.

Weiss, P. A., H. S. Scholz, J. Haas, K. F. Tamussino, J. Seissler, and M. H. Borkenstein. 2000. "Long-term follow-up of infants of mothers with type 1 diabetes: evidence for hereditary and nonhereditary transmission of diabetes and precursors." *Diabetes Care* 23 (7):905-11. doi: 10.2337/diacare.23.7.905.

Westermann, D., S. Rutschow, S. Jager, A. Linderer, S. Anker, A. Riad, T. Unger, H. P. Schultheiss, M. Pauschinger, and C. Tschope. 2007. "Contributions of inflammation and cardiac matrix metalloproteinase activity to cardiac failure in diabetic cardiomyopathy: the role of angiotensin type 1 receptor antagonism." *Diabetes* 56 (3):641-6. doi: 10.2337/db06-1163.

WHO. 2021. "GLOBAL REPORT ON DIABETES."

Wilkins, B. J., Y. S. Dai, O. F. Bueno, S. A. Parsons, J. Xu, D. M. Plank, F. Jones, T. R. Kimball, and J. D. Molkentin. 2004. "Calcineurin/NFAT coupling participates in pathological, but not physiological, cardiac hypertrophy." *Circ Res* 94 (1):110-8. doi: 10.1161/01.res.0000109415.17511.18.

Wobus, A. M., K. Guan, H. T. Yang, and K. R. Boheler. 2002. "Embryonic stem cells as a model to study cardiac, skeletal muscle, and vascular smooth muscle cell differentiation." *Methods Mol Biol* 185:127-56. doi: 10.1385/1-59259-241-4:127.

Wobus, A. M., G. Wallukat, and J. Hescheler. 1991. "Pluripotent mouse embryonic stem cells are able to differentiate into cardiomyocytes expressing chronotropic responses to adrenergic and cholinergic agents and Ca2+ channel blockers." *Differentiation* 48 (3):173-82. doi: 10.1111/j.1432-0436.1991.tb00255.x.

Wren, C., G. Birrell, and G. Hawthorne. 2003. "Cardiovascular malformations in infants of diabetic mothers." *Heart* 89 (10):1217-20. doi: 10.1136/heart.89.10.1217.

Xu, X., L. Ruan, X. Tian, F. Pan, C. Yang, and G. Liu. 2020. "Calcium inhibitor inhibits high glucose-induced hypertrophy of H9C2 cells." *Mol Med Rep* 22 (3):1783-1792. doi: 10.3892/mmr.2020.11275.

Yan, S. D., A. M. Schmidt, G. M. Anderson, J. Zhang, J. Brett, Y. S. Zou, D. Pinsky, and D. Stern. 1994. "Enhanced cellular oxidant stress by the interaction of advanced glycation end products with their receptors/binding proteins." *J Biol Chem* 269 (13):9889-97.

Yang, H. T., D. Tweedie, S. Wang, A. Guia, T. Vinogradova, K. Bogdanov, P. D. Allen, M. D. Stern, E. G. Lakatta, and K. R. Boheler. 2002. "The ryanodine receptor modulates the spontaneous beating rate of cardiomyocytes during development." *Proc Natl Acad Sci U S A* 99 (14):9225-30. doi: 10.1073/pnas.142651999.

Yang, P., X. Chen, S. Kaushal, E. A. Reece, and P. Yang. 2016. "High glucose suppresses embryonic stem cell differentiation into cardiomyocytes : High glucose inhibits ES cell cardiogenesis." *Stem Cell Res Ther* 7 (1):187. doi: 10.1186/s13287-016-0446-5.

Yang, P., and H. Li. 2010. "Epigallocatechin-3-gallate ameliorates hyperglycemia-induced embryonic vasculopathy and malformation by inhibition of Foxo3a activation." *Am J Obstet Gynecol* 203 (1):75.e1-6. doi: 10.1016/j.ajog.2010.02.008.

Yang, P., E. A. Reece, F. Wang, and R. Gabbay-Benziv. 2015. "Decoding the oxidative stress hypothesis in diabetic embryopathy through proapoptotic kinase signaling." *Am J Obstet Gynecol* 212 (5):569-79. doi: 10.1016/j.ajog.2014.11.036.

Yao, H., X. Han, and X. Han. 2014. "The cardioprotection of the insulin-mediated PI3K/Akt/mTOR signaling pathway." *Am J Cardiovasc Drugs* 14 (6):433-42. doi: 10.1007/s40256-014-0089-9.

Yao, R., and G. M. Cooper. 1996. "Growth factor-dependent survival of rodent fibroblasts requires phosphatidylinositol 3-kinase but is independent of pp70S6K activity." *Oncogene* 13 (2):343-51.

Yung, C. K., V. L. Halperin, G. F. Tomaselli, and R. L. Winslow. 2004. "Gene expression profiles in end-stage human idiopathic dilated cardiomyopathy: altered expression of apoptotic and cytoskeletal genes." *Genomics* 83 (2):281-97. doi: 10.1016/j.ygeno.2003.08.007.

Zhang, J., M. Klos, G. F. Wilson, A. M. Herman, X. Lian, K. K. Raval, M. R. Barron, L. Hou, A. G. Soerens, J. Yu, S. P. Palecek, G. E. Lyons, J. A. Thomson, T. J. Herron, J. Jalife, and T. J. Kamp. 2012. "Extracellular matrix promotes highly efficient cardiac differentiation of human pluripotent stem cells: the matrix sandwich method." *Circ Res* 111 (9):1125-36. doi: 10.1161/circresaha.112.273144.

Zhang, L., M. B. Cannell, A. R. Phillips, G. J. Cooper, and M. L. Ward. 2008. "Altered calcium homeostasis does not explain the contractile deficit of diabetic cardiomyopathy." *Diabetes* 57 (8):2158-66. doi: 10.2337/db08-0140.

Zhang, Y. L., and J. R. Wei. 2013. "3-nitrotyrosine, a biomarker for cardiomyocyte apoptosis induced by diabetic cardiomyopathy in a rat model." *Mol Med Rep* 8 (4):989-94. doi: 10.3892/mmr.2013.1644.

Zhao, F., B. Li, Y. Z. Wei, B. Zhou, H. Wang, M. Chen, X. D. Gan, Z. H. Wang, and S. X. Xiong. 2013. "MicroRNA-34a regulates high glucose-induced apoptosis in H9c2 cardiomyocytes." *J Huazhong Univ Sci Technolog Med Sci* 33 (6):834-839. doi: 10.1007/s11596-013-1207-7.

Zhao, Y., G. M. Cui, N. N. Zhou, C. Li, Q. Zhang, H. Sun, B. Han, C. W. Zou, L. J. Wang, X. D. Li, and J. C. Wang. 2016. "Calpain-Calcineurin-Nuclear Factor Signaling and the Development of Atrial Fibrillation in Patients with Valvular Heart Disease and Diabetes." *J Diabetes Res* 2016:4639654. doi: 10.1155/2016/4639654.

Zhao, Z., P. Yang, R. L. Eckert, and E. A. Reece. 2009. "Caspase-8: a key role in the pathogenesis of diabetic embryopathy." *Birth Defects Res B Dev Reprod Toxicol* 86 (1):72-7. doi: 10.1002/bdrb.20185.

Zhou, P., and W. T. Pu. 2016. "Recounting Cardiac Cellular Composition." *Circ Res* 118 (3):368-70. doi: 10.1161/circresaha.116.308139.

Zima, A. V., and L. A. Blatter. 2006. "Redox regulation of cardiac calcium channels and transporters." *Cardiovasc Res* 71 (2):310-21. doi: 10.1016/j.cardiores.2006.02.019.

Ziyadeh, F. N., K. Sharma, M. Ericksen, and G. Wolf. 1994. "Stimulation of collagen gene expression and protein synthesis in murine mesangial cells by high glucose is mediated by autocrine activation of transforming growth factor-beta." *J Clin Invest* 93 (2):536-42. doi: 10.1172/jci117004.

Appendices

Appendix 1: Cell culture recipes and reagents

1- Preparation of culture media

To keep the condition of sterility, bottles, measuring cylinders were autoclaved before used for culture medium preparation. The bottle culture medium was used in this study.

MEF media (Recipe for 50 ml media):

Content	Amount
DMEM (25mM)	43.95 ml
FBS	5 ml
Glutamax	0.5 ml
Pen/Step	0.5 ml
Mercaptoethanol	50 ul

mES media (Recipe for 50 ml media):

Content	Amount
DMEM (25mM)	41.45 ml
FBS	7.5 ml
Glutamax	0.5 ml
Pen/Step	0.5 ml
Mercaptoethanol	50 µl
LIF	50 µl

After preparation, the culture medium was filtered through 0.22 µm filter and kept at 4^{o}C.

2- Preparation of 0.1% gelatine

Add 0.1g of type A gelatine to100 ml double distilled water and autoclave it. Store at room temperature.

3- Preparation of dispase II solution

To prepare 5 mg/ml, weigh 100 mg in of dispase lyophilized form and add it to 20ml basal DMEM, mix well and vortex to dissolve filter with through 0.22 µm filter syringe filter and aliquoted in well labelled eppendorf 1ml each and store at -20^{o}C.

4- Preparation of foetal bovine serum (FBS)

FBS was heat inactivation at 60C for 20 minutes in a water bath well balanced. The FBS allowed to cool down to room temperature were then aliquoted and stored at -20^{o}C in 50 ml aliquots.

5- Preparation of penicillin G and streptomycin sulphate

Penicillin G (Sigma, SA, P- 3032), Streptomycin sulphate (Sigma, SA, S-91370). Final concentration required Penicillin 100 U/ml, Streptomycin 100 µg/ml. To prepare 500 ml, weigh 3 g Penicillin, and 5 g Streptomycin, then dissolve them in 500 ml autoclaved double distilled water. Sterile filter through 0.22 µm filter, aliquot and store at -20^{o}C.

6- Preparation of 4% PFA solution

Work in the fume-hood, wear gloves and face mask.

For preparation of 100ml 4% PFA solution, the requirements include:

100 ml 1 x PBS 4g PFA powder
Weighing boat Spatula/spoon
250 ml Beaker 100 ml Measuring cylinder
pH strips filter paper
Funnel 100 ml Schott bottle
50 ml labelled tubes for storage in the freezer.

Protocol:

1- Measure 80 ml 1x PBS and add to a beaker.
2- Weigh 4 g PFA and add that to the PBS.
3- Cover the beaker with foil.
4- Place onto magnetic stirrer and stir for about 20 min.
5- Turn on heat in the stirrer to dissolve the PFA powder. The temperature should never exceed 60°C using a thermometer to check the temperature
6- Wait for the PFA to be completely dissolved.
7- Leave to cool to room temperature for about 2-3 hours.
8- Adjust pH to 7.4
9- Pour the PFA solution into a 100 ml measuring cylinder and top it up to a 100 ml with 1x PBS.
10- Filter it into a 100 ml Schott bottle.
11- Store in the fridge short term or aliquot in 50 ml tubes and freeze at -20°C for long term use.

Appendix 2: Cell culture methods

1- Thawing cells

Switch on water bath to 37^{o}C. Pipette 5 ml of medium into a 15 ml tube. Transfer the vial of the cells from liquid nitrogen tank to water bath wrapped with tissue paper sprayed with 70% alcohol. Thaw cell vial in the water bath (2-4 minutes), transfer cells to the warmed medium in tube. Spin cells at 1000 rpm for 5 minutes. The supernatant removed and the cell pellet re-suspended in 1ml of medium and triturate into a single cell suspension. After titration of cell pellet transferred to a gelatinized cell culture dish and distribute the cells all-over the dish. Incubate the cells at 37 ^{o}C with 5% CO_2 and 95% humidity.

2- Freezing down cells

Cells were lifted with Dispase II centrifuged, and the cell pellet re-suspended in filtered ice-cold freeze down medium consisting of DMEM supplemented with 20% FBS and 10% dimethyl sulfoxide and transferred to cold cryogenic tubes, which kept on ice until transferred to -80°C overnight. The cells were then placed in liquid nitrogen store for long term storage.

3- Preparation of feeder layer

Culture and passage: Mouse embryonic fibroblast (MEFs) were originally from ATCC. MEFs were seeded and maintained in MEF medium containing DMEM 4.5 g/L glucose supplemented with FBS (10%), glutamax (1%), penicillin/ streptomycin (1%), and B-mercaptoethanol (0.1%). The medium was changed every 3-4 days. The cells were passaged at confluency of 80-90%, the medium aspirated and the cells washed with 1x PBS then trypsin/EDTA was added, and the cells incubated for 5 minutes at 37 ^{o}C to lift the cells. Trypsin/ EDTA was then inactivated with equal volume of MEF medium. The cells were transferred into 15 ml tubes and centrifuged at 1500 rcf for 5 minutes. The cell pellets were triturated with MEF medium and plated at 1:4 splits into new culture dishes. The MEFs were mycoplasma tested with every passage to exclude mycoplasma infection. The MEFs were passaged to passage 6 were the mitotic inactivation done.

Mitotic inactivation: Mitotic inactivation was done to prevent growth of the cells to become stable as a feeder layer for embryonic cell culture. Mitomycin C (Sigma-Aldrich, USA) was used for mitotic inactivation, which based on the principle that Mitomycin C breaks the cell cycle by cross linking with MEFs DNA thus preventing cell mitosis but permitting cell metabolism to continue (Ishii 1981). For MEFs inactivation, the medium removed, and the cells washed with1x PBS. Fresh MEF medium added containing with mitomycin C (10 µg/ml sterilize by filtration) and the cells were incubated at 37^{o}C in incubator for 2.5-3 hours. Thereafter, the MEF media with Mitomycin C removed and the cells were washed 3 times with 1XPBS. The cells were then lifted with trypsin/EDTA, centrifuged, and then frozen down at a specific concentration 0.3 x10^{6}, 0.6 x10^{6}, 1x10^{6} cells/vial.

4- Mycoplasma test

The cells were regularly (with every new vial used from MESCs stocks in liquid nitrogen) it was tested for mycoplasma infection to ensure that uninfected cells were used in experiments. Mycoplasma is a gram-negative bacterium that have no cell membrane and is more resistant to common antibiotics. These microorganisms depend on their host cells for survival and have harmful effects on their host cells. Mycoplasma infections induce disturbances in cell metabolism, alteration in cell morphology, causes disorders in cell growth and promote apoptosis (Gong et al. 1999). Therefore, testing the cells for mycoplasma infection is an important step in cell culture model. Mycoplasma infection is a subtle infection difficult to detect in cell culture and can be detected through nuclear staining, which stains both mycoplasma and nuclei of the cell (Nikfarjam and Farzaneh 2012).

The cells were cultured on sterile coverslips in in 35mm dishes in antibiotic-free culture medium consisting of Dulbecco·s Modified Eagles Medium (DMEM) 4.5 g/L glucose (Catalog Numbers 31966047, Thermofisher Scientific, SA) supplemented with foetal bovine serum (FBS) (10%), glutamax (1%), penicillin/ streptomycin (1%), and B-mercaptoethanol (0.1%) for 5 days. For mycoplasma staining, the medium was discarded, and the cells washed in 1XPBS then the cells were fixed using mixture 1:3 of glacial acetic acid and methanol at room temperature for 10 seconds, washed with distilled water for 3 minutes. The cells were stained with Hoechst 33258 (0.5 µg/ml) for 30 seconds, washed with distilled water 3 times and mounted on a glass slide using mounting fluid. The slides were allowed to dry 1-2 hours before viewing under a fluorescent microscope (Zeiss Axiovert 200M) using the DAPI filter. Hoechst stain binds to all nuclear components and consequently a positive mycoplasma result is detected as fluorescent dots on the cellular membrane and in the cytoplasm of the cells. Mycoplasma negative cells stained positive with Hoechst only in the nucleus. None of the cell batch staining were positive for mycoplasma.

5- Cell counting on a haemocytometer

A hemocytometer was cleaned with 70% ethanol. Resuspended cells were vortexed and 10 µL of cell suspension was transferred on the hemocytometer chamber.

4 Blocks (A-D) containing cells were counted under the microscope and cell number was determined as follows:

Total cell number=number of total cells in all 4 blocks x 1000/4.

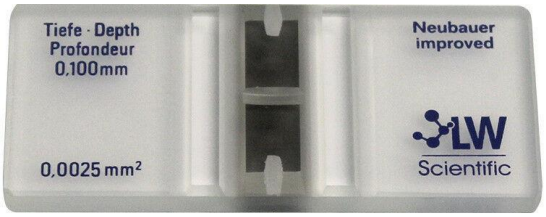

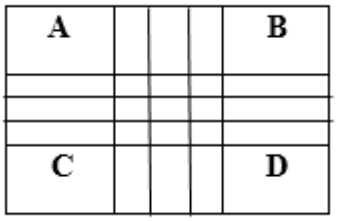

Hemocytometer chamber Counting blocks

6- Hanging drop

Following image shows how the drops placed onto the under surface of the lids of 10-cm culture dishes. The lids were then inverted and placed onto culture dishes filled PBS.

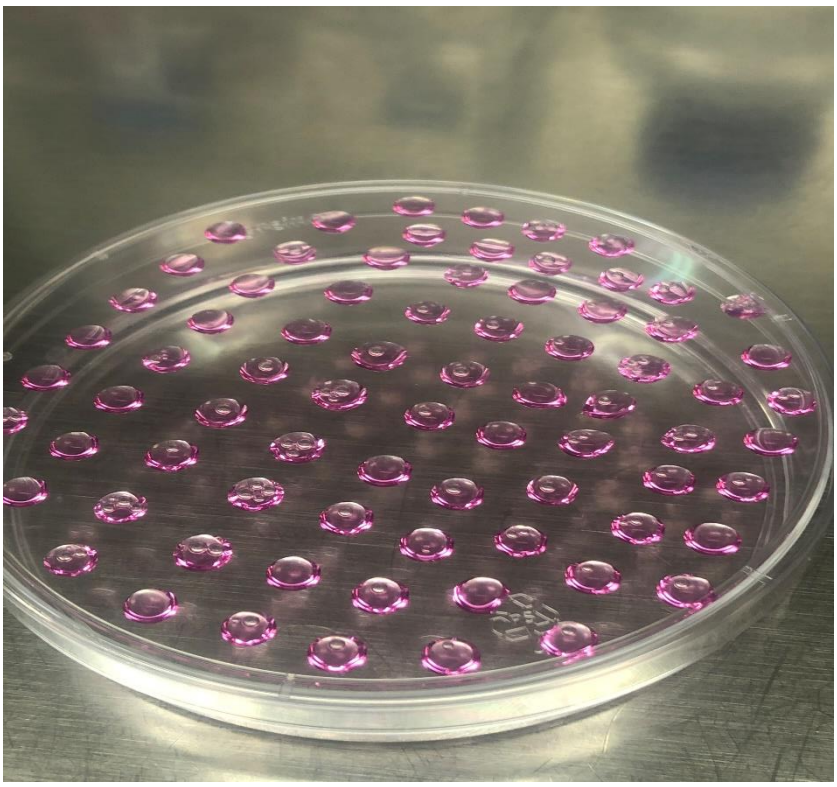

Hanging drop

Appendix 3: Calcium transient imaging optimization

Calcium transient imaging has been optimized throughout the period of the study. At first, the imaging was tried using LED light source, mightex camera using imaging software micromanager. The issue we had is the limitation of the camera frame rate it is just 5 frame/second which was the big limitation to use for calcium imaging or voltage sensitive dye imaging. Therefore, we optimized confocal calcium imaging. As all our experiments were conducted overall EBs, therefore also the calcium imaging needs to be overall EBs without dissociation of the cells which may disturb the cell

connection and impair the conduction and the contractile functionality. We used the confocal imaging and we found the signal were weak and also with the focus as the EBs the cells were in multilayers as there is difficulty in the focus which were later improved by using the imaging dishes which has a glass bottom and the EBs were platted early in these dishes for imaging, as in previous the EBs were plated on the glass coverslips and the coverslips were in the culture dishes so it is difficult to focus through two layers.

Appendix 4: Myocyter analysis of cellular contraction

Steps for analysis:

- Download Myocyter-Macroas.txt file.

- Create a folder with avi file for the confocal recorded cellular contraction.

- Open image J software and drag the myocyter txt file to open in the image j, it will open as following:

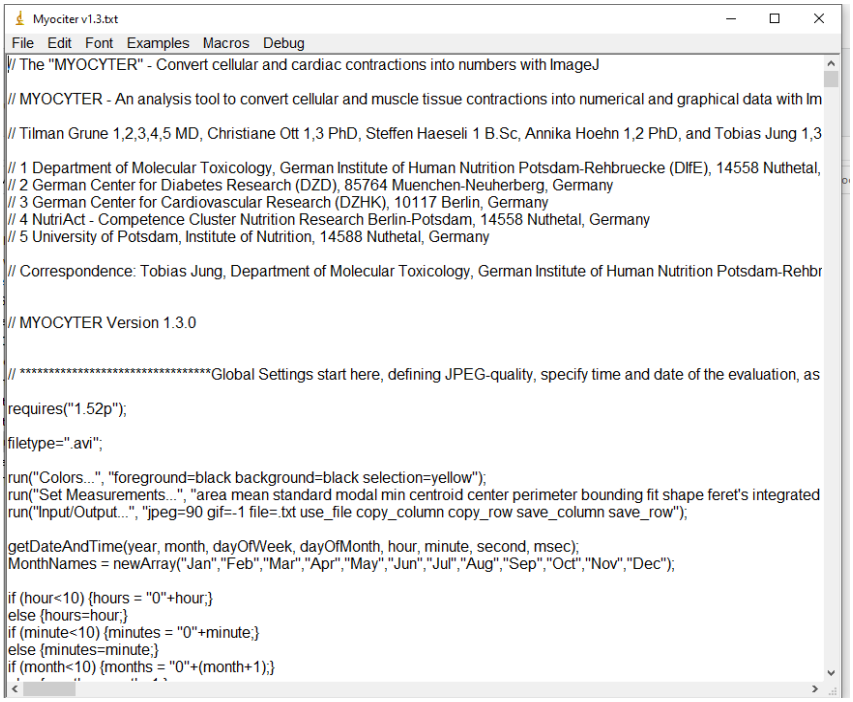

- Select run Macro from list under Macro list as follow:

-

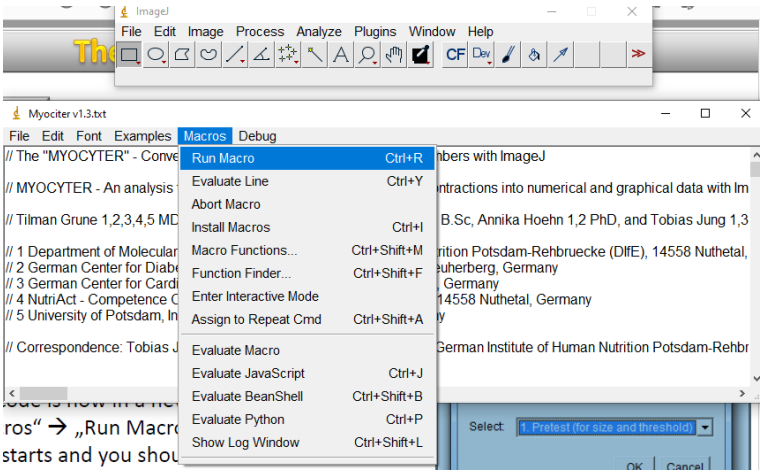

From run macro menu select pretest as follow:

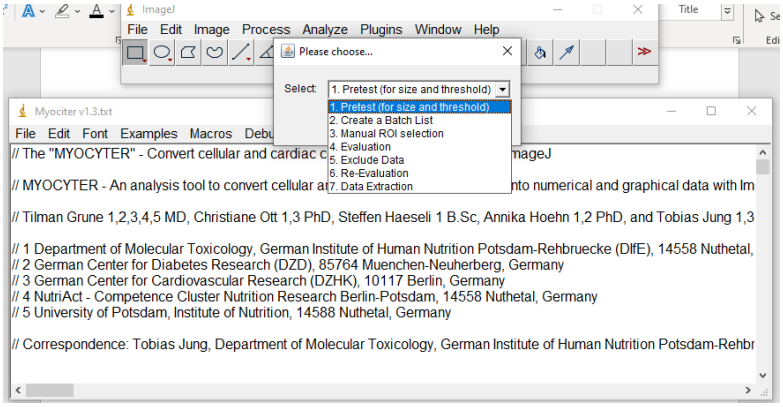

In the pretest window, use the default setting then click ok, then select folder containing avi video, without opening the folder. Once the pretest done, a new folder called pretest with created in the folder containing avi video.

- The next step is to create batch list, from macro list chose to create batchlist and from the widow select the folder containing pretest image without opening the folder and click ok.

- The next select manual ROI selection from macro list. This feature help for manual selecting the area of cellular beating to avoid analysing any artefact. Then select folder containing avi of cellular beating without opening the folder.

- The next is evaluation, from this window tick batching and ok as follow:

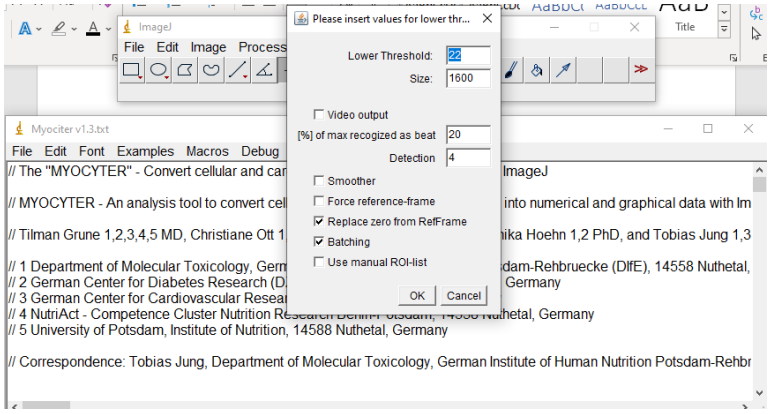

After evaluation done, new folders are created. The folder diffMove contain subfolder called data plots, which contains plots of amplitude of cellular contraction, and text file named results.

Appendix 5: TUNEL assay

We used in this study Click-it Plus TUNEL Assay for apoptosis detection with Alexa Fluor dyes Catalog No. C10617.

Following table shows the contents of the assays:

Material	Amount	Concentration
TdT Reaction Buffer (Component A)	8.0 mL	1X Solution
EdUTP nucleotide mixture (Component B)	55 µL	50X Solution
TdT (terminal deoxynucleotidyl transferase) *recombinant* (Component C)	3 vials (34 µL per vial)	15 U/µL in glycerol
Click-iT Plus TUNEL Reaction Buffer, 10X (Component D)	500 µL	10X Solution in Tris-buffered saline
Click-iT Plus TUNEL Reaction Buffer Additive (Component E)	400 mg	NA
Copper protectant (Component F)	100 µL	NA
Alexa Fluor picolyl azide dye	1 vial of Alexa Fluor	DMSO Solution

(Component G)	488 picolyl azide (25 µL)	

Preparations of working solutions

1- Allow assay contents to warm to room temperature before opening.

2- Prepare a working solution of 1X Click-iT Plus TUNEL Reaction buffer (Component D): Transfer all the solution in the Component D vial to 4.5 mL of deionized water.

To create smaller amounts of 1X Click-I-It Plus TUNEL Reaction buffer, dilute volumes from the Component D bottle 1:10 with deionized water.

3- Prepare a working solution of 1X Click-iT Plus TUNEL super mix according to following table:

Super mix components	Picolyl azide Alexa Fluor 488	Picolyl azide Alexa Fluor 594	Picolyl azide Alexa Fluor 647
1X Click-iT Plus TUNEL Reaction Buffer	2630 µL	2625 µL	2625 µL
Copper Protectant (Component F)	67 µL	67 µL	67 µL
Alexa Fluor picolyl azide (Component G)	3.7 µL	8.3 µL	8.3 µL
Total volume	2.7 mL	2.7 mL	2.7 mL

4- To prepare a 100X stock solution of the Click-iT Plus TUNEL Reaction Buffer Additive (Component E): Transfer 2 mL of deionized water to the vial (400 mg), then mix to dissolve the contents.

5- Following table preparation of TdT reaction mixtures.

Reaction components	Number of coverslips					
	1	2	5	10	25	50
TdT reaction buffer (Component A)	47 µL	94 µL	235 µL	470 µL	1,175 µL	2,350 µL
EdUTP (Component B)	1 µL	2 µL	5 µL	10 µL	25 µL	50 µL
TdT enzyme (Component C)	2 µL	4 µL	10 µL	20 µL	50 µL	100 µL

Total volume	50 µL	100 µL	250 µL	500 µL	1,250 µL	2,500 µL

6- Following table for the preparation of Click-iT Plus TUNEL reaction cocktails:

. Reaction components	Number of coverslips					
	1	2	5	10	25	50
Click-iT Plus TUNEL Supermix	45 µL	90 µL	225 µL	450 µL	1,125 µL	2,250 µL
10X Click-iT Plus TUNEL Reaction buffer additive	5 µL	10 µL	25 µL	50 µL	125 µL	250 µL
Total volume	50 µL	100 µL	250 µL	500 µL	1,250 µL	2,500 µL

Appendix 6: EdU cell proliferation assay

Table: Click-iT reaction cocktails.

Click-iT reaction cocktail	Number of coverslips		
Reaction components	1	2	5
1X Click-iT reaction buffer (prepared in step 1.4)	430 µL	860 µL	2.2 µL
$CuSO_4$ (Component E)	20 µL	40 µL	100 µL
Alexa Fluor azide	1.2 µL	2.5 µL	6 µL
Reaction buffer additive	50 ul	100ul	250ul
Total volume	500 µL	1ml	2.5 ml

Appendix 7: Western blot protocol

Process of western blot analysis

1- Preparation of buffers 2- Protein extraction

3- Protein Quantification 4- Sodium-dodecyl-sulphate polyacrylamide gel electrophoresis (SDS-PAGE)

5- Protein transfer 6- Blocking of the membrane and antibody probing

7- Western blot detection

8- Stripling and re-probing 9- Western blot analysis

1-Prepartion of the buffers:

A- Radioimmunoprecipitation assay buffer (RIPA buffer).

recipe for 50 ml include: NaCl (5 molar) 1.5 ml, Triton X -100 (100%) 500 ul, SDS (10%) 500 ul, Tris (1molar, Ph 7.5), Deoxycholate sodium 0.5 g and distilled water 46.5 ml.

B- Phosphate Buffered Saline-Tween (PBS-T).

(PBS-T×1): 8 g NaCl, 0.2 g KCl, 1.44 g Na_2HPO_4, 0.24 g KH_2PO_4, 2 ml Tween 20 and up to1000 ml distilled water, stir for 20 minutes and adjust the pH to 7.4.

C- Running (tank) buffer.

Using a Bio- Rad buffer (10× Tris/Glycine/SDS TGS Buffer, Bio Rad Laboratories. Inc. U.S). Mix 100 ml of TGS with 900 ml of distilled water.

D-Transfer buffer

Using Bio Rad buffer (Trans -BlotTurbo x5 Transfer buffer, Bio Rad Laboratories. Inc. U.S). Mix 200 ml of 5× transfer buffer with 600 ml of distilled water and 200 ml of ethanol.

E-Stripling buffer

8 g NaOH in 1 liter distilled water.

2-Protein extraction

The culture media were aspirated, and the cells were washed two times with ice-cold PBS. Add 70-100 ul/ 12 well culture plates RIPA buffer with protease and phosphatase inhibitor cocktail (Halt protease &phosphatase inhibitor, ThermoScientific, USA) 10 µl of inhibitor per 1 ml of RIPA buffer. The cells were scraped with cold rubber tip of 1ml syringe and transferred to eppendorf tubes on the ice. The samples were then vortexed then putted in the tubes on the roller in 4C for 30 minutes to complete the homogenization. The samples were then centrifuged at 15 000 RCF at 4 °C for 30 minutes (Labnet International, NJ07095 USA), then the supernatant transferred into well labelled Eppendorf tube and make aliquot of 20 µl for protein assay and store at -80°C.

3- Protein quantification

The bicinchoninic acid (BCA) components were used to determine the protein concentrations, using the Pierce BCA Assay kit (Thermo Scientific, US) (Thermo Scientific, Rockford, U.S.A.). This assay applies a sensitive and selective colorimetric recognition where a specific reagent containing BCA detects the reduction of Cu2+ to Cu1+ in an alkaline medium. A standard curve is generated using bovine serum albumin (BSA) at a range of concentrations (2000 µg/ml, 1000 µg/ml, 500 µg/ml, 125 µg/ml and 0 µg/ml).

A- Preparation of diluted bovine serum Albumin (BSA) standards using RIPA buffer as diluent and standard Bovine serum solution as follows:

Vial	volume of Diluent(ul)	volume of BSA(ul)
A	0	300 of stock
B	125	375 of stock
C	325	325 of stock
D	175	175 of vial B dilution
E	325	325 of vial C dilution
F	325	325 of vial E dilution
G	325	325 of vial F dilution
H	400	100 of vial G dilution
I	400	0

B- Preparation of BCA working reagent

To calculate the amount of working reagent required use the following formula: Number of standards used + number of samples ×2 (for duplicate) +1 for pipetting error ×200 (amount required per well). To prepare WR mix 50 parts of reagent A and one part of reagent B giving a clear green solution.

C- For a microplate procedure using 96 wells plate, add 25 µl of standards in duplicate,10 µl of samples in duplicate. Add 50 µl of RIPA buffer to the samples and 200 µl of working reagent to both standards and samples. Cover with parafilm and incubate in the oven at 37°C for 30 minutes.

D- Measure the absorbance in plate reader (RT-2100C, Microplate Reader, Germany) at 562 nm, and prepare the samples according to the result in excel datasheet as follow:

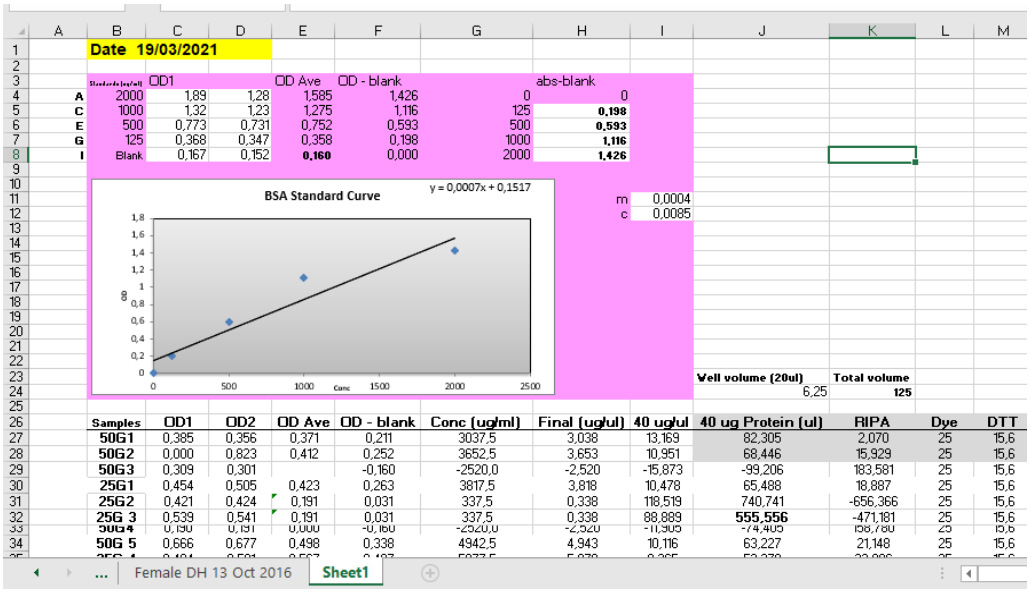

Date 19/03/2021

	OD1		OD Ave	OD - blank		abs-blank
A	2000	1,89	1,28	1,585	1,426	0	0
C	1000	1,32	1,23	1,275	1,116	125	0,198
E	500	0,773	0,731	0,752	0,593	500	0,593
G	125	0,368	0,347	0,358	0,198	1000	1,116
I	Blank	0,167	0,152	0,160	0,000	2000	1,426

m 0,0004
c 0,0085

Vell volume (20ul)	Total volume
6,25	125

Samples	OD1	OD2	OD Ave	OD - blank	Conc (ug/ml)	Final (ug/ul)	40 ug/ul	40 ug Protein (ul)	RIPA	Dye	DTT
50G1	0,385	0,356	0,371	0,211	3037,5	3,038	13,169	82,305	2,070	25	15,6
50G2	0,000	0,823	0,412	0,252	3652,5	3,653	10,951	68,446	15,929	25	15,6
50G3	0,309	0,301		-0,160	-2520,0	-2,520	-15,873	-99,206	183,581	25	15,6
25G1	0,454	0,505	0,423	0,263	3817,5	3,818	10,478	65,488	18,887	25	15,6
25G2	0,421	0,424	0,191	0,031	337,5	0,338	118,519	740,741	-656,366	25	15,6
25G 3	0,539	0,541	0,191	0,031	337,5	0,338	88,889	555,556	-471,181	25	15,6
50G4	0,190	0,191	0,000	-0,160	-2520,0	-2,520	-11,905	-74,405	158,780	25	15,6
50G 5	0,666	0,677	0,498	0,338	4942,5	4,943	10,116	63,227	21,148	25	15,6

... Female DH 13 Oct 2016 Sheet1

4- Sodium-dodecyl-sulphate polyacrylamide gel electrophoresis (SDS-PAGE)

Prepare 12% SDS -PAGE gels prepared solution for gel casting (TGX Fast Cast Acrylamide Kit,10% Cat.161-0173, Bio Rad Laboratories. Inc. U.S). Prepare resolving and stacking gel. Add 10% Ammonium persulphate (ASP) and Tetramethylethylendiamine (TEMED) just before use. Clean glass plates with 70% alcohol and fix them well in the casting stand. Load the resolving gel and add layer of 20% SDS or 100% isopropanol to allow polymerization without oxygen for 10 minutes. Load the stacking gel after drain the SDS or isopropanol and insert the comb. Allow the gel to set for 30 minutes at room temperature. The hand casted gel can be stored at 4°C for later use.

Samples were denatured at 95 °C for 5 minutes, vortexed and centrifuged briefly prior to loading. The gels placed in the electrophoresis chamber, which filled with tank buffer. Load 40 µg/20ul of samples and 2.5 µl molecular weight marker (Figure below) into wells and record the order of loading. Using Mini-PROTEN Tetra Cell System (Bio Rad. SA), the electrodes connected red to red and black to black and run consonant voltage at 150 V for 90 minutes.

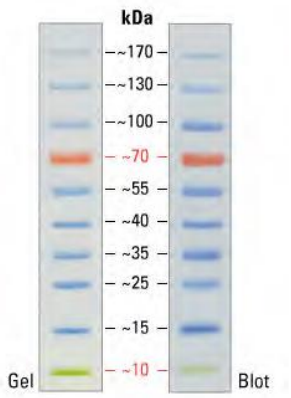

PageRuler Pre-stained Protein Marker

5- Transfer process:

The protein transfer process was performed using semidry transfer unit (Trans-Blot Turbo Transfer system, Bio Rad, SA)). The Polyvinylidene fluoride (PVDF) transfer membranes (Immuno-Blot PVDF Membrane for Protein Blotting, Bio-Rad Laboratories, inc. U.S) were activated in 100% methanol for 30 seconds then in transfer buffer. The transfer sandwiches were prepared and consists of pre-wet set of filters paper / PVDF membrane / gel / pre-wet set of filters paper and the bubbles were removed using a roller. The sandwiches then placed carefully into transfer cassette then placed in transfer unit and switch on. Choose List / Bio-Rad / low molecular weight protein 5 minutes / run. Once the transfer done remove the membrane from transfer unit and rinse briefly with PBST. The protein transfer was confirmed by staining the membrane for 5 minutes with ponceau stain (light sensitive, mix 2.5 ml of stain with 22.5 ml distilled water). The membrane then washed to remove stain three times with distilled water before membrane blocking.

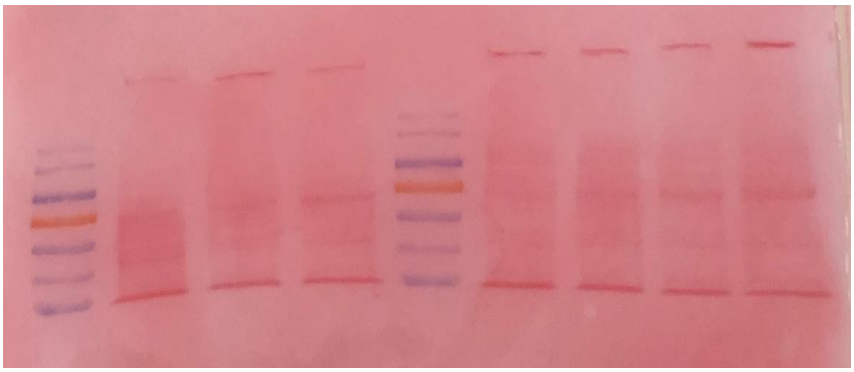

PVDF membrane stained with poceau stain

6- Blocking and antibody probing

The membranes were blocked for one hour at room temperature on the shaker with either 5% bovine serum albumin (BSA) (2,5 g in 50ml PBS-T) or with 5% non-fat milk in PBST (dissolve 25 g milk powder in 500 ml PBST and filter it with filter paper (Whatman, Germany)). After blocking, the membranes with primary antibody (mouse monoclonal anti-troponin T) at a dilution of 1:5000 in 5% non-fat milk overnight at 4 °C on shaker. Next day, the membranes were washed in PSBST 3 times 10 minutes each, then incubated with secondary antibody (Goat Anti-Mouse IgG(H+L)-HRP conjugate, 170-6516, Bio-Rad, GAM) at dilution 1:10000 in 5% non-fat milk solution. Incubate with secondary antibody for two hours at room temperature with gentile agitation on shaker. Afterthought wash in PBST three times.

7- Western blot detection

Prepare a detection reagent (Clarity Western ECL Substrate, Cat. 70-5060, Bio- Rad Laboratories. Inc. U.S) mix 1ml of each one, first white bottle which is super signal stable peroxide then brown bottle which is super signal west Pico Luminal / Enhancer. Use forceps to remove membrane from PBST and place it in a clean dry transparency. After one minute, close the transparency and remove excess fluid. Stick a fleshy sticker on the protein marker where expect the protein band signal to appear then keep it detection cassette. In a dark room cut x-ray film (Agfar

Healthcare, RSA), and lay it on the membrane (without removing the transparency) for 1-3 minutes. Take the x-ray film and immerse it in the developer solution and remove it once the band signal coming up Rinse briefly in water then immerse it in the fixer solution for 2 minutes then rinse in water and hang up to dry.

8- Stripling and re-probing of the membrane

The purpose of stripling of the membrane is to incubate it with other antibody to detect other protein or for loading control. Immediately after ECL detection process wash the membrane shortly with PBST then with distilled water 2 times for 10 minutes each. Wash with stripling buffer for 5 minutes then in distilled water two times for 10 minutes each finally wash briefly with PBST.

Block the membrane with 5% non-fat milk for 1 hour at room temperature then incubate with housekeeping primary antibody (Monoclonal Anti-alpha actin antibody produced in mouse) at dilution of 1:5000 in 5% non-fat milk in PBS-T overnight at 4°C. Wash with PBST 3 times 10 minutes each. Incubate with horseradish peroxidase (HRP) conjugated secondary antibody (Goat Anti-Mouse IgG (H+L)-HRP conjugate, 170-6516, Bio-Rad, GAM) at room temperature on the shaker. Wash three times with PBST 10 minutes each and proceed to ECL detection as that for protein of interest.

9- Scanning and analysis

Scan the x-ray film with scanner and analyse with image J software (NIH, USA) as following steps:

1- Open scanned image in image J software. Change the image to 8-bit mode, go to image / type / 8bit.

2-Using rectangular tool from the image J toolbar draw rectangle shape around the first band, then go analyse / gel / select first lane, then drag the rectangle over the next band, go analyse / gel / select next lane, repeat this step until all bands selected

4- Once all the bands selected go analyse / gel / plot lanes to give a profile plot for each lane. The profile plot represents the mean density of each lane; higher peak represents dark band while wider peak represents large band size**.** Choose the straight-line tool from image J toolbar and draw a line at the base of the peak to enclose the peak. Select wand tool from image J toolbar and click inside the peak and highlight all the peaks.

5- Choose analyse / gel / label peaks, the results are expressed as a percentage of the mean density of all the bands representing the protein of interest. Copy the result to excel datasheet.

6- Same steps (1-6) needed for the housekeeping protein.

7- Calculate the relative density of each band by dividing the percentage value of the mean density of the protein of interest over the percentage value of the mean density of the protein of housekeeping protein beta actin.